– 17 –

Bacterial Cellulose from *Glucanacetobacter xylinus*: Preparation, Properties and Applications

Édison Pecoraro, Danilo Manzani, Younes Messaddeq and Sidney J.L. Ribeiro

ABSTRACT

This chapter deals with the cellulose produced by the *Glucanacetobacter xylinus* strain, called bacterial cellulose, which is a remarkably versatile biomaterial usable in wide variety of domains, such as papermaking, optics, electronics, acoustics and biomedical devices. Its unique structure shows entangled ultrafine fibres, which provide excellent mechanical strength, besides biodegradability, biocompatibility, high water-holding capacity and high crystallinity. Some of its applications are described, such as complementary nutrition (*nata de coco*), artificial temporary skin for wounds and burns, dental aid, artificial blood vessels and micronerve surgery, DNA separation, composite reinforcement, electronic paper, light emitting diodes and fuel cell membranes.

Keywords

Bacterial cellulose, *Glucanacetobacter xylinus*, Biosynthesis, Structure, Properties, Applications, Biocompatibility, Biomaterial, DNA separation, Biodegradability

17.1 INTRODUCTION

Cellulose is the most abundant biopolymer on earth with an estimated output of over 10^{11} tons per year. Most of its biosynthesis takes place in the cellular walls of plants, but four other sources are known, animal, bacterial, chemical and enzymatic.

The cellulose thus produced exists naturally in two native forms (native cellulose): The first is called *pure cellulose,* and includes celluloses produced in their natural state, such as cotton, bacterial cellulose and those present in some algae and some marine animals like tunicates. The second is called *complex cellulose*, and includes most of the celluloses present in nature, as the fundamental component of the cellular wall of higher plants.

Notwithstanding its specific origin in nature, cellulose is a linear polymer in which β-1,4 glycosidic moieties are joined to form cellobiose repeat units. What vary from one form of cellulose to another are, on the one hand, its degree of polymerization, which can span hundreds to thousands and, on the other hand, the supramolecular organization of its chains, which can give rise to amorphous and several types of crystalline structures. The cellulose hydroxyl groups can form intra and intermolecular hydrogen bonds which are responsible for its chemical stability, structure rigidity and tensile strength. All these fundamental aspects related to cellulose are thoroughly documented, as pointed out in Chapter 1.

The present chapter is devoted to a specific form of cellulose, bacterial cellulose, which has been gaining growing attention because of the property of the actual material associated with it.

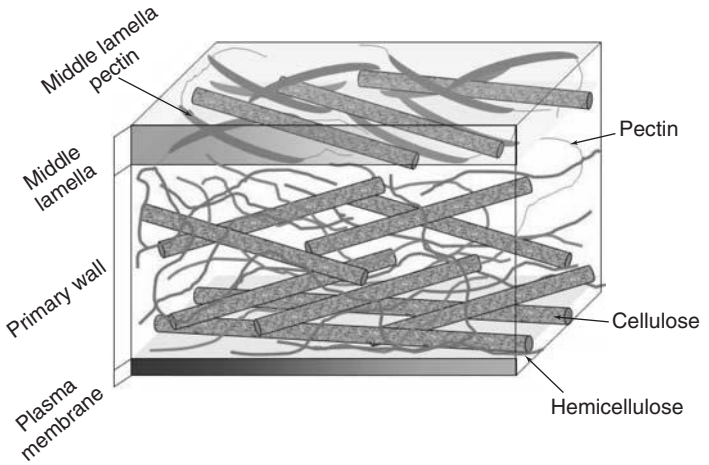

Figure 17.1 Schematic representation of the components in higher-plant cellulose.

Table 17.1

Properties of plant (PC) and bacterial (BC) cellulose

Properties	PC	BC
Fibre width	$1.4–4.0 \times 10^{-2}$ mm	70–80 nm
Crystallinity	56–65%	65–79%
Degree of polymerization	13 000–14 000	2 000–6 000
Young's modulus	5.5–12.6 GPa	15–30 GPa
Water content	60%	98.5%

Bacterial cellulose is obtained through the biosynthesis induced by bacteria belonging to genera *Glucanacetobacter*, *Rhizobium*, *Sarcina*, *Agrobacterium*, *Alcaligenes*, etc. Among them, the one possessing the best efficiency to produce cellulose, and for that reason the most studied, is *Glucanacetobacter xylinus* (also denominated as *Acetobacter xylinum*) [1]. These are gram-negative bacteria, strictly aerobic and non-photosynthetic, capable to convert glucose, glycerol and other organic substrates into cellulose within a period of a few days. They are usually found in fruits, vegetables, vinegar and alcoholic beverages.

The cellulose biosynthesized by *G. xylinus* is identical to that produced by plants, regarding its molecular formula and polymeric structure, but presents a higher crystallinity. The other fundamental difference between bacterial cellulose and its widespread plant-based counterpart stems from the fact that the former is chemically pure, free of lignin, hemicelluloses and the other natural components usually associated with the latter (Fig. 17.1).

Table 17.1 compares some properties of vegetal and bacterial cellulose.

The specific properties of bacterial cellulose make it interesting for important applications, such as a nutritional component (additive of low caloric contents, stabilizer, texture modifier, *nata de coco*), a pharmacological agent (temporary dressing, excipient, cosmetics, drug carriers), as well in telecommunications and papermaking, as summarized in Table 17.2.

17.2 CELLULOSE SYNTHESIS BY *G. XYLINUS*

G. xylinus was first described by Brown in 1886 [2, 3] who identified a jelly-like film formed over the surface of a vinegar broth fermentation. A microscopic analysis revealed the presence of bacteria distributed within the whole film. Still today, *G. xylinus* is taken as the model microorganism in the research on the biosynthesis, crystallization and structural properties of bacterial cellulose [4]. The cellulose produced by *G. xylinus* contains approximately

Table 17.2

Examples of applications of bacterial cellulose

Area	Application
Cosmetics	Stabilizer of emulsions; component of artificial nails
Textile industry	Artificial textiles; highly absorbent materials
Sports and tourism	Sporting clothes; tents; camping material
Mining and refinery	Sponges for recovery spilled oil; material for toxin adsorption
Wastes treatment	Recycling of minerals and oils
Sewage purification	Urban sewage purification; water ultrafiltration
Broadcasting	Sensitive diaphragms for microphones and stereo headphones
Forestry	Artificial wood replacer, multi-layer plywood, heavy-duty containers
Paper industry	Specialty papers, archival documents repairing, more durable banknotes, diapers, napkins
Machine industry	Car bodies, airplane parts, sealing of cracks in rocket casings
Food production	Edible cellulose (*nata de coco*)
Medicine	Temporary artificial skin for therapy of burns and ulcers, component of dental implants
Laboratory	Immobilization of proteins, cells; chromatographic techniques; medium for tissue cultures
New applications	Cellulose thin films for documents and book recovery; fibres (including optical); biodegradable plastics; oriented templates; liquid crystal displays; luminescent materials; fuel cell membranes; drug delivery; stents covering; ophthalmic, cardiovascular and neurological prostheses; bulletproof materials

98 per cent (w/w) of water. Visually, the difference between bacterial and plant cellulose relates both to appearance and water content viz. the latter has a fibrous aspect, while the former resembles a gel.

In the laboratory, the cultivation is conducted in a liquid Hestrin–Schramm medium (glucose, yeast extract, peptone, citric acid and sodium phosphate) at pH 5 and 28°C. The cultures are grown in static containers or air flow (airlift bioreactors). The growing time depends on the desired thickness of the ensuing cellulose membrane. Several studies can be found on the growth kinetics of those microorganisms, based on fermentative processes [5].

The cells of *G. xylinus* possess 100 or more pores in their membrane for cellulose extrusion. Each pore produces a cellulose chain that groups with another 36 chains to form an elementary fibril, which has a diameter of approximately 3.5 nm. About 46 adjacent fibrils join through hydrogen bonds to form a ribbon, which has a width ranging from 40 to 60 nm (Fig. 17.2(a)). The ribbons roll up to form the fibre (Fig. 17.2(b)), which gets tangled with the other fibres dispersed in the culture medium (Fig. 17.2(c)) [6]. The entangled fibres form a jelly-like film on the surface of the liquid culture medium. The film containing the bacteria is called zooglea (Fig. 17.2(d)). Its thickness depends on the cultivation time and can usually reach 1 or 2 cm (Fig. 17.2(e)).

Each extrusion pore bears a site for cellulose chains production called terminal complex (TC) and each TC accomplishes several different processes, all controlled genetically within the biosynthetic route. Many studies have been undertaken for both plant and bacterial cellulose, in order to find the proteins, enzymes and to map the genes that are involved in each synthesis step [4, 7], but, until now, none is conclusive. According to Iguchi *et al.* [8], the cellulose membrane is a shelter for the bacteria. It protects them from the lethal effect of solar ultraviolet radiation, keeps them moist in an aerobic environment, allows the diffusion of nutrients from the culture medium and protects them against predators and contamination by heavy metals. According to Borzani and de Souza [9], in a static culture, the cellulose zooglea grows towards the atmosphere, leaning on the first film formed in the liquid–gas interface. In an agitated culture, bubble columns or airlift reactors, the growing also follows to the liquid-gas interface [10].

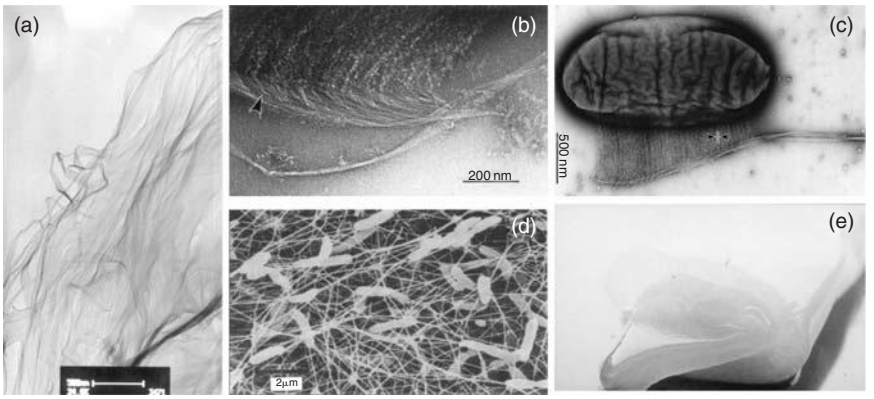

Figure 17.2 (a) Transmission electron micrograph showing the ribbons of approximately 60 nm widths; (b) on the left, the arrow indicates the place where the fibrils are rolling up; (c) SEM of *G. xylinus* producing a cellulose fibre. The suitable place among two arrows display the dimension of the fibrils: (d) SEM of the zooglea; (e) recently harvested zooglea of static culture container. (Figure 2(b) and (c) reprinted from Reference [6], with kind permission of Springer Science and Business Media. Figure 2(d) reprinted from Reference [8], with kind permission of Springer Science and Business Media.)

The more suitable purification method for the bacterial cellulose calls upon distilled water, sodium hydroxide and sodium hypochlorite solutions, since it guarantees the elimination of bacteria cells and culture medium residues from the membrane. For clinical applications, the suitable sterilization processes are gamma radiation and ethylene oxide treatment, but the latter should be avoided for bacterial cellulose dry or wet membrane, because it can cause allergic reactions, mostly when used internally.

In the bacterial cellulose biosynthesis, the cellulose chains (formed by glucose units linked through β-1,4-glycosidics bonds) interact through hydrogen bonds, assuming a parallel orientation among them. The structure and rigidity of bacterial cellulose is provided by the OH intra and intermolecular hydrogen bonds, as shown in Fig. 17.3.

The cellulose microcrystallinity results from isolated areas with orderly chains within the microfibril structures. The arrangement of those chains in an ordered structure is driven by hydrogen bonding. The remaining areas show chains distributed in a paracrystalline or amorphous phases [11]. Two crystalline allomorph phases, Iα and Iβ, were proposed for cellulose I (bacterial cellulose) [12]. The Iα phase is found predominantly in cellulose produced by algae and bacteria, while the Iβ phase is present in higher percentages in higher-plant cellulose. Atalla

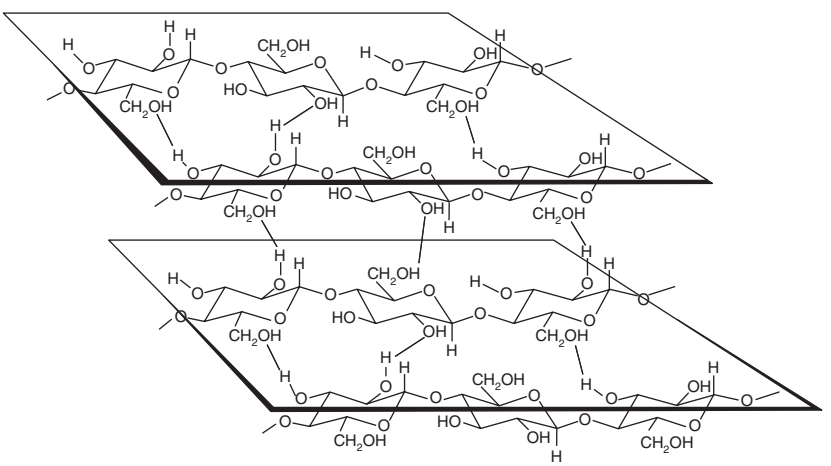

Figure 17.3 Outline of intra- and inter-molecular hydrogen bonds among cellulose chains.

Table 17.3

Iα/Iβ ratio for different cellulose sources

Type	Class	Ratio Iα/Iβ(%)
Glucanoacetobacter	Bacterial	64/36
Valonia	Vegetal (algae)	60/40
Halocynthia	Animal	10/90

and Van der Hart showed in 1984 [12] that phase Iβ is formed by cellulose chains arranged in a monoclinic unit cell, whereas phase Iα displays a triclinic arrangement. The ratio between the Iα and Iβ phases depends on the cellulose source, as shown in Table 17.3.

The structural characteristics of bacterial cellulose are directly related to two factors, namely (1) the origin of the strain, which determines the Iα/Iβ ratio and (2) the culture medium composition that influences the chain size. Such characteristics determine the degree of crystallinity of bacterial cellulose and consequently, their physico-chemical properties. Structural modifications can be accomplished in a post-production step, since it is possible to functionalize the hydroxyl groups (—OH) by methylation [13], esterification [14], sulphonation [13], nitration [13], deoxyamination [15], etc.

17.3 PROPERTIES

The results presented here refer specifically to membranes synthesized by Bionext®'s strain. Bionext is a Brazilian company that produces bacterial cellulose for medical applications. At this company, bacterial cellulose wet membranes are dried by compression and heating, a process that confers unique texture characteristics.

17.3.1 Morphology

Figure 17.4 shows the surface map of a Bionext dry membrane recorded in a Taylor Hobson Form Talysurf Series 2 profilometer.

The dry membrane can be obtained in different thicknesses, from 20 to 500 μm, depending on the need. Figure 17.5 compares the electron scanning photomicrograph of the membrane shown in Fig. 17.4 with that of one obtained by freeze drying. In both cases the fibres are made of ribbons, which are composed of a group of about 36 fibrils

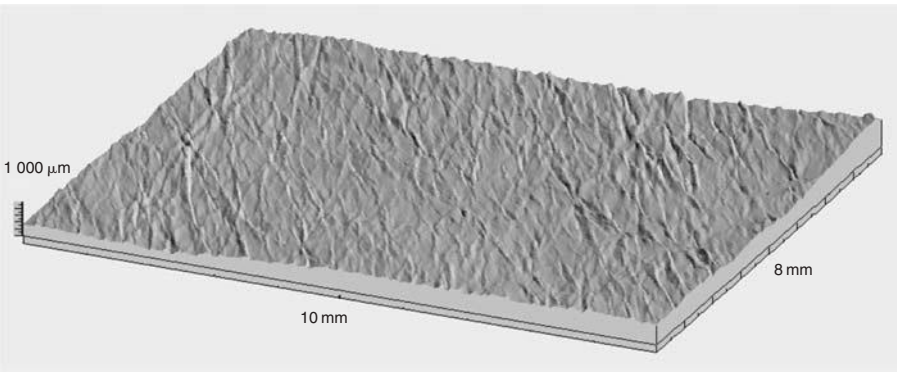

Figure 17.4 Surface map of a bacterial cellulose membrane dried by compression and heating. The scanned area is 10 mm × 8 mm. The average thickness is 200 μm.

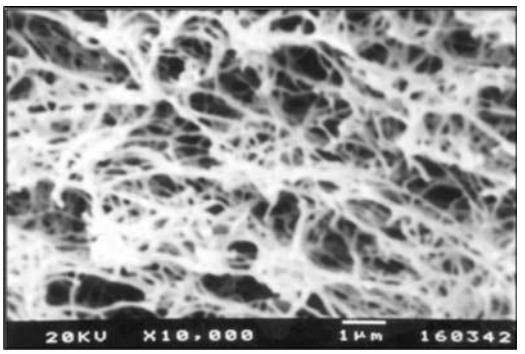

(a)

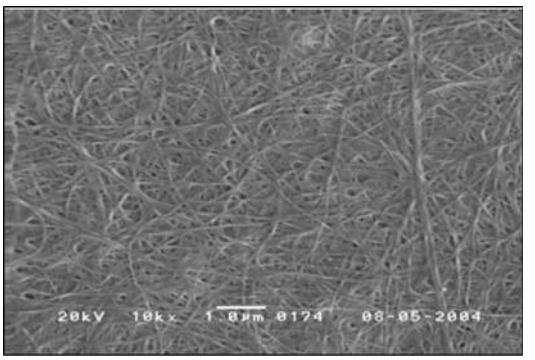

(b)

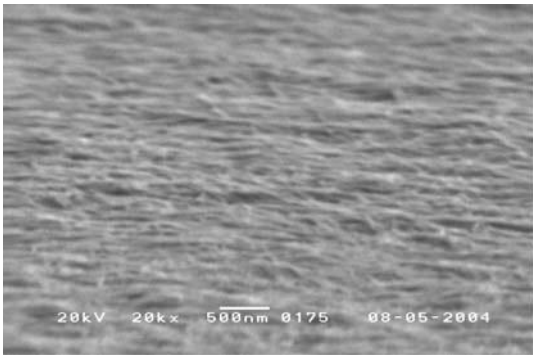

(c)

Figure 17.5 Electron scanning microscopy of (a) Surface of a membrane prepared by freeze drying; (b) surface of a membrane dried in a laboratory oven; (c) cross section of the membrane in (b).

interacting through hydrogen bonds. Figure 17.6 shows the transmission electron microscopy microphotographs of ribbons.

Under compression, the original open network, shown in Fig. 17.5(a), collapses in a fibre entanglement and this new network is so dense that it can be used as a filter for microorganisms or blood components, as shown in Fig. 17.7. Specific surface area and porosity can also be modified by a dry process. Thus, the specific area for samples pressed and heated is *ca*. $25\,m^2\,g^{-1}$, while for those freeze dried is about $45\,m^2\,g^{-1}$.

17.3.2 Vibrational spectroscopy

Figure 17.8 shows a typical FTIR spectrum of a pressed and heated bacterial cellulose membrane. Of course, the functional groups that characterize bacterial cellulose are the same as those of vegetable cellulose and the corresponding peaks are assigned in Table 17.4 [16].

Infrared spectroscopy can also be used for the determination of the Iα/Iβ ratio. The method is based on the difference in the stretching energies, and the peaks, assigned to the OH groups present in each phase. The peak at $750\,cm^{-1}$ corresponds to the triclinic phase Iα, while that at $710\,cm^{-1}$ is attributed to monoclinic phase Iβ. Hence, the ratio between the area under these peaks gives the ratio between the phases. The Iα/Iβ ratio shows variations related to the origin of cellulose. Algae and bacteria forms are rich in triclinic phase (Iα), while higher plants are rich in monoclinic phase (Iβ). For Valonia algae, Atalla [12] found a ratio of 6/4. For different *G. xylinus* strains, ratios of 6/4 and 7/3 have been reported [17, 18]. However for the Bionext strain, the ratio is 2/8, that is these bacteria produce cellulose similar to that found in higher plants, in terms of the proportion between the crystalline phases. As this strain is an over producer, its cellulose synthesis seems to be directed towards the thermodynamically most stable phase, viz. Iβ.

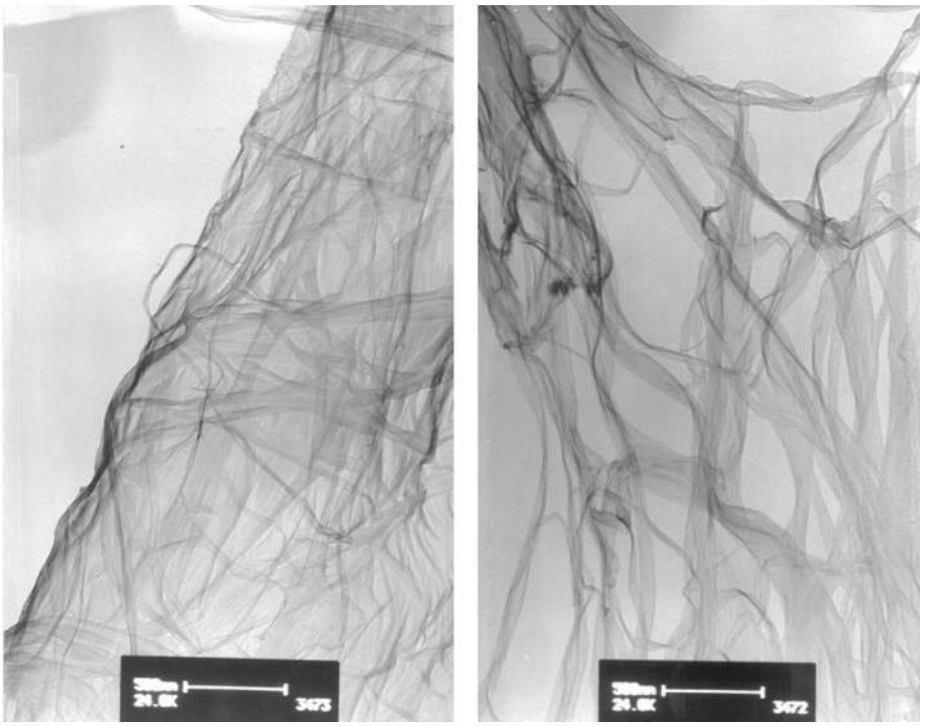

Figure 17.6 Transmission electron microscopy photomicrographs showing ribbons of 60 nm width. In this case, the ribbons compose the structure of the fibres in a membrane prepared by freeze drying (the bars correspond to 500 nm).

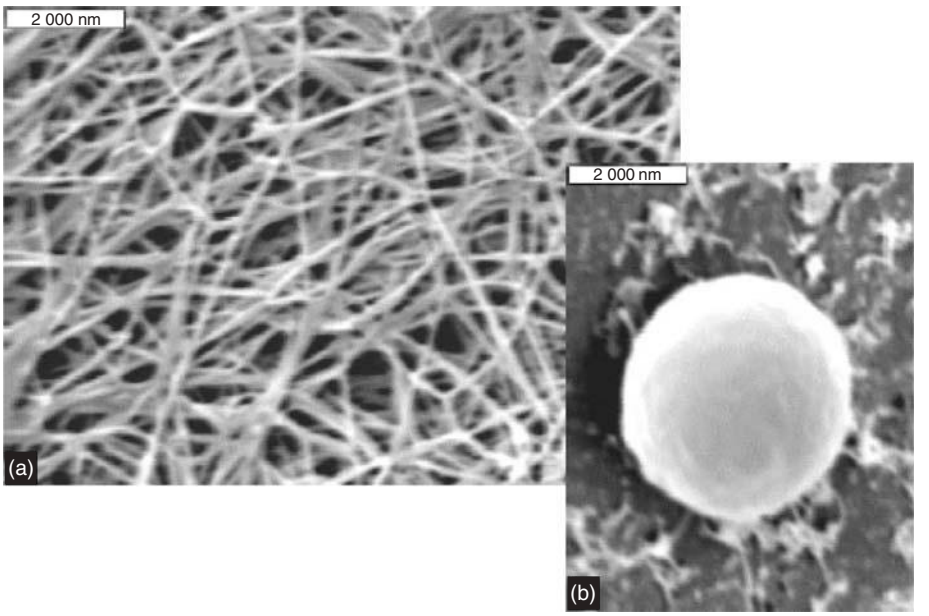

Figure 17.7 (a) Bacterial cellulose dry membrane mesh and (b) a thrombocyte (blood component). (Reprinted from Reference [5] with permission from Elsevier Science Ltd.)

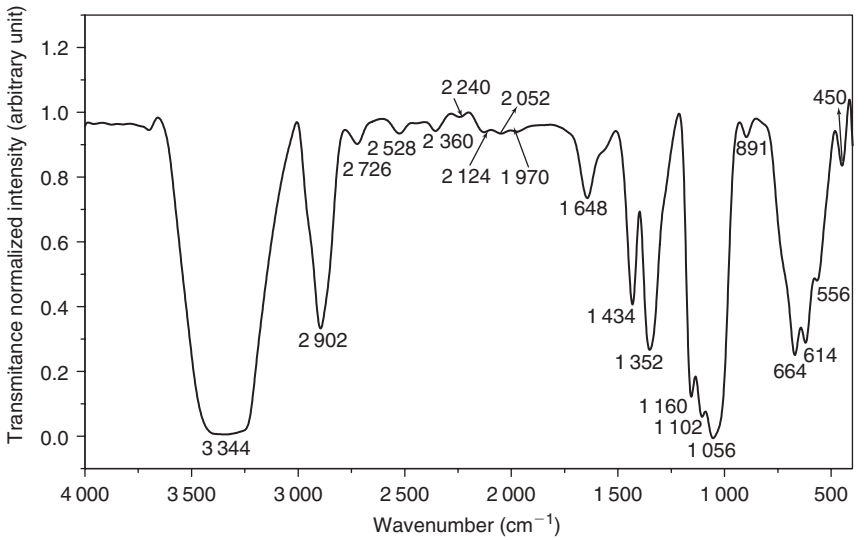

Figure 17.8 FTIR spectrum of a 200-μm thick bacterial cellulose membrane.

Table 17.4

Typical infrared absorption frequencies for bacterial cellulose [16]

Range (cm^{-1})	Assignment[a]
3 500–3 300	ν OH
3 000–2 870	ν CH and CH_2 (CHOH; CH_2OH)
1 645	δ_s HOH
1 430–1 330	δ C—OH e CH
1 200–1 000	ν C—O (—C—O—H)
1 150–1 000	ν C—O (C—O—C)
900–700	δ_{as} in plane CH_2 δ C—H
700–400	δ out of the plane OH

[a] ν = stretching; δ = angular bending; s = symmetric; as = asymmetric.

17.3.3 X-ray diffraction

The X-ray diffractogram of bacterial cellulose, Fig. 17.9, shows the presence of crystalline peaks and amorphous haloes. Due to the overlapping of the reflections from Iα and Iβ phases, it is not possible to separate the contribution of each one on the peaks at approximately $2\theta = 15°$ and 23°. The peak at 15° corresponds to the diffractions from triclinic (100) and monoclinic (110) plans, whereas the peak at 23° corresponds to the reflections from triclinic (110) and monoclinic (200) plans [19]. Through the *Ruland* method [20], it is possible to quantify the degree of crystallinity of cellulose. The method relates the contribution of the amorphous phase on the reflexions of the crystalline phases through the expression $\%C = [I_c/(I_c + K \times I_a)] \times 100$, where $\%C$ is the percentage of the crystalline phase, I_c the integral under all the crystalline reflexion peaks, I_a the integral under the haloe that corresponds to the amorphous phase, and K is a proportionality constant, which in the case of bacterial cellulose is taken as unity.

The crystallinity of bacterial cellulose has an influence on its mechanical properties. In 1990, Brown *et al*. [21] showed that under an intense magnetic field (1.8 T), their *G. xylinus* strain produced cellulose with no crystalline regions. One characteristic of that cellulose was a lower tensile strength, compared to that of a sample obtained without magnetic field. Therefore, an increase in the amount of crystalline phase can lead to an improvement of the mechanical properties of bacterial cellulose membranes.

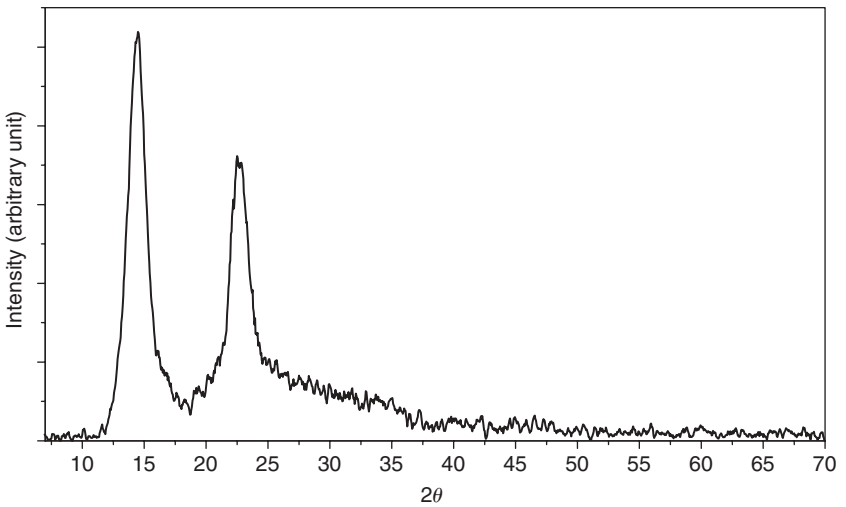

Figure 17.9 X-ray diffractogram of a bacterial cellulose membrane. The sample was supported on a borosilicate glass holder.

17.3.4 UV–visible and near-infrared absorption

Another important characteristic of bacterial cellulose is its capacity to block most of the ultraviolet radiation from sunlight. The UV spectral region is subdivided into UV-A (320–400 nm), UV-B (280–320 nm) and UV-C (below 280 nm). UV-C is not considered here, since it is absorbed by the atmosphere. Figure 17.10 shows the transmittance spectrum of a bacterial cellulose membrane from the UV (250–400 nm) to the near-infrared

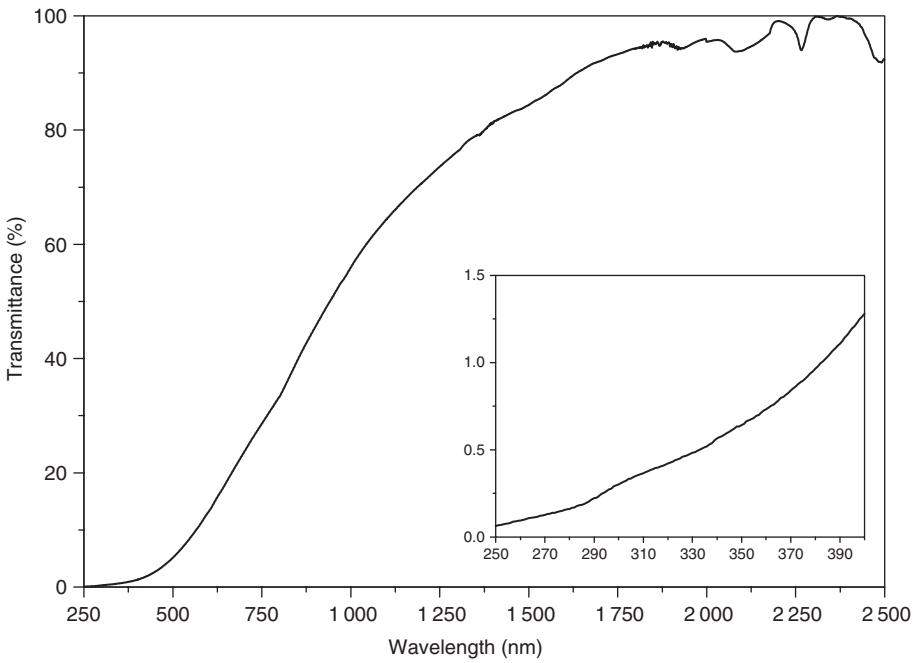

Figure 17.10 UV–Visible and near-infrared transmittance spectrum of a 200-μm thick bacterial cellulose membrane. The insert shows the magnification of the 250–400 nm range.

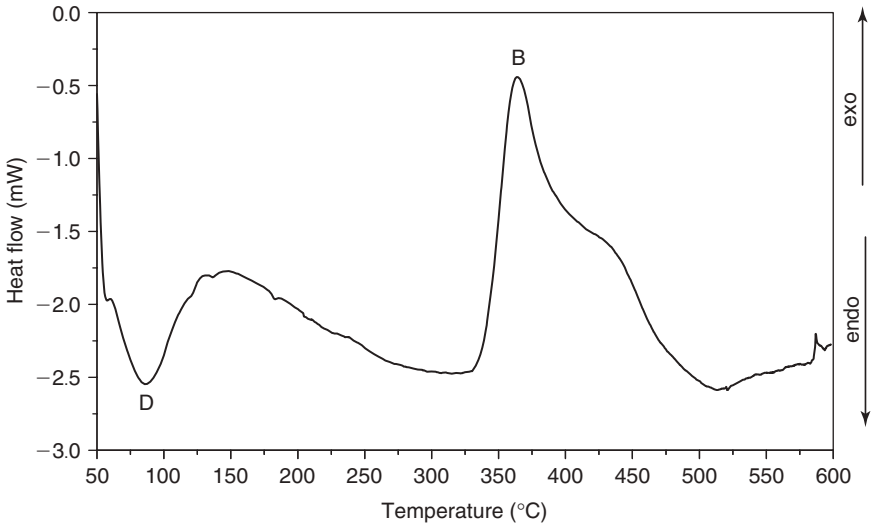

Figure 17.11 DSC thermogram of a bacterial cellulose membrane. The temperatures at D and B refer to the dehydration (87°C) and burning (363°C) peak temperatures, respectively.

(750–2 500 nm), including the visible region of the electromagnetic spectrum. The insert shows that for a 200-μm thick membrane, only 0.4 per cent of all UV-B and 1.3 per cent of UV-A radiation pass through it. For medical applications, such as temporary artificial skin, that feature is an important issue. Besides its transparency in the visible region, another characteristic of bacterial cellulose is its transparency at 1 550 nm, suggesting that it can be used for telecommunication applications.

17.3.5 Thermal behaviour

As shown in Fig. 17.11, a bacterial cellulose dry membrane can be heated up to 325°C before it starts to burn, which is at least 75°C above the burning temperature of conventional office paper. This higher thermal resistance can is attributed to the absence of additives in its composition, which are common in papermaking.

Not only by its thermal, but also by its mechanical properties (tensile strength of 200–300 MPa [22]), bacterial cellulose could also be an alternative material for industrial seals and connections.

17.4 APPLICATIONS

The applications of bacterial cellulose dry and wet membranes have increased considerably in last couple of decades, mainly in the biomedical field, as recently thoroughly reviewed [23], and high technology areas, and also in other sectors, as summarized below.

17.4.1 Food (*nata de coco*)

Probably the most popular use of bacterial cellulose is in the form of a dessert called *nata de coco.* It is a glycidic food obtained by surface fermentation with *G. xylinus*. It is well known in some Asiatic countries, mainly the Philippines. Coconut milk or water, low economical value by-products of coconut processing, are employed as

culture media. Other agricultural residues such as milk, whey and even fruit juices, may also be used. The recipe to prepare *nata de coco* from bacterial cellulose is [24] as follows:

Ingredients

- 1 kg of bacterial cellulose wet membrane (bacteria free).
- Three cups white sugar.
- Three cups water.

Preparation

- Cover the wet membrane with water and boil for 10 min.
- Repeat 3 times and rinse every time.
- Boil sugar and water until syrupy. Put in membrane and cook for 10 min.
- Let stand overnight. Next day, boil again in its syrup, reduce heat and continue cooking until syrup is absorbed by membrane.
- Make another syrup (1 part sugar to 1 part water).
- Cook the membrane in second syrup for 10 min.

To preserve pack the *nata de coco* in sterilized bottle, then pour hot syrup (second syrup) and seal tightly.

17.4.2 Artificial temporary skin for wounds and burns

The idea to use bacterial cellulose for wound care started in the early 1980s with the exploratory investigation at Johnson & Johnson [25]. After that, a Brazilian company called *Biofill Industrias* (now *Fibrocel*) [26], continued to investigate the properties of microbial cellulose and nowadays *Fibrocel* commercializes *Nexfill*®, a bacterial cellulose dry bandage for burns and wounds. When the bandage made of dry or wet [27] bacterial cellulose membrane is applied on top of a burn area or wound, it relieves the pain almost completely in a few seconds and shows close adhesion to the wound bed. This effect will only be observed if the epidermis is exposed, that is it works for second or third degree burns. It is a one-time healing, since everyday clinical procedures are not necessary any longer, as in conventional treatments. The same is observed for chronic wounds, like those caused by diabetes or in bedridden patients. During cicatrization, the membrane does not develop rips or perforations, keeping the area as a closed wound, thus preventing contamination by bacteria or other infectious microorganisms. It also blocks ultraviolet radiation, besides restricting the loss of fluids by maintaining a constant evaporation rate. Furthermore, due to its transparency, it allows a straightforward wound inspection. The time of re-epithelialization is shorter than that associated with a traditional bandage. When cicatrization takes place, the membrane loses its adherence on the scarred area, breaking into small pieces and falling off. Its analgesic action mechanism is not elucidated yet. The likely mechanism involves ion capture by the cellulose hydrogen bonds. In conclusion, the treatment with bacterial cellulose membranes reduces the hospital residence time of the patient while improving his quality of life during recovery.

17.4.3 Dental wounds

Based on the results with artificial skin in burns or skin tissue loss, bacterial cellulose was tested in dental tissue regeneration. The bandage, called Gengiflex®, consists of two layers: the inner layer is composed of bacterial cellulose, which offers rigidity to the membrane, and the outer alkali-cellulose layer is chemically modified [28]. Salata *et al.* [29], in 1995, compared the biological performance of Gengiflex® and Gore-Tex® membranes using the *in-vivo* non-healing bone-defect model proposed by Dahlin *et al.* [30]. The study showed that Gore-Tex membranes (a composite with polytetrafluoroethylene, urethane and nylon) were associated with significantly less inflammation and both membranes promoted the same amount of bone formation during the same period of time. A greater amount of bone formation was present in bone defects protected by either Gore-Tex or bacterial cellulose membrane, when compared to the control sites. Gore-Tex is better tolerated by the tissues than Gengiflex.

Recently, in a similar vein, Macedo *et al.* [31] also compared bacterial cellulose and polytetrafluoroethylene (PTFE) as physical barriers used to treat bone defects in guided tissue regeneration. In this study, two osseous defects (8 mm in diameter) were performed in each hind-foot of four adult rabbits, using surgical burs with constant

sterile saline solution irrigation. The effects obtained on the right hind-feet were protected with PTFE barriers, while Gengiflex membranes were used over wounds created in the left hind-feet. After 3 months, the histological evaluation of the treatments revealed that the defects covered with PTFE barriers were completely repaired with bone tissue, whereas incomplete lamellar bone formation was detected in defects treated with Gengiflex membranes, resulting in voids and lack of continuity of bone deposition. This demonstrated that the non-porous PTFE barrier is a more effective alternative to treat osseous defects than a bacterial cellulose membrane.

17.4.4 Artificial blood vessels and micronerve surgery

This particular use for bacterial cellulose was proposed by Klemm *et al.* [5] in 2001. They used BASYC® (BActerial SYnthesized Cellulose), which consists of tubes of bacterial cellulose with no sewing. The tubes have an inner diameter of 1 mm, length of about 5 mm and wall thickness of 0.7 mm. For their use in microsurgery, they must resist both mechanical strains during microsurgical preparation and anastomozing and blood pressure of the living body. Bacterial cellulose has favourable mechanical properties, including shape retention and tear resistance and a better mechanical strength than organic sheets, like polypropylene, polyethylene terephthalate or cellophane. The BASYC tubes can resist to the blood pressure of the test animal (white rat) of 0.02 MPa (150 mmHg). Beside blood vessels, the tubes can also be used as a protective cover for micronerve sutures and in the form of a practice model for the application of microsurgical suture techniques in medical training.

The results for treated blood vessels showed that after 4 weeks, the BASYC®-prosthesis was wrapped up with connective tissue, pervaded with small vessels like *vasa vasorum*. The BASYC®-interposition was completely incorporated in the body without any rejection reaction. Results from micronerve surgery (white rat sciatic nerve) showed similar results. From 4 to 26 weeks following the intervention, the bacterial cellulose tube was covered with connective tissue and contained small vessels. No inflammation reaction or capsulation of the implant was observed. The regeneration nerve was improved after 10 weeks, compared to an uncovered anastomosed nerve.

The use of bacterial cellulose in medical prosthesis is exciting, considering the perspectives of applications in cardiac bypass surgery and self-transplanted derivation vessels [23].

17.4.5 DNA separation

DNA analysis or replication for forensic investigation, clinical diagnosis or even for molecular biology procedures, demands the separation of molecular fragments from ten to thousands of base pairs (bp). Electrophoresis is one of the most powerful techniques to provide DNA separation. This method takes advantage of the sieving effect of gels or polymer solutions. The design of the optimal mesh size for DNA separation has been a major issue [32]. Recently, a new concept for separation has been developed that takes advantage of the nanospaces in nanofluid structures, for example pillars [33–35], magnetic structures [36] or nanospheres [37].

Tabuchi *et al.* in 2004 [37], proposed the use of bacterial cellulose fibrils suspension for DNA separation. A solution of 0.49 per cent hydroxypropylmethyl cellulose containing 0.3 per cent of bacterial cellulose fragments allowed excellent separation for a wide range of DNA sizes (10 bp–15 kbp). Two different types of mesh structure coexisted in the medium, viz. the mesh derived from the conventional polymer solution and that associated with the bacterial cellulose fibrils. Thus, the structure is composed of $\sim$10 μm fragments containing 10 nm to 1 μm mesh of bacterial cellulose rigid fibrils and the several 10 nm meshes of the flexible polymer network.

The system also allowed a high resolution of single-nucleotide polymorphisms, even though the viscosity was less than 5 cP. According to the authors [37], the results suggest that the ability of this medium to separate DNA is due to its double-mesh concept, combined with a stereo (obstacle) effect and that this is therefore a powerful medium currently available for the separation of DNA fragments.

17.4.6 Separation of mixtures

Bacterial cellulose can be used as a selective pervaporation membrane in water–organic mixtures. An easy experiment can be set up if a bacterial cellulose membrane is available. The membrane should be tightly fixed between two transparent containers, like a partition. Both containers should have an aperture for the introduction of the

feed mixture (*e.g.*, water and olive oil) or the individual liquids. For mixtures, just fill up one container and close it, while leaving the opposite container open. For individual liquids, fill each container with the respective liquid and close both. In the case of individual liquids, the water will be pumped through the membrane for the oil container, even with the containers closed. In the case of mixtures, water will be pumped through the membrane, if at least part of the liquid is in contact with it.

Pandey *et al.* [38], in 2005, described the use of a bacterial cellulose membrane to separate water–organic mixtures (acetone, formalin, ethanol, ethylene glycol and glycerol) by a pervaporation process. The membrane showed a high sorption affinity for compounds, like glycerol and ethylene glycol, which form extensive hydrogen bonding with the cellulose chains in the membrane. The presence of water in the aqueous binary mixtures of organic chemicals, in general, increases the overall sorption via the plasticization of the membrane, which preferentially sorbs water from the binary mixtures. The total flux for the pervaporation of the aqueous (40 per cent (v/v)) binary mixtures ranged from $92\,g\,m^{-2}h^{-1}$ for glycerol/H_2O to $614\,g\,m^{-2}h^{-1}$ for ethanol/H_2O at 35°C, which further increased to $1\,429\,g\,m^{-2}h^{-1}$ at 75°C. The permeation selectivity was highest for glycerol/H_2O and lowest for ethanol/H_2O and decreased with increasing temperature. The comparatively high pervaporative separation index of $103–104\,g\,m^{-2}h^{-1}$ and the relatively low activation energy of $10\,kJ\,mol^{-1}$ emphasized the potential of bacterial cellulose membranes in the pervaporative separation of aqueous binary mixtures with organic compounds.

17.4.7 Fibre reinforcement

Because of their dimensions, ribbons and microfibrils found in the bacterial cellulose morphology, are a subject of interest for composites and the mechanical enhancement of materials. The development of new cellulose-reinforced composite materials is based on both industrial and techno-economical criteria and is therefore dominated by the search for adequate mechanical performance at the lowest cost, as thoroughly discussed in Chapter 19, which also highlights the facts that cellulose nanocrystals have the potential for excellent mechanical performances, due to a low density combined with high *moduli* and tensile strength, and are biodegradable and inexpensive, making them very attractive for industrial purposes. Grunert and Winter [39] were the first in 2000 to develop new materials containing cellulose nanocrystals from bacterial cellulose topochemically modified by trimethylsilylation. The unreacted and the surface trimethylsilylated crystals were exploited as the particulate phase in nanocomposites with crosslinked polydimethylsiloxane as the matrix. This study aimed at demonstrating that cellulose nanocrystals can improve the mechanical properties of polymers and that the surface modification of the cellulose provides an enhanced adhesion between the two components of the composite, a fundamental point which is systematically treated in Chapter 18. The dynamic mechanical analysis of the nanocomposites revealed reinforcement with regard to the pure polymer for both the composite with unmodified and that with surface trimethylsilylated cellulose fibres. The extent of reinforcement depended strongly on the temperature and on the surface chemistry of the particulate phase [39].

Nogi *et al.* [40], in 2005, used bacterial cellulose nanofibres to reinforce transparent polymers. The composites exhibited a highly luminous transmittance at a fibre content as high as 60 wt%, and a low sensitivity to matrices with a variety of refractive indices. The optical transparency was also insensitive to temperature increases up to 80°C.

In a recent original contribution to this topic, Brown and Laborie [41] prepared finely dispersed nanocomposites of bacterial cellulose in poly(ethylene oxide) by introducing the latter polymer in the former growth medium. This integrated manufacturing approach opens a novel promising route to fibre-reinforced nanocomposites based on bacterial cellulose.

17.4.8 Electronic paper

The transparency, paper-like appearance and unique microfibrillar nanostructure of bacterial cellulose sheets are characteristics that were taken into account by Shah and Brown Jr. [42], to propose the use of this material as electronic paper in 2005. The technique involved first making the cellulose sheet electrically conducting (or semiconducting) by depositing ions around the microfibrils to provide conducting pathways and then immobilizing electrochromic dyes within the microstructure. The whole system was then cased between transparent electrodes and upon the application of switching potentials (2–5 V), a reversible colour change was activated, down to a standard pixel-sized area of *ca.* $100\,\mu m^2$. Using a standard backplane or an in-plane drive circuit, a high-resolution dynamic display device using bacterial cellulose as a substrate could thus be constructed. The major advantages of

such a device are its high paper-like reflectivity, flexibility, contrast and biodegradability and its potential applications could extend to e-book tablets, e-newspapers, dynamic wall papers, rewritable maps and learning tools.

17.4.9 Fuel cell membranes

Chemically modified bacterial cellulose also finds applications in electric power generation. Bacterial cellulose has the ability to catalyze the precipitation of palladium within its structure to generate a high surface area with catalytic potential [43]. Palladium-bacterial cellulose could have applications in the manufacture of both electrical and electronic devices. Since bacterial cellulose fibrils are extruded by the bacterium and then self-assemble to form a three-dimensional network structure that resembles a sponge, its physical morphology is therefore compatible with polyelectrolyte membrane technology and fuel cell development. The palladium-cellulose can be combined with enzymes immobilized in cellulose membranes for the design of biosensors and biofuel cells. The work of Evans *et al*. [43] suggests that bacterial cellulose possesses reducing groups capable of initiating the precipitation of palladium, gold and silver from aqueous solutions. Since the bacterial cellulose contained water equivalent to at least 200 times its dry weight, they dried it to a thin foil, suitable for the construction of membrane electrode assemblies. Results with palladium-cellulose showed that it was capable of catalyzing the generation of hydrogen, when incubated with sodium dithionite and generated an electrical current from hydrogen in a membrane electrode assembly containing native cellulose as the polyelectrolyte membrane. The advantages of using native and metallized bacterial cellulose membranes over other polyelectrolyte membranes such as Nafion 117®, include their higher thermal stability and lower gas crossover.

17.5 CONCLUSIONS

Although it is a reality for medical applications and exotic desserts, bacterial cellulose is still only a potential promise for other applications. This is partly due to the absence of overproducer strains, which can supply the demand for this raw material. The global production is considered small and it is made up of producing companies in Brazil, farmers in the Asian southeast and some research laboratories in Europe and the USA. Cheng *et al*. [10] published in 2002 a study for the production of bacterial cellulose pellets in airlift bioreactors. Based on their data, it would be possible to produce 1 ton of pure bacterial cellulose in a facility comprising 130 airlift bioreactors of 1 000 L capacity each, within 72 h. That pure cellulose could be used to substitute plant cellulose for papermaking. The environmental implications would be tremendous in terms of both the decrease in CO_2 emissions and the preservation of reforestry. That may be possible in the future, where genetically modified strains will produce a white and gelatinous forest.

ACKNOWLEDGEMENTS

We thank *Bionext® Produtos Biotecnológicos* and the Brazilian research agencies FAPESP and CNPq for financial support. E.P. acknowledges *Bionext* for a research grant.

REFERENCES

1. Steinbüchel A., Doi Y., *Biotechnology of Biopolymers*, Wiley-VCH Verlag, Weinheim, 2005, p. 381.
2. Brown A.J., On an acetic ferment that forms cellulose, *J. Chem. Soc.*, **49**, 1886, 172.
3. Brown A.J., The chemical action of pure cultivation of bacterium aceti, *J. Chem. Soc.*, **49**, 1886, 232.
4. Delmer D.P., Cellulose biosynthesis: Exciting times for a difficult field of study, *Annu. Rev. Plant Physiol. Plant Mol. Biol.*, **50**, 1999, 245.
5. Klemm D., Schumann D., Udhardt U., Marsch S., Bacterial synthesized cellulose – Artificial blood vessels for microsurgery, *Prog. Polym. Sci.*, **26**, 2001, 1561.
6. Hirai A., Tsuji M., Horii F., TEM study of band-like cellulose assemblies produced by *Acetobacter xylinum* at 4°C, *Cellulose*, **9**, 2002, 105.
7. Saxena I.M., Brown Jr. M., Cellulose biosynthesis: Current views and evolving concepts, *Ann. Bot.*, **96**, 2005, 9.
8. Iguchi M., Yamanaka S., Budhiono A., Bacterial Cellulose – A masterpiece of nature's arts, *J. Mater. Sci.*, **35**, 2000, 261.
9. Borzani W., de Souza S., Mechanism of the film thickness increasing during the bacterial producing of cellulose on non-agitated liquid media, *Biotechnol. Lett.*, **17**(11), 1995, 1271.

10. Cheng H.P., Wang P.M., Chen J.W., Wu W.T., Cultivation of *Acetobacter xylinum* for bacterial cellulose production in a modified airlift reactor, *Biotechnol. Appl. Biochem.*, **35**, 2002, 125.
11. Shawn D., Meder R., Cellulose hydrolysis – The role of monocomponent cellulases in crystalline cellulose degradation, *Cellulose*, **10**, 2003, 159.
12. Atalla R.H., van der Hart D.L., Native cellulose – A composite of two distinct crystalline forms, *Science*, **223**, 1984, 283.
13. Heinze T., Liebert T., Unconventional methods in cellulose functionalization, *Prog. Polym. Sci.*, **26**, 2001, 1689.
14. Greiner A., Hou H., Reuning A., Thomas A., Wendorff J.H., Zimmermann S., Synthesis and opto-electronic properties of cholesteric cellulose esters, *Cellulose*, **10**, 2003, 37.
15. Klemm D., Heublein B., Fink H-P., Bohn A., Cellulose: Fascinating biopolymer and sustainable raw material, *Angew. Chem. Int. Ed.*, **44**, 2005, 3358.
16. Zhbankov R.G., *Infrared Spectra of Cellulose and Its Derivates*, Consultants Bureau, New York, 1966, p. 304.
17. Wada M., Okano T., Sugiyama J., Allomorphs of native crystalline cellulose I evaluated by two equatorial d-spacings, *J. Wood Sci.*, **47**, 2001, 124.
18. Brown R.M., Cellulose structure and biosynthesis: What is in store for the 21st century?, *J. Polym. Sci.*, **A42**, 2004, 487.
19. Wada M., Sugiyama J., Okano T., Native celluloses on the basis of two crystalline phase (Ia/Ib) system, *J. Appl. Polym. Sci.*, **49**, 1993, 1491.
20. Ruland W., X-ray determination of crystallinity and diffuse disorder scattering, *Acta Crystallogr.*, **14**, 1961, 1180.
21. US Patent, 4,891,317, 1990.
22. Yamanaka S., Watanabe K., Applications of bacterial cellulose, in *Cellulosic Polymers – Blends and Composites*, Ed.: Gilbert R., Hanser Gardner, München, 1994, p. 207.
23. Czaja W.K., Young D.J., Kawecki M., Brown Jr. R.M., The future prospects of microbial cellulose in biomedical applications, *Biomacromolecule*, **8**, 2007, 1.
24. http://www.filipinovegetarianrecipe.com/fruit_preserves/nata_de_coco.htm (accessed 11-2006).
25. US Patent 4,655,758, 1987; 4,588,400, 1986.
26. http://www.fibrocel.com.br/ (accessed 11/2006).
27. Legeza V.I., Galenko-Yaroshevskii V.P., Zinov'ev E.V., Paramonov B.A., Kreichman G.S., Turkovskii I.I., Gumenyuk E.S., Karnovich A.G., Khripunov A.K., Effects of new wound dressings on healing of thermal burns of the skin in acute radiation disease, *Bull. Exp. Biol. Med.*, **138**, 2004, 331.
28. Novaes Jr. A.B., Novaes A.B., IMZ implants placed into extraction sockets in association with membrane therapy (Gengiflex) and porous hydroxyapatite: A case report, *Int. J. Oral Maxillofac. Implants*, **7**, 1992, 536.
29. Salata L.A., Craig G.T., Brook I.M., *In vivo* evaluation of a new membrane (gengiflex) for guided bone regeneration (GBR), in *Meeting of the British Society for Dental Research*, 1995, Manchester. *J. Dent. Res.*, **74**, 1995, 825.
30. Dahlin C., Linde A., Gottlow J., Nyman S., Healing of bone defects by guided tissue regeneration, *Plast. Reconstr. Surg.*, **81**, 1988, 672.
31. Macedo N.L., Matuda F.S., Macedo L.G.S., Monteiro A.S.F., Valera M.C., Carvalho Y.R., Evaluation of two membranes in guided bone tissue regeneration: Histological study in rabbits, *Braz. J. Oral Sci.*, **3**, 2004, 395.
32. Tabuchi M., Baba Y., Design for DNA separation medium using bacterial cellulose fibrils, *Anal. Chem.*, **77**, 2005, 7090.
33. Volkmuth W.D., Austin R.H., DNA electrophoresis in microlithographic arrays, *Nature*, **358**, 1992, 600.
34. Han J., Craighead H.G., Separation of long DNA molecules in a microfabricated entropic trap array, *Science*, **288**, 2000, 1026.
35. Hung L.R., Tegenfeldt J.O., Kraeft J.J., Strum J.C., Austin R.H., Cox E.C., A DNA prism for high-speed continuous fractionation of large DNA molecules, *Nat. Biotechnol.*, **20**, 2002, 1048.
36. Doyle P.S., Bibette J., Bancaud A.J.-L., Self-assembled magnetic matrices for DNA separation chips, *Science*, **295**, 2002, 2237.
37. Tabuchi M., Ueda M., Kaji N., Yamasaki Y., Nagasaki Y., Yoshikawa K., Kataoka K., Baba Y., Nanospheres for DNA separation chips, *Nat. Biotechnol.*, **22**, 2004, 337.
38. Pandey L.K., Saxena C., Dubey V., Studies on pervaporative characteristics of bacterial cellulose membrane, *Separation and Purification Technology*, **42**, 2005, 213.
39. Grunert M., Winter W.T., Progress in the development of cellulose-reinforced nanocomposites, *Abstr. Pap. Am. Chem. Soc.*, **219**, 2000. 126-PMSE Part 2, MAR 26.
40. Nogi M., Handa K., Nakagaito A.N., Yano H., Optically transparent bionanofiber composites with low sensitivity to refractive index of the polymer matrix, *Appl. Phys. Lett.*, **87**, 2005, 243110.
41. Brown E.E., Laborie M.-P.G., Bioengineering bacterial cellulose/poly(ethylene oxide) nanocomposites, *Biomacromolecules*, **8**, 2007, 3074.
42. Shah J., Brown Jr. R.M., Towards electronic paper displays made from microbial cellulose, *Appl. Microbiol. Biotechnol.*, **66**, 2005, 352.
43. Evans B.R., O'Neill H.M., Malyvanh V.P., Lee I., Woodward J., Palladium-bacterial cellulose membranes for fuel cells, *Biosens. Bioelectron.*, **18**, 2003, 917.

This page is intentionally left blank.

– 18 –

Surface Modification of Cellulose Fibres

Mohamed Naceur Belgacem and Alessandro Gandini

ABSTRACT

This chapter describes the most recent contributions to the realm of cellulose fibre modification, starting with a brief description of the materials and characterization techniques used in this context. The surface modification strategies are then reviewed, including the coupling with acids and anhydrides, the grafting with siloxanes, isocyanates and the grafting-from *via* free-radical initiation or ring opening polymerization, as well as the surface activation of the fibres by physical agents. The modification by admicellar configurations, the preparation of cellulose–inorganic particle hybrid materials and self-reinforced composites, are also discussed. All systems are assessed in terms of the specific type of application envisaged for the modified fibres, namely (i) as reinforcing elements in macromolecular matrices (composite materials); (ii) in textiles and (iii) for trapping organic pollutants.

Keywords

Surface modification, Cellulose fibres, Coupling by esterification, Grafting with siloxanes, Coupling by isocyanates, Grafting-from *via* free-radical initiation, Grafting-from *via* ring opening polymerization, Treatment with high energy sources, Modification by admicellar sleeving, Cellulose–inorganic hybrids, Self-reinforced composites

18.1 INTRODUCTION

The use of cellulose fibres in innovative areas of materials science has recently gained considerable attention because of three potential advantages they possess, namely: (i) their biorenewable character, (ii) their ubiquitous availability in a variety of forms, and (iii) their low cost. Cellulose fibres have been used for centuries in traditional industries, such as papermaking and textile in which they are used as a source of materials and medicine and analytical applications where they are employed as aids, excipients and column fillers among other applications. A recent addition to these numerous realms has concerned their surface modification aimed at extending their use to such novel fields as (i) reinforcing elements in macromolecular composite materials [1–5], replacing glass fibres; (ii) pollutant traps for organic molecules in a water medium [6–11]; (iii) metal-coated and magnetically active materials for microwave technologies [12, 13], (iv) conducting and photo-luminescent materials for electronic and optoelectronic devices [14–17], etc.

The driving forces related to the use of cellulose fibres in these new fields of applications resides additionally in the ease with which they can be recycled at the end of their life cycle, whether through their actual re-employment, or through combustion (energy recovery). Finally, cellulose fibres possess additional advantages like low density and modest abrasive impact.

The term ‘functionalization of cellulose fibres’, as used in this chapter, describes the grafting of new chemical groups at the surface or within a limited depth, in order to generate novel specific properties compared with

those of the pristine material. The chemical entities involved in these transformations are predominantly the cellulose OH groups, which have also been exploited for their bulk modifications, not only in traditional processes like the synthesis of esters and ethers, but also for the preparation of new derivatives, as described in Chapter 16. The fundamental difference between bulk and surface treatments is not to be found in the underlying chemistry, but instead in the fact that the former leads to a radical transformation of the entire fibre, which almost always destroys its morphology and semi-crystalline phase, whereas the latter maintains these features virtually intact, except for a very thin outer layer whose thickness can vary from a few nanometres to a few micrometres. An extended meaning of this term includes the attachment of nanoparticles or macromolecules at the surface of the fibres through physico-chemical interactions.

The purpose of this chapter is to deal with the surface modification of cellulose fibres in order to provide them with specific functionalities, so that they can play determining roles in such applications as reinforcing elements for composite materials, self-contained composite structures, anti-pollution aids, hybrid materials, superhydrophobic surfaces and conductive and magnetic materials. Other types of surface modifications, such as those associated with dying or the manufacture of chromosorb, enzymatic and ion-exchange supports, fall outside the scope of this review. Within the structure of this book, this chapter constitutes in many ways a bridge between the chemistry associated with bulk modification treated in Chapter 16 and the processing and properties of composite materials in Chapter 19, with the addition of more specific aspects.

The surface modification of cellulose fibres, in view of their incorporation into macromolecular matrices in order to produce composite materials, has been extensively reviewed by us in recent years [18,19]. The corresponding materials have also been the subject of recent monographs [1, 5, 20–23] and are thoroughly updated in Chapter 19.

18.2 SUBSTRATES AND METHODS OF CHARACTERIZATION

A wide variety of cellulose fibres, typically going from unmodified wood fibres to very pure cellulose, have been studied in this context, which implies, on the one hand, that the modification might also involve other natural polymers, like lignin and hemicelluloses and, on the other hand, that the actual morphology can influence the kinetics and the extent of the surface modification. More specifically, the choice of materials used includes wood and annual plant fibres, as such or as obtained from delignification and bleaching processes, regular diameter regenerated filled filaments, cellophane films, semi-crystalline powders, commercial Whatman filter paper made of 'pure' cellulose and laboratory-made additive-free tracing paper.

A whole host of characterization techniques have been employed to assess the occurrence and the extent of the modification. These tools include FTIR and XPS spectroscopy, elemental analysis, contact angle measurements, inverse gas chromatography (IGC) and scanning electron microscopy (SEM). New emerging techniques, such as the take-off angle photoelectron spectroscopy, secondary ion mass spectrometry (SIMS), solid state NMR, confocal fluorescence microscopy and atomic force microscopy (AFM) have recently started to be used in this field.

18.3 SURFACE MODIFICATION STRATEGIES

Since this topic was recently reviewed [18, 19], only those past contributions characterized by a qualitative impact will be discussed again, together with the relevant publications which appeared since then.

18.3.1 Coupling with acids and anhydrides

The hydrophobization of cellulose surface was often achieved thanks to the well-known aptitude of cellulose macromolecules to undergo esterification reactions. The main coupling agents used to esterify cellulose using non-swelling solvents, in order to limit the reaction to the fibre's surface, are summarized in Scheme 18.1, namely: the classical acetic anhydride [24] (**I**), alkyl ketene dimer (AKD) **II**, alkenyl succinic anhydride (ASA) **III**, fatty acids (**IV**, with *n* varying from 6 to 22) or their chlorides, poly-(propylene-*graft*-maleic anhydride) (**V**), trifluoroethoxyacetic acid (**VI**) and its anhydride, as well as several other perfluoro-derivatives, pyromellitic anhydride (**VII**), styrene–maleic anhydride copolymer (**VIII**) and methacrylic anhydride (**IX**).

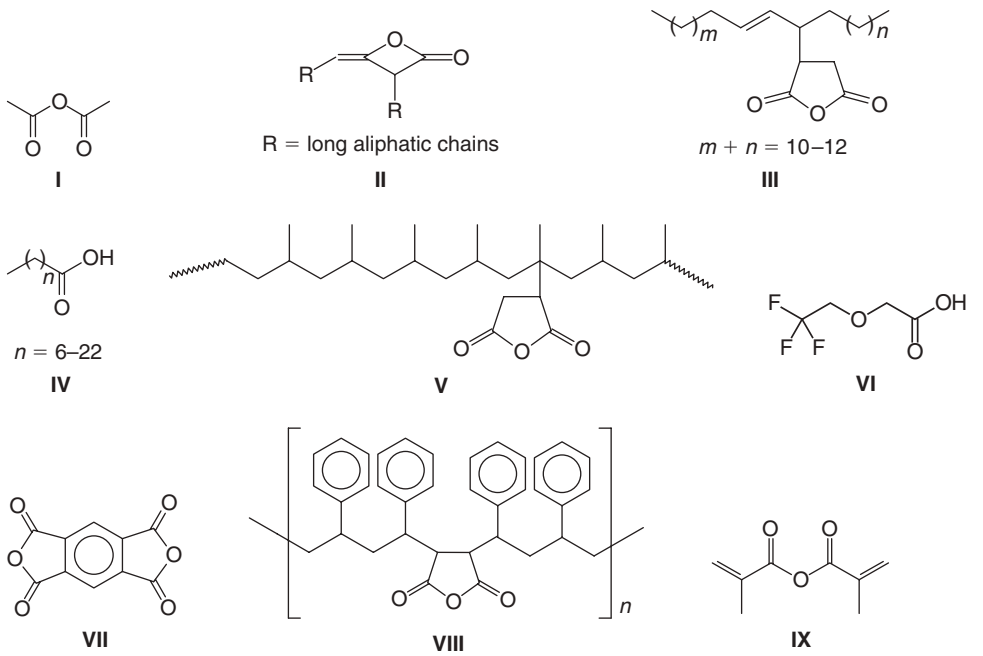

Scheme 18.1

Treating cellulose fibres with coupling agents **II**, **III** and **IV** (with $n = 16$) lowered the dispersive and polar components of the surface energy when the modifications were conducted with emulsions of the coupling agents [25]. This treatment was carried out in order to compatibilize the surface of cellulose fibres with a polypropylene matrix. The same strategy was used to graft cellulose fibres with **III** or **V** [26–30]. The grafting efficiency was assessed by ESCA, FTIR, IGC, SEM and contact angle measurements. The first technique showed that the peaks at 285 and 290 eV, relative to the C—H and O—C═O moieties, respectively, increased after the treatment, particularly with **V**. FTIR showed the appearance of a peak at 1 740 cm^{-1} associated with the ester function. Finally, contact angle measurements showed that a drop of water formed an angle of 140° when deposited onto the surface of **V**-modified cellulose fibres and that the polar contribution to the surface energy decreased significantly, *i.e.* from 43 to 4.9 $mJ\,m^{-2}$ for the most efficient grafting agent, namely **V** with a molecular weight of 39 000 [28]. IGC and SEM corroborated the importance of the modification.

The esterification of cellulose was also carried out using lauric acid (**IV** with $n = 10$) and trifluoroethoxyacetic acid [31]. The occurrence of grafting with the latter reagent was proven by XPS, which showed the presence of a peak at 292.4 eV, assigned to CF_3 moieties and confirmed by IGC data.

Among the more recent contributions to this field, some [32–35] call upon the use of new characterization techniques, like diffuse reflectance infra red fourier transform (DRIFT) and cross polarized magic angle spinning (CP-MAS) ^{13}C-NMR spectroscopy.

The dianhydride **VII** was used to graft cellulose samples in the presence of 4-dimethylaminopyridine as the catalyst [36, 37]. FTIR spectroscopy revealed the presence of peaks at 1 852, 1 785, 1 730 and 1 645 cm^{-1} associated, respectively, with anhydride, ester and carboxylic acid carbonyl functions, proving that only one anhydride group had reacted with the substrate, leaving the other available for further modification (*e.g.* its participation in the growth of a polyester matrix).

Cellulose fibres modified by **I** were characterized by FTIR, SEM and WAXS to prove that the modification had preserved the substrate from structural changes and that the biodegradability of the modified fibres was maintained, albeit at a lower rate [38]. Interestingly, even bacterial cellulose (*Acetobacter xylinum*), an original novel material discussed in Chapter 17, has been submitted to surface modification with **I** [39].

A very recent investigation called upon trifluoroacetic anhydride as the esterification reagent for the surface of cellulose fibres. The reaction was carried out both in the gas [40, 41] and the liquid phase [42]. The presence of the CF_3 groups on the cellulose surface gave rise to very hydrophobic and lipophobic properties [42]. Given the

high sensitivity to hydrolysis of the trifluoroacetate moiety, this modification was shown to be readily reversed by liquid water and even by a moist atmosphere. This peculiar feature has an obvious bearing in the context of applications in which the biphobic character of the fibres' surface only constitutes a temporary requirement, after which the fibres can be readily recycled following rapid hydrolysis.

Nyström *et al*. [43] recently reported the surface modification of cellulose fibres with a long perfluoroalkyl chain, which was appended either directly or through an intermediate layer of OH-bearing polymers. Again, a highly hydrophobic character was obtained, but the authors failed to recognize the hydrolytic sensitivity of the grafted perfluoroester moieties.

18.3.2 Grafting with silane coupling agents

Scheme 18.2 regroups the silane coupling molecules tested to graft cellulose fibres, namely: vinyldimethylethoxyethylsilane (**X**), vinyltrimethoxysilane ($n = 0$) (**XIa**) and vinyltriethoxysilane (n = 1) (**XIb**), γ-glycidylpropyltrimethoxysilane (**XII**), phenyltrimethoxysilane (**XIII**), γ-mercaptopropyltriethoxysilane (**XIV**), hexadecyltrimethoxysilane (**XV**), γ-methacrylopropyltrimethoxysilane (**XVI**), γ-aminopropyltriethoxysilane (**XVII**), (2-aminoethylamino)-propyltriethoxysilane (**XVIII**), 3-(phenylamino)-propyl-triethoxy silane (**XIX**), 3-(2-(2-aminoethylamino)-ethylamino)-propyl-triethoxysilane (**XX**) and cyanoethyltrimethoxysilane (**XXI**).

Although several papers related to the use of silane coupling agents are available in the literature, only few of them deal with a clear-cut proof of the actual occurrence of grafting and with a serious study of the reaction mechanisms involved [18, 19, 44–54]. In fact, the majority of the other studies deal with the use of the addition of a silane coupling agent to the cellulose fibres and their subsequent incorporation into polymeric matrices and evaluate the supposed grafting indirectly by monitoring the changes in the mechanical properties of the ensuing composites.

The more thorough studies showed that, contrary to glass fibre chemistry, (*i.e.*≡Si—OR + ≡Si—OH) the direct condensation reaction between the siloxane alkoxy groups and the cellulose OH functions (≡Si—OR + ≡C—OH, cellulose) *does not occur*, unless traces of water are present to generate Si—OH groups [46, 47, 53]. The occurrence of the condensation of silanol groups with cellulose (≡Si—OH + ≡C—OH, cellulose) was proven by FTIR spectroscopy, (the presence of bands at 1 134 and 1 038 cm^{-1} associated with Si—O—C), XPS spectroscopy (peaks at 102, 150 and 160 eV attributed to Si-signals) and elemental analyses (detection of silicon), but only about above 90°C. Of course, some other typical features, specific to the use of a given siloxane, were

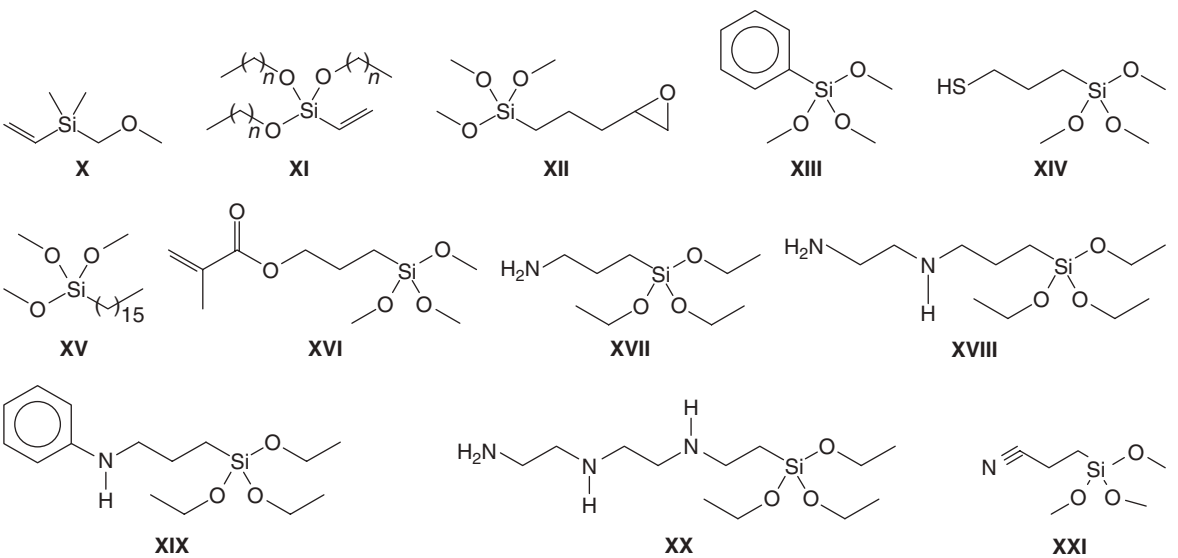

Scheme 18.2

detected in the FTIR spectra, namely peaks at 1 712 and 1 637 cm^{-1}, associated with the presence of C═O and C═C groups, respectively, for methacrylic and vinylic siloxanes [49, 52, 53] and a band at 2 250 cm^{-1} for **XXI**-treated fibres revealed the presence of C≡N groups [53]. The contact angles of a drop of water were also measured in the case of the use of **XV**. The fact that their value increased from 40°, for the pristine cellulose surface to more than a 100°, for the modified surface clearly indicated the efficiency of the coupling [52, 53].

A double-grafting strategy was also applied in this context, consisting in the use of siloxanes bearing a polymerizable function [52, 53]. In this study, **XVI**-modified fibres were 'copolymerized' with styrene (**ST**) or methyl methacrylate (**MMA**) and the ensuing surface energy displayed a negligible polar component, whereas the dispersive component of the fibres, before and after the single and/or double-grafting procedures, remained practically unchanged [52]. With similar systems, **XII**- and **XVII**-modified substrates were subsequently treated with an aliphatic amine and an aliphatic oxirane, respectively, to simulate the formation of an epoxy resin. The ensuing doubly grafted fibres showed the same strong decrease of the polar component of the surface energy, which indicated that the surface had become highly hydrophobic [52].

18.3.3 Coupling with isocyanates

The chemical reaction of isocyanate-bearing molecules with cellulose fibres has been the subject of numerous studies, because urethane formation provides many advantages, namely: (i) relatively high reaction rates, (ii) the absence of elimination products and (iii) the chemical stability of the urethane moiety [18, 19, 36, 55]. The most relevant reagents used in this context are summarized in Scheme 18.3, namely: poly(styrene-*co*-isopropenyl-α-α′-dimethylbenzyl isocyanate) (**XXII**), *O*-(2-isocyanatopropyl-*O′*(methoxy)polyoxypropylene (**XXIII**), **3-**isopropenyl-α-α′-dimethylbenzyl isocyanate (**XXIV**), 2-isocyanatoethyl methacrylate (**XXV**), 1,4-butylenediisocyanate (**XXVI**), 1,4-phenyldiisocyanate (**XXVII**) and 2,4-toluene diisocyanate (**XXVIII**). More reagents were tested, as we recently reported in detail elsewhere [18, 19].

Typically, the reaction of the isocyanate functions with the OH groups of cellulose was assessed by weight gain and FTIR (bands at 3 343 and 1 690 cm^{-1} associated with NH, 1 705 cm^{-1}, attributed to C═O and around 2 900 cm^{-1} relative to aliphatic CH moieties, in the case of long chain aliphatic isocyanate). This evidence was often corroborated by XPS, contact angle measurement and IGC. When the reaction is carried out with stiff molecules bearing two NCO functions [36] or two different functions (an NCO at one end and insaturations at the other) [55], it leaves the second moieties for further exploitation. Thus, the use of reagents **XXIV** and **XXV** was followed by the 'copolymerization' with **MMA** or **ST** which confirmed the occurrence of this double-grafting through the dramatic increase in the water contact angle, the drastic reduction of the polar component of the surface energy and the notable weight gain, after the extraction of the unbound polymer [18, 19]. When the

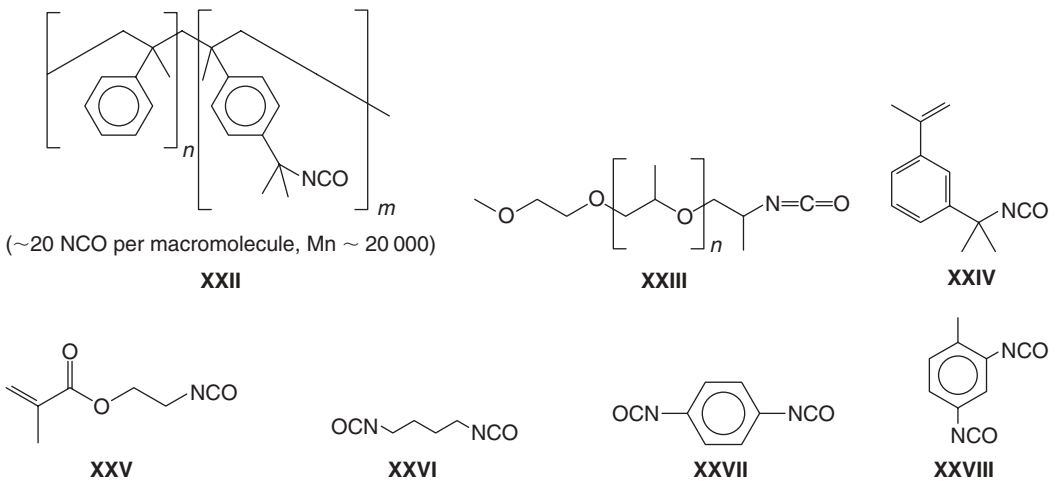

Scheme 18.3

diisocyanate **XXVII** was grafted onto the fibre surface, the remaining NCO group was shown to participate as a comonomer in the growth of a polyurethane matrix around the fibres.

18.3.4 Grafting-from *via* free-radical initiation

For several decades after the Second World War, the direct activation of the surface of cellulose fibres aimed at generating free radicals capable of initiating the polymerization of various monomers in an aqueous medium was the subject of a very large number of studies [56–58]. This 'grafting-from' strategy gave interesting results with several optimized systems, but was never upgraded to an industrial process mainly because of the inevitable formation of appreciable quantities of homopolymers and side reactions which tended to degrade the cellulose macromolecules and discolour the ensuing materials. These classical systems were critically reviewed recently [18].

The recent discovery and rapid progress of controlled radical polymerizations [59], notably atom transfer radical polymerization (ATRP) and reversible addition-fragmentation chain transfer (RAFT), has revived interest in the possibility of grafting different macromolecular structures from the cellulose backbone [43, 60–65].

Most of these recent studies have called upon the ATRP strategy and successfully grafted various polymers on the cellulose surface. An example of this approach is shown in Scheme 18.4 [60, 61], in which 2-bromoisobutyl bromide was made to react with the cellulose surface OH groups before soaking the modified fibres into neat methyl acrylate (**MA**), in the presence of tris(2-dimethylamino)ethyl-amine and CuBr, sacrificial initiator and ethyl acetate. The grafting efficiency was evaluated by weight gain, FTIR and AFM, as shown in Fig. 18.1, which displays the images of filter paper at different grafting stages. The possibility of building grafted block copolymers was also explored and achieved through a second monomer addition, as shown in the last step of Scheme 18.4.

The use of xyloglucan as a molecular anchor constitutes an alternative approach to cellulose grafting through ATRP, as sketched in Scheme 18.5 [65].

The application of the RAFT strategy to induce a grafting-from process applied to cellulose surface has also been recently reported [66]. In this system, the cellulose surface OH groups were converted into thiocarbonyl–thio

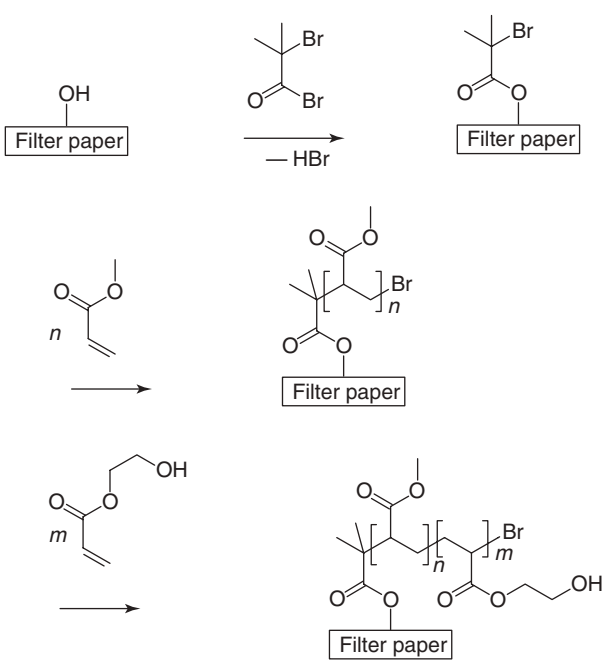

Scheme 18.4

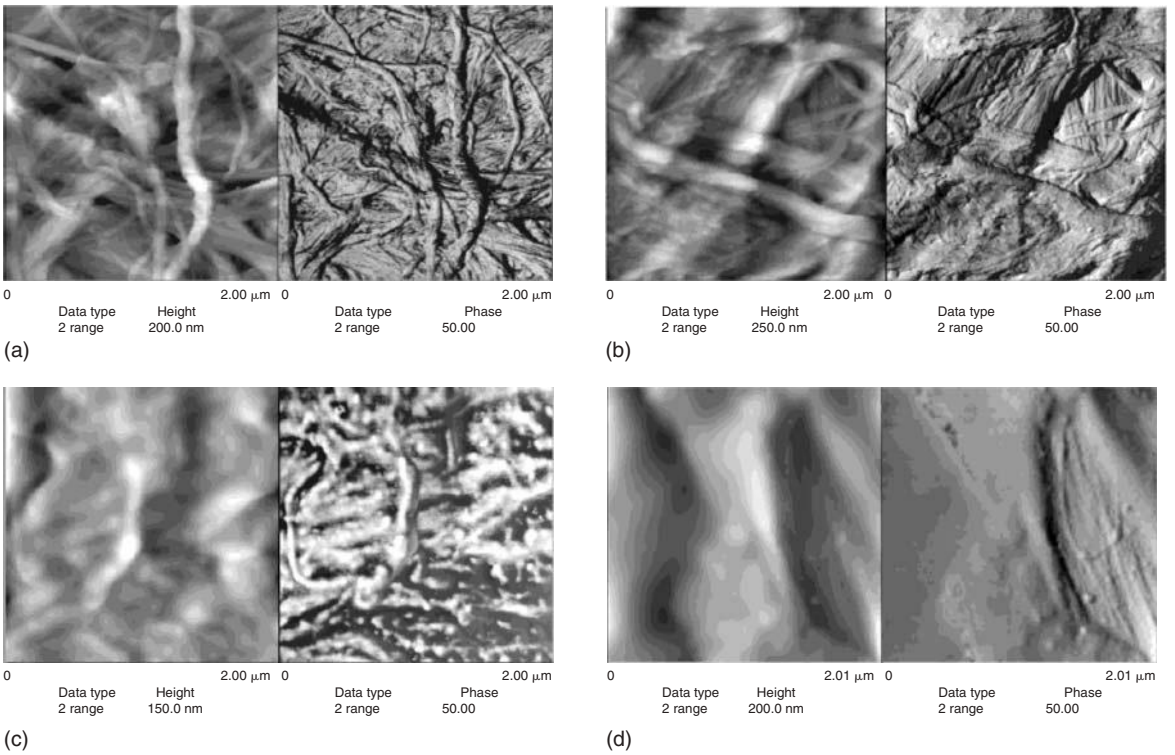

Figure 18.1 AFM-images of (a) virgin filter paper, (b) paper with the grafted initiating moieties, (c) paper grafted with **PMA** and (d) paper grafted with **PMA**-block-**PHEMA**. (Reproduced by permission of the American Chemical Society. Copyright 2003. Reprinted from Reference [61].)

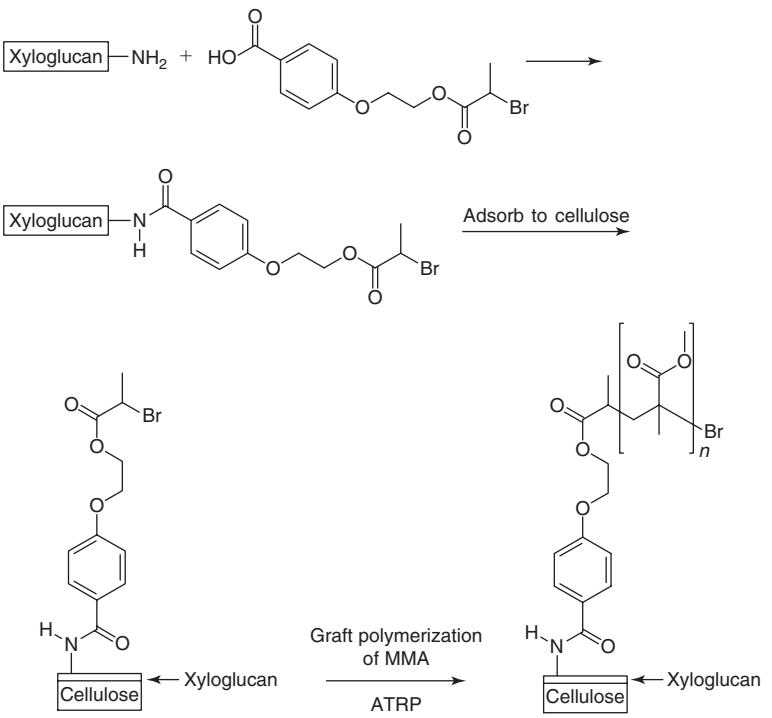

Scheme 18.5

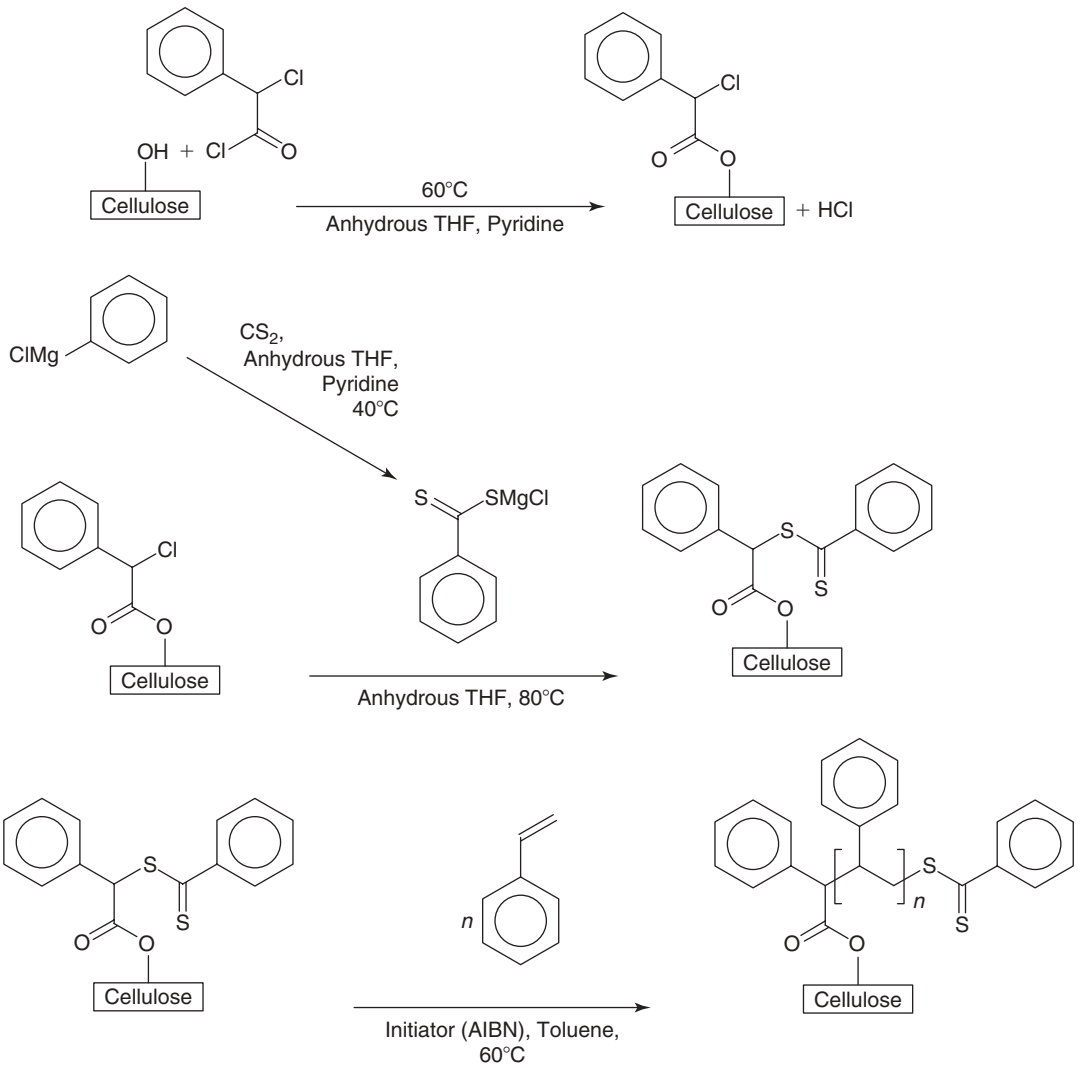

Scheme 18.6

moieties, to be used as mediators for the RAFT polymerization of **ST**, as seen in Scheme 18.6. Clear-cut proof of the successful grafting was provided by several pieces of evidence.

An alternative way to achieve this goal has recently been proposed [67–69]. It calls upon the oxidation of the fibre surface with sodium periodate and the subsequent UV photolysis of the ensuing moieties in the presence of conventional monomers, so that the free radicals generated by the cleavage of the oxidized structures can initiate their polymerization. This approach gave interesting results although the oxidation procedure was found to degrade considerably the cellulose macromolecules.

18.3.5 Grafting-from *via* ring opening polymerization

Chain extension reactions based on the activation of the cellulose surface aimed at provoking the grafting-from through the ring opening polymerization of heterocyclic monomers have been practiced industrially in the specific instance of the synthesis of hydroxypropyl and hydroxyethyl cellulose. The aim of these processes is, however, to

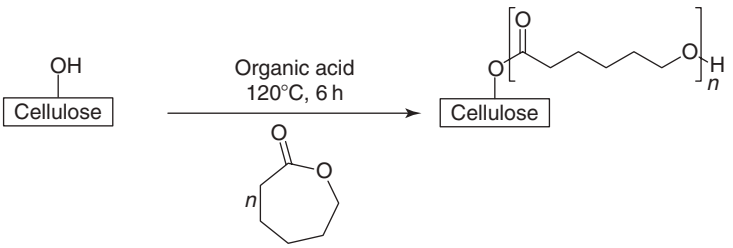

Scheme 18.7

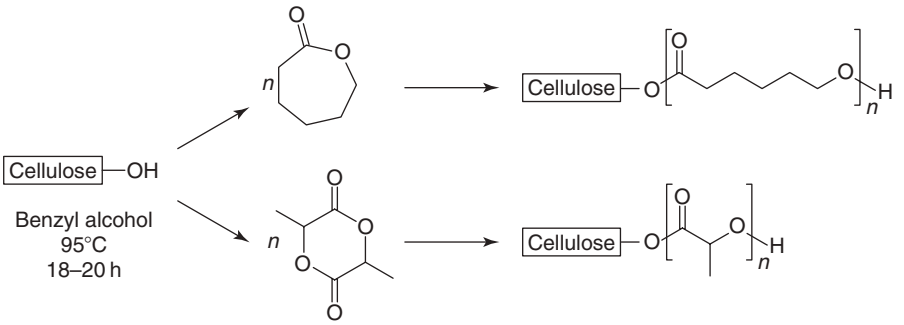

Scheme 18.8

convert the bulk of the fibres and produce novel thermoplastic polymers. A recent modification of this approach describes the partial oxypropylation of cellulose fibres in order to limit their modification to a minimum depth, thus generating a soft sleeve around them [70]. Hot-pressing of these novel materials gives rise to composites in which the matrix is made up of the oligo-(propylene oxide) grafts, and the reinforcing elements are the unmodified inner cores of the fibres. Details of this study are given in Chapter 12, together with similar approaches applied to other natural polymers.

In another vein, Haren and Cordova investigated the grafting of poly-(caprolactone) using an organic acid to activate the cellulose surface, as shown in Scheme 18.7 [71]. Ample evidence was provided for the occurrence of this reaction, which was shown to generate a weight gain of 10 per cent. A similar strategy was adopted in a later study [72] by another group in which, however, benzyl alcohol was the activating species and L-lactic acid (**LA**) was also grafted, as shown in Scheme 18.8.

Surprisingly, a water contact angle of about 110° was measured at the surface of these modified fibres, *viz.* a value which seems exceedingly high considering the structure of the grafts with their terminal OH groups. In the same publication, two other approaches were tackled in order to graft the same monomers, but through different initiation mechanisms, which provided a multiplication of the OH groups of cellulose.

Henequen microfibres were treated with two different epoxides (1,2-epoxy-5-hexene and 1,2-epoxy-5-octene), in order to append insaturations at their surface, which were then used as potential comonomer units when acrylic acid was polymerized in their presence [73]. The ensuing materials displayed a substantial increase in water absorption given the well-known hydrophilic character of acrylic acid.

18.3.6 Grafting by electrical discharges and irradiation techniques

Corona, dielectric barrier and plasma discharges, and, more recently, laser, γ-ray and vacuum UV irradiations, have been used to modify the surface of cellulose fibres. This topic was recently reviewed [18] and here we will limit our coverage to the most significant results and to an update of recent contributions.

XPS analysis showed that corona treatment oxidizes the surface of cellulose fibres [74, 75]. Thus, for example, for filter paper, regenerated cellulose films and pulps, a corona discharge induced the formation of 6.8, 1.5 and 2.1

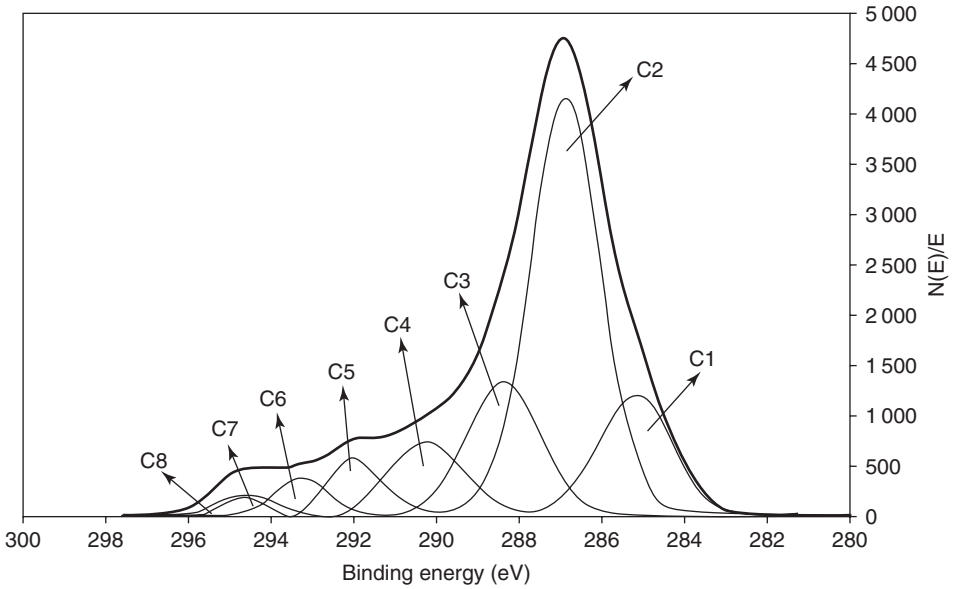

Figure 18.2 C_{1s} XPS spectra of paper (wire side) treated with RF–CF_4 plasma ($P = 300$ W, $t = 10$ min, $p = 300$ mTorr). (Reproduced by permission of Elsevier. Copyright 2007. Reprinted from Reference [80].)

carboxyl groups, respectively, per hundred sugar residues. An increase in both the acidic character of the surface and the dispersive energy was also established, as determined from contact angle, capillarity and IGC measurements. The increase of the dispersive energy indicated that a sort of purification of the surface took place, since there was a removal of low molecular weight substances (extractives and lignin fragments), as confirmed by XPS analysis. The electrical conductance and pH of the water suspensions of the treated fibres confirmed the formation of COOH groups.

The use of cold-plasma can be applied to modify the fibres' surface properties in two opposite directions, namely an increase in the hydrophilic character when the treatment is carried out in Argon or air [18, 76] and, on the contrary, the formation of a super-hydrophobic surface when fluorinated gases are used [18, 77–80]. A very recent publication illustrates clearly the latter approach [80]. In this study, paper sheets were plasma irradiated in the presence of CF_4 and the surface modification characterized by XPS, ATR–FTIR as a function of the power parameters and the CF_4 pressure. Interestingly, no significant difference was observed in the extent of modification to either side of the sheet. Figure 18.2 shows a typical XPS spectrum of one of these modified surfaces.

The laser treatment of cellulose surfaces is a very recent topic [81–84]. Kolar *et al*. [81] were the first to irradiate cellulose fibres and papers with both an excimer laser at 308 nm and a Nd:YAG laser at 532 nm, with the purpose of cleaning their surfaces. The use of the shorter wavelength, however, also induced some cellulose degradation. In a later study, the use of a Nd:YAG pulsed laser at 1 064 nm showed that pure microcrystalline cellulose was unaffected by the treatment [82]. This observation was challenged by a later investigation [83] which showed that the same irradiation conditions led to the surface chemical modifications of various cellulose samples, similar to those associated with thermal degradation of this natural polymer.

The effect of other excimer lasers (ArF, KrF and XeCl with wavelengths of 193, 248 and 308 nm, respectively) has also been studied on rayon [84]. The treatment at 193 nm induced significant changes in the cloth surface, as shown by cracks detected by SEM micrographs and an increase in oxidized moieties detected by XPS.

To the best of our knowledge, only one study has been published on the effect of vacuum UV irradiation on cellulose surfaces [85]. It was found that significant oxidation reactions took place (Fig. 18.3), whose effect was similar to that of strong chemical attacks, (*e.g*. chromic or nitric acid).

The γ-irradiation of cellulose in the atmosphere associates oxidation and degradation mechanisms, as one would expect from the particularly high energy involved. A recent investigation has also shown that this type of treatment favours some cellulose crosslinking [86, 87], as well as a decrease in crystallinity accompanied by thermal degradation, whose extent increases with increasing irradiation doses [88].

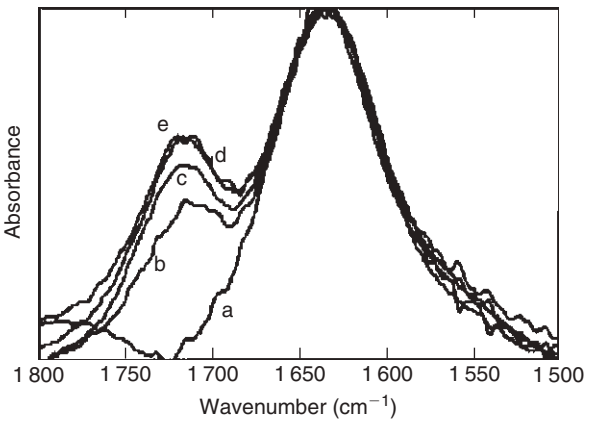

Figure 18.3 IR spectra of rayon fabrics irradiated with Vacuum UV for (a) 0, (b) 5, (c) 15, (d) 40 and (e) 60 min. (Reproduced by permission of Wiley and Sons, Inc. Copyright 1999. Reprinted from Reference [85].)

18.3.7 Modification by admicellar configurations

Boufi *et al.* have recently tackled in a systematic fashion the formation of admicelles around cellulose fibres using cationic surfactants [6–10] or fatty-esterified surfaces [11]. The purpose of this strategy is to exploit these admicellar sleeves as hydrophobic reservoirs for water-insoluble organic molecules. The first study of this series [6] made use of the admicelles to adsorb alkenyl monomers, which were then polymerized, thus generating a hydrophobic polymer sleeve around the fibres.

Subsequent investigations [7–10] were aimed, on the one hand, at enhancing the extent of admicellization by increasing the density of carboxylate groups along the fibres through TEMPO-mediated oxidations and, on the other hand, at studying quantitatively the adsorption of various organic compounds inside the admicelles. Table 18.1 gives the maximum adsorbed quantity of water-insoluble organic compounds as a function of the nature of the surfactant or the presence of the fatty acid graft.

The most relevant conclusions gathered from this ongoing investigation can be summarized as follows:

- The amount of adsorbed cationic surfactants increases with increasing cellulose surface charge, as shown in Fig. 18.4.
- Different water-insoluble organic pollutants can be successfully sucked into the admicelles by adsolubilization.

Table 18.1

Adsolubilization of organic compounds on cellulose fibres bearing surface admicelles or grafted hydrophobic chains

Organic solute	$C_{max.adsol}$ (μmol/g)		
	Cationic surfactant C18 [7, 8]	Anionic surfactant C18 [9]	Chemically grafted C12 [11]
Benzene	390–396	–	–
Naphthalene	304–295	–	–
Chlorobenzene	310–336	300	190
1,3,5-Trichlorobenzene	185–187	–	470
Nitrobenzene	194–223	340	150
2-Naphthol	290–295	660	320
Quinoline	202–374	–	330
2-Chlorophenol	169	–	–
1,4-Dichlorobenzene	223	296	250
Aniline	368	–	–
Diphenylmethane	232	410	–

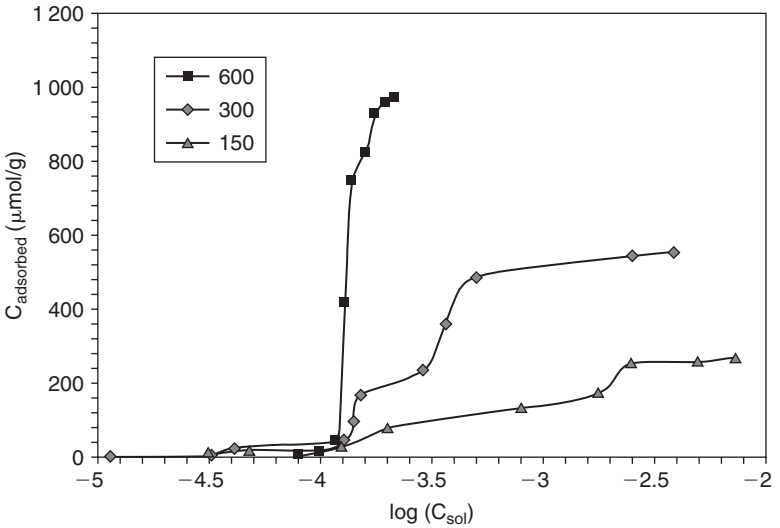

Figure 18.4 Adsorption isotherm of the C16 cationic surfactant onto oxidized cellulose fibres, as a function of the cellulose charge density, expressed in μmol/g. (Reproduced by permission of the American Chemical Society. Copyright 2005. Reprinted from Reference [10].)

- The longer the hydrophobic tail of the surfactant, the better the adsolubilization capacity of the modified surface. Thus, for example, the maximum adsolubilized quantities of 2-naphtol were 290, 180, 140 and 120 μmol/g for C18-, C16-, C14- and C12-based admicelles, respectively.
- The preliminary adsorption of cationic polyelectrolytes at the cellulose surface allowed anionic surfactants to be adsorbed at the fibre surface and form the corresponding admicelles [9].

The adsorbed surfactant molecules were found to desorb from the cellulose surface during the recycling of the substrate [7–10]. This drawback was overcome by joining the aliphatic chains chemically to the cellulose surface by esterification with fatty acid chlorides [11]. Thus, the substrates could be recycled easily and indefinitely, without any loss of their adsorption capacity.

18.3.8 Modification for advanced technologies

Beneventi *et al*. recently reported the preparation of a cellulose poly(pyrrole) composite generated by the impregnation of the fibres with $FeCl_3$ solution, followed by the *in situ* polymerization of pyrrole [14]. An alternative way of preparing conductive cellulose, based on the incorporation of carbon nanotubes into a cellulose sheet, has also been proposed recently [15, 16].

A different approach aimed at elaborating composite materials for microwave technology called upon the coating of cellulose fibres with a metal like copper [12]. Finally, magnetically active cellulose-based composites have also been described [13] by the incorporation of barium ferrite into a regenerated fibre structure.

In all these investigations, physical interactions between the active charge and the cellulose matrix dominate, rather than actual chemical bonds associated with most of the systems described previously.

18.3.9 Cellulose–inorganic particle hybrid materials

Another new field related to the use of cellulose for high value-added materials concerns the incorporation of inorganic nanoparticles into a cellulose fibre assembly. Three interesting studies are mentioned here in this context, *viz*. (i) the growth of cadmium sulphide (CdS) semi-conducting nanocrystals on the surface of regenerated cellulose fibres [89] and the study of the photoluminescence of the ensuing composite; (ii) the precipitation of titanium dioxide

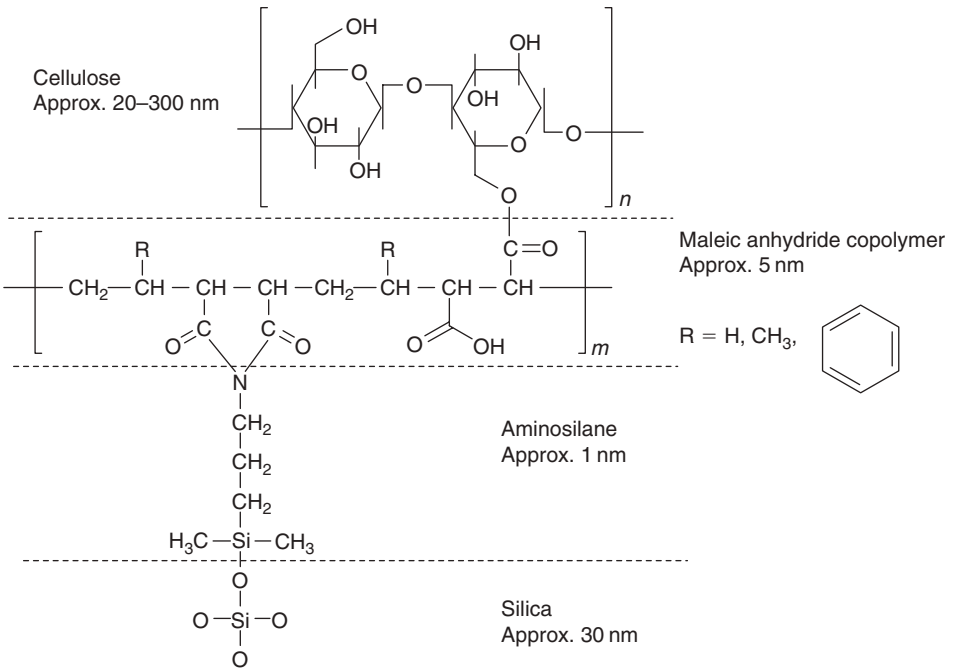

Scheme 18.9

nanoparticles on the surface of Eucalyptus pulp fibres [90], which resulted in a remarkable enhancement of the cellulose optical properties and (iii) the immobilization of cellulose macromolecules onto a silica surface mediated by maleic anhydride copolymers and silane coupling agent 3-aminopropyl-dimethylethoxysilane, as illustrated in Scheme 18.9 [91].

18.3.10 Self-reinforced composites

We already mentioned in Section 3.5 [70] the partial oxypropylation of cellulose fibres and the interest of the ensuing composite materials in which the unmodified fibre cores represent the reinforcing elements and their thermoplastic sleeves the source of a matrix. Other interesting approaches have been recently put forward to prepare composite materials in which cellulose or one of its derivatives prepared *in situ* are the only component. Glasser was the first to tackle this problem through the combination of cellulose esters and fibres by two distinct approaches, *viz.* (i) the incorporation of lyocell fibres into a cellulose acetate matrix [92] and (ii) the partial esterification of wood pulp fibres with *n*-hexanoic anhydride in an organic medium [93] that produced thermally deformable materials in which the thermoplastic cellulose ester constituted the matrix and the unmodified fibres the reinforcing elements.

The latter approach was also applied to the partial benzylation of sisal fibres in an aqueous medium [94]. The isolation, drying and hot-pressing of these benzylated fibres gave materials whose morphology showed features resembling those of a composite material in which the modified cellulose played the role of the thermoplastic matrix.

In another vein, a recent report [95] describes the preparation of an all-cellulose composite by dissolving pretreated ramie fibres in DMAc/LiCl and introducing untreated fibres into the ensuing solution. The composites were then isolated by coagulation with methanol and dried.

18.4 CONCLUSIONS

Together with the other three chapters devoted to cellulose-based materials, this survey has been conceived to emphasize that after a relatively dormant period, the interest in the use of cellulose fibres to participate in the

technological revolution associated with a search of functional materials for highly specific and efficient purposes has became a lively reality. This is true of both the need to replace conventional reinforcing elements for composite materials for ecological and energy reasons, *i.e*. an aspect involving massive quantities of fibres, and the need to prepare high-tech devices in which cellulose-based components, even if only present in modest proportions, play a decisive role.

REFERENCES

1. Eichhorn S.J., Baillie C.A., Zafeiropoulos N., Mwaikambo L.Y., Ansell M.P., Dufresne A., Entwistle K.M., Herraro-Franco P.J., Escamilla G.C., Groom L., Hughes M., Hill C., Rials T.G., Wild P.M., *J. Mater. Sci.*, **36**, 2001, 2107.
2. *Compos. Sci. Technol.*, **63**, 2004. Eco-Composites: A special issue of 14 publications devoted to cellulose-based composite materials.
3. Mohanty A.K., Misra M., Hinrichsen G., *Macromolecular Mater. Eng.*, **1**, 2000, 276–277.
4. Gassan J., Bledzki A.K., *Prog. Polym. Sci.*, **24**, 1999, 221.
5. *Compos. Interface*, **12**, 2005. A special issue devoted to cellulose-based composites.
6. Boufi S., Gandini A., *Cellulose*, **8**, 2001, 303.
7. Aloulou F., Boufi S., Belgacem M.N., Gandini A., *Colloid Polym. Sci.*, **283**, 2004, 344.
8. Aloulou F., Boufi S., Chakchouk M., *Colloid Polym. Sci.*, **282**, 2004, 699.
9. Aloulou F., Boufi S., Beneventi D., *J. Colloid Interface Sci.*, **280**, 2004, 350.
10. Alila S., Boufi S., Belgacem M.N., Beneventi D., *Langmuir*, **21**, 2005, 8106.
11. Boufi S., Belgacem M.N., *Cellulose*, **13**, 2006, 81.
12. Zabetakis D., Dinderman M., Schoen P., *Adv. Mater.*, **17**, 2005, 734.
13. Rubacha M., *J. Appl. Polym. Sci.*, **101**, 2006, 1529.
14. Beneventi D., Alila S., Boufi S., Chaussy D., Nortier P., *Cellulose*, **13**, 2006, 725.
15. Yoon S.H., Jin H.J., Kook M.C., Pyun Y.R., *Biomacromolecules*, **7**, 2006, 1280.
16. Shah J., Brown Jr. R.M., *Appl. Microbiol. Biotechnol.*, **66**, 2005, 352.
17. Ruang D., Huang Q., Zhang L., *Macromol. Mater. Engin.*, **290**, 2005, 1017.
18. Belgacem M.N., Gandini A., *Compos. Interface*, **12**, 2005, 41.
19. Belgacem M.N., Gandini A., Natural Fibre-Surface Modification and Characterisation, in *Cellulose Fibre Reinforced Polymer Composites* (Eds. Sabu T. and Pothan L.), Old City Publishing, 2007. Chapter 3
20. Sabu T., Pothan L., *Cellulose Fibre Reinforced Polymer Composites*, Old City Publishing, 2007.
21. Pandey J.K., Kumar A.P., Misra M., Mohatny A.K., Drzal L.T., Singh R.P., *J. Nanosci. Nanotechnol.*, **5**, 2005, 497.
22. Wool R.P., Sun X.S., *Bio-Based Polymers and Composites*, Elsevier, Amesterdam, 2005. pp. 620.
23. Stevens C.V., Verhé R.G., *Renewable Bioresources: Scope and Modification for Non-Food Applications*, John Wiley & Sons, Ltd, Chichester, 2004. pp. 310.
24. Rowell R.M., *ASC Symp. Ser.*, **476**, 1990, 242.
25. Quilin D.T., Caulfield D.F., Koutsky J.A., *Mat. Res. Soc. Symp. Proc.*, **266**, 1992, 113.
26. Felix J., Gatenholm P., *J. Appl. Polym. Sci.*, **42**, 1991, 609.
27. Klason C., Kubat J., Gatenholm P., *ACS Symp. Ser.*, **489**, 1992, 82.
28. Felix J., Gatenholm P., *J. Appl. Polym. Sci.*, **50**, 1993, 699.
29. Felix J., Gatenholm P., *Nordic Pulp Paper Res. J.*, **2**, 1993, 200.
30. Felix J., Gatenholm P., *Polym. Compos.*, **14**, 1993, 449.
31. Garnier G., Glasser W.G., *Polym. Eng. Sci.*, **36**, 1996, 885.
32. Freire C.S.R., Silvestre A.J.D., Pascoal Neto C., Belgacem M.N., Gandini A., *J. Appl. Polym. Sci.*, **100**, 2006, 1093.
33. Pasquini D., Belgacem M.N., Gandini A., Curvelo A.A.S., *J. Colloid Interface. Sci.*, **295**, 2006, 79.
34. Jandura P., Kokta B.V., Riedl B., *J. Appl. Polymer Sci.*, **78**, 2000, 1354.
35. Freire C.S.R., Silvestre A.J.D., Pascoal Neto C., Gandini A., Fardim P., Holbom B., *J. Colloid Interface Sci.*, **301**, 2006, 205.
36. Gandini A., Botaro V.R., Zeno E., Bach S., *Polym. Int.*, **50**, 2001, 7.
37. Belgacem M.N., Gandini A., *ACS Symp. Ser.*, **945**, 2007, 93.
38. Frisoni G., Baiardo M., Scandola M., Lednicka D., Cnockaert M.C., Mergaert J., Swings J., *Biomacromolecules*, **2**, 2001, 476.
39. Kim D.Y., Nishiyama Y., Kuga S., *Cellulose*, **9**, 2002, 361.
40. Yuan H., Nishiyama Y., Kuga S., *Cellulose*, **12**, 2005, 543.
41. Ostenson M., Järund H., Toriz G., Gatenholm P., *Cellulose*, **13**, 2006, 157.

42. Freire C.S.R., Gandini A., Silvestre A.J.D., Pascoal Neto C., Cunha A.G., *J. Colloid Interface Sci.*, **301**, 2006, 333.
43. Nyström D., Lindqvist J., Ostmark E., Hult A., Malström E., *Chem. Commun.*, **3594**, 2006.
44. Pothan L.A., Bellman C., Kailas L., Sabu T., *J. Adhes. Sci. Technol.*, **16**, 2002, 157.
45. Sreekala M.S., Thomas S., *Compos. Sci. Technol.*, **63**, 2003, 861.
46. Valdez-Gonzalez A., Cervantes-Uc J.M., Olayo R., Herrera-Franco P.J., *Composites, Part B: Engineering*, **30**, 1999, 309.
47. Valdez-Gonzalez A., Cervantes-Uc J.M., Olayo R., Herrera-Franco P.J., *Composites, Part B: Engineering*, **30**, 1999, 321.
48. Matuana L.M., Balatinecz J.J., Park C.B., Sodhi R.N.S., *Wood Sci. Technol.*, **33**, 1999, 259.
49. Redondo S.U.A., Radovanovic E., Gonçalves M.E., Yoshida I.V.P., *J. Appl. Polym. Sci.*, **85**, 2002, 2573.
50. Ahdelmouleh M., Boufi S., Ben Salah A., Belgacem M.N., Gandini A., *Langmuir*, **18**, 2002, 3203.
51. Pickering K.L., Abdalla A., Ji C., McDonald A.G., Franich R.A., *Composites, Part A*, **34**, 2003, 915.
52. Ahdelmouleh M., Boufi S., Ben Salah A., Belgacem M.N., Gandini A., *Int. J. Adhes. Adhes.*, **24**, 2004, 43.
53. Castellano M., Fabbri P., Gandini A., Belgacem M.N., *J. Colloid Interface Sci.*, **273**, 2004, 505.
54. Park B.D., Wi S.G., Lo K.H., Singh A.P., Yoon T.H., Kim Y.S., *Biomass Bioenergy*, **27**, 2004, 353.
55. Botaro V., Gandini A., Belgacem M.N., *J. Thermoplast. Comp. Mater.*, **18**, 2005, 107.
56. Hebeish A., Guthrie J.T., *The Chemistry and Technology of Cellulosic Copolymers*, Springer-Verlag, Berrlin, 1981.
57. Samal R.K., Sahoo P.K., Samantaray H.S., *J. Macromol. Sci., Rev. Macromol. Chem.*, **C26**, 1986, 81.
58. Stannett V.T., Some recent developments in cellulose science and technology in North America, in *Cellulose: Structure and Functional Aspects* (Eds. Kennedy J.P., Phillips G.O. and Williams P.A.), Ellis Horwood, Chichester, UK, 1989, pp. 19–31.
59. Braunecker W.A., Matyjaszewski K., *Prog. Polym. Sci.* **32**, 2007, 93.
60. Carlmark A., Malmström E., *J. Am. Chem. Soc.*, **124**, 2002, 900.
61. Carlmark A., Malmström E., *Biomacromolecules*, **4**, 2003, 1740.
62. Plackett D., Jankova K., Egsgaard H., Hvilsted S., *Biomacromolecules*, **6**, 2005, 2474.
63. Coskun M., Temüz M.M., *Polym. Int.*, **54**, 2005, 342.
64. Bontempo D., Masci G., De Leonardis P., Mannina L., Capitani D., Crescenzi V., *Biomacromolecules*, **54**, 2006, 2474–2784.
65. Zhou Q., Greffe L., Baumann M.J., Malmström E., Teeri T.T., Baumer H., *Macromolecules*, **38**, 2005, 3547.
66. Roy D., Guthrie J.T., Perrier S., *Macromolecules*, **38**, 2005, 10363.
67. Margutti S., Vicini S., Proietti N., Capitani D., Conio G., Pedemonte E., Segre A.L., *Polymer*, **43**, 2002, 6183.
68. Princi E., Vicini S., Proietti N., Capitani D., *Eur. Polym. J.*, **41**, 2005, 1196.
69. Princi E., Vicini S., Pedemonte E., Gentile G., Cocca M., Mastuscelli E., *Eur. Polym. J.*, **42**, 2006, 51.
70. Gandini A., Curvelo A.A.S., Pasquini D., de Menezes A.J., *Polymer*, **46**, 2005, 10611.
71. Harén J., Cordova A., *Macromol. Rapid Commun.*, **26**, 2005, 82.
72. Lonnberg H., Zhou Q., Brumer H., Teeri T.T., Malmström E., Hult A., *Biomacromolecules*, **7**, 2006, 2178.
73. Thompson T.T., Lorià-Bastarrachea M.I., Aguilar-Vega M.J., *Carbohydrate Polym.*, **62**, 2005, 65.
74. Belgacem M.N., Czeremuszkin G., Sapieha S., Gandini A., *Cellulose*, **2**, 1995, 145.
75. Gassan J., Gutowski V.S., Bledzki A.K., *Macromolecular Mater. Eng.*, **283**, 2000, 132.
76. Yuan X., Jayaraman K., Bhattacharyya D., *J. Adhes. Sci. Technol.*, **18**, 2004, 1027.
77. Vander Wielen L.C., Ostenson M., Gatenholm P., Ragauskas A.J., *Carbohydr. Polym.*, **65**, 2006, 179.
78. Sahin H.T., Manolache S., Young R.A., Denes F., *Cellulose*, **9**, 2002, 171.
79. Navarro F., Dávalos F., Denes F., Cruz L.E., Young R.A., Ramos J., *Cellulose*, **10**, 2003, 411.
80. Sahin H.T., *Appl. Surface Sci.*, **253**, 2007, 4367.
81. Kolar J., Strlic M., Müller-Hess D., Gruber A., Troschke K., Pentzien S., Kautek W., *J. Cult. Heritage*, **1**, 2000, S221.
82. Botaro V.R., Santos C.G., Arantes Jr. G., Da Costa A.R., *Appl. Surface Sci.*, **183**, 2001, 120.
83. Strlic M., Kolar J., Vid-Simon S., Marincek M., *Appl. Surf. Sci.*, **207**, 2003, 236.
84. Kensaku M., Masatsugu I., Shunsuke O., Akihiro Y., Akihiko O., Masako S., Takahiro I., Osamu S., *Compos. Interfaces*, **7**, 2001, 497.
85. Koichi K., Victor V.N., Mikhail F.N., Masashi M., Yoshito I., Katsuhiko N., *J. Polym. Sci., Part A: Polym. Chem.*, **37**, 1999, 357.
86. Földváry C., Takács E., Wojnárovits L., *Radiat. Phys. Chem.*, **67**, 2003, 505.
87. Tóth T., Borsa J., Takács E., *Radiat. Phys. Chem.*, **67**, 2003, 513.
88. Khan F., Ahmad S.R., Kronfli E., *Biomacromolecules*, **7**, 2006, 2303.
89. Ruang D., Huang Q., Zhang L., *Macromol. Mater. Engin.*, **290**, 2005, 1017.
90. Marques P.A.A.A., Trindade T., Neto C.P., *Compos. Sci. Technol.*, **66**, 2006, 1038.
91. Freudenberg U., Zschoche S., Simon F., Janke A., Schmidt K., Behrens S.H., AUweter H., Werner C., *Biomacromolecules*, **6**, 2005, 1628.

92. Seavy K.C., Gosh I., Davis R.M., Glasser W.G., *Cellulose*, **8**(161), 2001; Franko A., Seavy K.C., Gumaer J., Glasser W.G., *Cellulose*, **8**(171) 2001.
93. Mutsumura M., Sugiyama J., Glasser W.G., *J. Appl. Polym. Sci.*, **78**(2241) 2000; Mutsumura H., Glasser W.G., *J. Appl. Polym. Sci*., **78**(2254) 2000.
94. Lu X., Zhang M.Q., Rong M.Z., Shi G., Yang G.C., *Compos. Sci. Technol.*, **63**, 2003, 177.
95. Lu X., Zhang M.Q., Rong M.Z., Yue D.L., Yang G.C., *Compos. Sci. Technol.*, **64**, 2004, 1301.

– 19 –

Cellulose-Based Composites and Nanocomposites

Alain Dufresne

ABSTRACT

Environmental issues have recently generated considerable interest in the development of composite materials based on renewable resources such as natural fibres as low cost alternatives for glass fibres. A large number of interesting applications are emerging for these materials. In Europe, the emphasis is on the automotive industry which is looking into the use of plant fibre-based composites as a way to serve the environment and at the same time save weight (and therefore fuel). In North America, wood fibre-based composite building materials have been developing for some time. In India and South America, jute and sugar cane fibres are used in low cost housing. Wherever the industry, there will be a locally grown lignocellulosic fibre to suit the application. In addition, natural fibres present a multi-level organization and consist of several cells formed out of semi-crystalline oriented cellulose microfibrils that open opportunities in the field of nanoscience and nanotechnology.

Keywords

Cellulose, Composites, Nanocomposites, Natural fibres, Lignocellulosic fibres, Cellulose whiskers, Chitin Whiskers, Starch nanocrystals

19.1 INTRODUCTION

Composite materials (or composites for short) are engineered materials made from two or more constituents with significantly different mechanical properties, which remain separate and distinct within the finished structure. There are two categories of constituent materials: matrix and reinforcement. At least one portion of each type is required. The matrix surrounds and supports the reinforcements by maintaining their relative positions. The reinforcements impart special physical (mechanical and electrical) properties to enhance the matrix properties. A synergism produces material properties unavailable from naturally occurring materials. Due to the wide variety of matrixes and reinforcements available, the design potential for composite is huge.

The so-called natural composites like bones and woods are constructed by biological processes. The most primitive man-made composite materials comprised straw and mud in the form of bricks for building constructions. The most advanced examples are used on spacecrafts in highly demanding environments. The most visible applications are pave roadways in the form of either steel and Portland cement concrete or asphalt concrete. Engineered composite materials must be formed to shape. This involves strategically placing the reinforcements while manipulating the matrix properties. A variety of methods are used according to the end-item design requirements. These fabrication methods are commonly named moulding or casting processes, as appropriate, and both have numerous variations. The principle factors impacting the methodology are the nature of the chosen matrix and reinforcement materials. Another important factor is the gross quantity of material to be produced. Large quantities can be used to justify high capital expenditures for rapid and automated manufacturing technology. Small production quantities are accommodated with lower capital expenditures, but higher labour costs at a correspondingly lower rate.

Many commercially produced composites use a polymer matrix often called a resin. The reinforcements are often fibres but also commonly ground minerals. Strong fibres such as fibreglass, quartz, Kevlar or carbon fibres give the composite its tensile strength, while the matrix binds the fibres together, transferring the load from broken fibres to unbroken ones and between fibres that are not oriented along the tension lines. Also, unless the matrix chosen is especially flexible, it prevents the fibres from buckling in compression. In terms of stress, any fibre will provide resistance to tension, the matrix will resist shear, and all materials present will resist compression. Composite materials can be divided into two main categories, normally referred to as short-fibre reinforced materials and continuous-fibre reinforced materials, the latter often constituting a layered or laminated structure. Shocks, impacts, loadings or repeated cyclic stresses can cause the laminate to separate at the interface between two layers, a condition known as delamination. Individual fibres can separate from the matrix through a mechanism called fibre pull-out.

Nanoscience and nanotechnology correspond to science and technology that extend from about 100 nm down to atomic orders of magnitude around 0.2 nm, and to the physical phenomena and material properties observed when operating in this size range. Conceptually, nanocomposites refer to multiphase materials where at least one of the constituent phases has one dimension less than 100 nm. This field has attracted the attention, scrutiny and imagination of both scientific and industrial communities in recent years, and has opened a large window of opportunities to overcome the limitations of traditional micrometre-scale composites. Research in this area is literally exploding, because of the intellectual appeal of building blocks on the nanometre scale and because the technical innovations permit the designing and creation of new materials and structures with unprecedented flexibility, improvements in physical properties and significant industrial impact.

The large interest in the nanoscale range originates from outstanding properties. Enhanced properties can often be reached for low filler volume fraction, without a detrimental effect on other properties such as impact resistance or plastic deformation capability. Though industrial exploitation of nanocomposites is still in its infancy, the rate of technology implementation is increasing.

19.2 NATURAL FIBRES

Agro-based resources, also referred to as lignocellulosics, are resources that contain cellulose, hemicelluloses and lignin. When considering lignocellulosics as possible engineering materials, there are several basic concepts that must be taken into account [1]. First, lignocellulosics are hygroscopic resources that were designed to perform, in nature, in a wet environment. Second, nature is programmed to recycle lignocellulosics in a timely way through biological, thermal, aqueous, photochemical, chemical and mechanical degradation. In simple terms, nature builds a lignocellulosic structure from carbon dioxide and water and has all the tools to recycle it back to the starting chemicals.

There is a wide variety of agro-based or natural fibres to consider for utilization. They can be subdivided based on their origin, viz. vegetable, animal or minerals. Cellulose as a material is used by the natural world in the construction of plants and trees, and by man to make shipping sails, ropes and clothes, to give but a few examples. It is also the major constituent of paper and further processing can be performed to make cellophane and rayon. Depending on the part of the plant from which they are taken, cellulose fibres can be classified as:

- *Grasses and reeds*: The fibres come from the stem of plants, such as bamboo or sugar cane.
- *Leaf or hard fibres*: These fibres are most commonly used as reinforcing agents in polymers. They can be extracted for instance from sisal, henequen, abaca or pineapple.
- *Bast or stem fibres*: These fibres come from the inner bark of the stem of plants. Common examples are jute, flax, hemp, kenaf and ramie.
- *Straw fibres*: Examples include rice, wheat and corn straws.
- *Seed and fruit hairs*: These fibres come from seed-hairs and flosses and are primarily represented by cotton and coconut.
- *Wood fibres*: Examples include maple, yellow poplar and spruce.

In any commercial development, there must be a long-term guaranteed supply of resources. The growing of natural fibres is spread across all five continents. Quality and yield depend on the kind of plant, the grown variety, the soil and the climatic conditions. Tanzania and Brazil are the two largest producers of sisal. Henequen is produced in Mexico, kenaf is grown commercially in the United States and flax is a commodity crop grown in the European Union, as well as in many diverse agricultural systems and environment throughout the world, including Canada,

Table 19.1

Inventory of major potential bast fibre sources for the year 2000/2001 [2]

Fibre source	World production (metric tons)
Jute	2 900 000
Linseed	942 240
Kenaf	470 000
Flax	464 650
Sisal	380 000
Ramie	170 000
Hemp	157 800
Abaca	98 000

Argentina, India and Russia. Hemp originated in Central Asia, from where it spread to China, the Philippines and many other countries. Ramie fibres, mostly available and used in China, Japan and Malaysia, are the longest and one of the strongest textile fibres. The largest producers of jute are India, China and Bangladesh and coir is produced in tropical countries. The price for natural fibre varies depending on the economy of the countries where such fibres are produced. Table 19.1 shows the inventory of some of the larger sources of agricultural bast fibre that could be utilized for fibre–polymer composites. However, only a small part of these fibres has been used for industrial applications up to now, which shows that the potential of the existing bast plants has not yet been exhausted and that huge natural resources are still available.

The traditional source of natural fibres has been wood and for many countries, this will continue to be the case. Other large sources come from recycling agro-fibre-based products such as paper, waste wood and point source agricultural residues. Recycling paper products back into paper requires a wet processing and the removal of inks, salts and adhesives. Recycling the same products into composites can be done by using dry processing whereby all components are incorporated into the composite, eliminating the need of costly separation procedures. The major point source fibres are rice hulls from a rice processing plant, sun flower seed hulls from an oil processing unit and bagasse from a sugar mill.

In order to maintain the high quality of the fibres, their separation from the original plant is best done by retting, scrapping or pulping. Basically, there are two working principles to separate the bast fibres from the wood [3]. The conventional method uses breaking rollers, which alternatingly bend, buckle and soften the stalks. This method requires an intensive retting before processing which is induced by microorganisms that dissolve the lignin and pectins of the stalk. Modern technologies use swing hammer mills in most cases. The fibre decortication is provoked by the impact stress of the hammers directly on the surface of the stalks. This working principle ensures a complete separation of the fibres from the wood, even when processing freshly harvested, non-retted plants. The effective mechanical separation of the fibres and the wood inside the decorticator simplifies the subsequent fibre cleaning. The availability of large quantities of lignocellulosic fibres with well-defined mechanical properties is a general prerequisite for the successful subsequent use of these materials.

Plant fibres are bundles of elongated thick-walled dead plant cells. They are like microscopic tubes, that is cell walls surrounding the centre lumen that contributes to their water uptake behaviour (Fig. 19.1). Natural fibres display

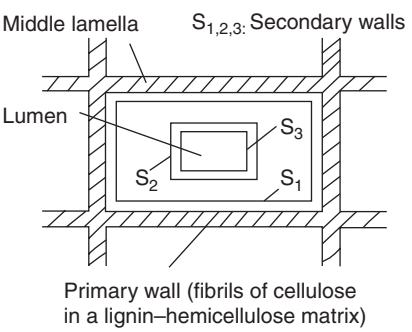

Figure 19.1 Schematic structure of a natural fibre cell. Reproduced with permission from Reference [4].

Table 19.2

Mean chemical composition of some natural fibres [7]

	Cotton	Jute	Flax	Ramie	Sisal
Cellulose	82.7	64.4	64.1	68.6	65.8
Hemicelluloses	5.7	12.0	16.7	13.1	12.0
Pectin	5.7	0.2	1.8	1.9	0.8
Lignin	–	11.8	2.0	0.6	9.9
Water soluble	1.0	1.1	3.9	5.5	1.2
Wax	0.6	0.5	1.5	0.3	0.3
Water	10.0	10.0	10.0	10.0	10.0

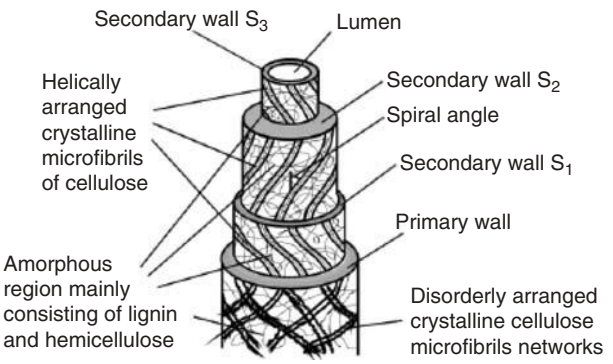

Figure 19.2 Schematic structure of an elementary plant fibre (cell). The secondary cell wall, S2, makes up about 80 per cent of the total thickness. Reproduced with permission from Reference [5].

a multi-level organization and consist of several cells formed out of semi-crystalline oriented cellulose microfibrils connected to a complete layer by lignin, hemicelluloses and in some cases pectins. Climatic conditions, age and digestion process influence not only the structure of the fibres but also their chemical composition. Table 19.2 reports the mean chemical composition of some natural fibres. With the exception of cotton, the components of natural fibres are cellulose, hemicelluloses and lignin, which determine their physical properties. Several of such cellulose–lignin/hemicellulose layers in one primary and three secondary cell walls stick together to form a multiple-layer composite. Such microfibrils have typically a diameter of about 2–20 nm, are made up of 30–100 cellulose macromolecules in extended chain conformation and provide the mechanical strength to the fibre.

The cell walls differ among themselves in their composition and orientation of the cellulose microfibrils. In most plant fibres, these microfibrils are oriented at an angle to the normal axis called the microfibrillar angle (Fig. 19.2). The characteristic value for this structural parameter varies from one plant fibre to another.

The outer cell wall is porous and contains almost all of the non-cellulose compounds, except proteins, inorganic salts and colouring matters and it is this outer cell wall that creates poor absorbency, poor wettability and other undesirable textile properties. In most applications, fibre bundles or strands are used rather than individual fibres. Within each bundle, the fibre cells overlap and are bonded together by pectins that give strength to the bundle as a whole. However, the strength of the bundle structure is significantly lower than that of the individual fibre cell and thus the potential of the individual fibres is not fully exploited.

The properties of natural fibres are strongly influenced by many factors, particularly chemical composition, internal fibre structure, microfibrillar angle, cell dimensions and defects, which differ between different parts of a plant, as well as between different plants. A weak correlation between strength and cellulose content and microfibril or spiral angle is found for different plant fibres. In general, the fibre strength increases with increasing cellulose content and decreasing spiral angle with respect to the fibre axis. This means that the most efficient cellulose fibres are those that have a high cellulose content, coupled with a low microfibril angle. Other factors that may affect the fibre properties are the maturity, the separating process, the microscopic and molecular defects, such as

Table 19.3

Physical properties of some natural fibres. Properties of some synthetic organic and inorganic fibres are added for comparison

Fibre	Density ($g\,cm^{-3}$)	Young's modulus (GPa)	Tensile strength (MPa)	Elongation (%)	Microfibrillar angle (°)
Cotton	1.5	5.5–27.6	300–1 500	3–8	–
Jute	1.3–1.5	13–26.5	393–800	1.2–1.8	8
Flax	1.5	27.6	345–1 500	2.7–3.2	5–10
Hemp	1.5	70	690	1.6	2–6.2
Ramie	1.55	61.4–128	400–938	1.2–3.8	7.5
Sisal	1.45	9.4–22	468–700	2–7	10–22
Coir	1.15–1.46	4–6	130–220	15–40	30–49
Viscose	–	11	593	11.4	–
Soft wood kraft	1.5	40	1 000	–	–
E-glass	2.5	70	2 000–3 500	2.5	–
S-glass	2.5	86	4 570	2.8	–
Aramide	1.4	63–67	3 000–3 150	3.3–3.7	–
Carbon	1.4	230–240	4 000	1.4–1.8	–

pits and knots, the type of soil and the weather conditions under which the vegetable was grown. Differences in fibre structure due to the environmental conditions during growth result in a broad range of characteristics. The mechanical properties of plant fibres are in general much lower when compared to those of the most widely used reinforcing glass fibres (Table 19.3). However, because of their low density, the specific properties which are property-to-density ratio dependent, viz. strength and stiffness, are comparable to those of glass fibres. Thus, natural fibres are in general suitable to reinforce polymer matrices, both thermoplastics and thermosets.

19.3 COMPOSITES

The use of additives in polymers is likely to grow with the introduction of improved compounding technologies and new coupling agents that permit the use of high filler/reinforcement contents. Fillings up to 75 pph could be common in the future and this would have a tremendous impact in lowering the use of petroleum-based polymers [6]. Since the price of plastics has risen sharply over the past few years, adding a natural powder or fibre to them provides a cost reduction to industry (and in some instances increases performance as well). To the agro-based industry, this represents an increased value for the agro-based component. Ideally, of course, a bio-based renewable polymer reinforced with agro-based fibres would be the most environment-friendly material.

Over the past decade there has been a growing interest in the use of lignocellulosic fibres as reinforcing elements in polymeric matrices [7, 8]. A number of researchers have been involved in investigating the exploitation of cellulosic fibres as load bearing constituents in composite materials. Prior work on lignocellulosic fibres in thermoplastics has concentrated on wood-based flour or fibres [9–13]. The majority of these studies has been on polyolefins, mainly polypropylene (PP). Compared to inorganic fillers, the main advantages of lignocellulosics are listed below:

(1) Low density: Their density, around $1.5\,g\,cm^{-3}$, is much lower than that of glass fibres, around $2.5\,g\,cm^{-3}$.
(2) Low cost and low energy consumption.
(3) High specific strength.
(4) Renewability and biodegradability.
(5) Abundant availability in a variety of forms throughout the world.
(6) Flexibility: Unlike brittle fibres, lignocellulosic fibres will not be fractured during processing.
(7) Non-abrasive nature to processing equipment, which allows high filling levels, resulting in significant cost savings and high stiffness properties.
(8) Non-toxicity.
(9) Ease of handling.

(10) Reactive surface, facilitating its chemical modification.
(11) Organic nature, resulting in the possibility to generate energy without residue after incineration at the end of their life-cycle.
(12) Economic development opportunity for non-food farm products in rural areas.

Despite these attractive aspects, lignocellulosic fibres are used only to a limited extent in industrial practice due to difficulties associated with surface interactions. It is important to keep these limitations in perspective when developing end-use applications. The primary drawback of agro-based fibres is associated with their inherent polar nature and the non-polar characteristics of most thermoplastics, which causes difficulties in compounding the filler and the matrix and, therefore, in achieving acceptable dispersion levels, which in turn generates inefficient composites. Another drawback of lignocellulosic fillers is their hydrophilic character which favours moisture absorption with a consequent swelling of the fibres and the decrease in their mechanical properties. Moisture absorption and the corresponding dimensional changes can be largely prevented if the hydrophilic filler is thoroughly encapsulated by the hydrophobic polymer matrix and there is a good adhesion between both components. However, if the adhesion level between the filler and the matrix is not good enough, diffusion pathways for moisture can pre-exist or can be created under mechanical solicitation. The existence of such pathways is also related to the filler connection and therefore to its percolation threshold.

The various approaches to the surface modification of these fibres aimed at minimizing the above drawbacks are thoroughly discussed in Chapter 18.

Yet another limitation associated with the use of lignocellulosic fillers is the fact that the processing temperature of composites must be restricted to just above 200°C (although higher temperatures can be used for short periods of time), because of their susceptibility to degradation and/or the possibility of volatile emissions that could affect the composite properties. This limits the types of thermoplastics that can be used to polymers like polyethylene, PP, poly-vinyl chloride and polystyrene, which constitute, however, about 70 per cent of all industrial thermoplastics. Nevertheless, technical thermoplastics like polyamides, polyesters and polycarbonates, which are usually processed at temperatures higher than 250°C, cannot be envisaged as matrices for these types of composite.

19.4 COMPOSITE PROCESSING

Drying the fibres is an essential prerequisite that must be applied before processing, because water on the fibre surface acts as a separating agent at the fibre–matrix interface. In addition, because of the water evaporation during processing at temperatures higher than 100°C, voids appear in the matrix. Both phenomena obviously lead to a decrease in the mechanical properties of the ensuing composites. Fibre drying can be done under different conditions, which results in different degrees of their residual moisture.

Extrusion and injection-moulding are the economically most attractive processing methods of thermoplastic-based composites. The extrusion press processing (express-processing) has been developed for the production of flax fibre reinforced PP at the research centre of Daimler Benz [7]. In this process, flax fibre non-wovens and PP melt films are alternatively deposited and moulded. A production process for PP semi-products reinforced with lignocellulosic fibres in the form of mats has been developed by BASF AG [7]. Fibre mats are produced by stitching together layers of fibres which have previously been crushed.

Beginning with bakelite in the early 1900s, engineers and scientists have continued to work to improve the various attributes of thermosets through the addition of natural fibres. Unsaturated polyester, epoxy, and vinylester resins are commonly used for preparing such composites. Fabrication techniques suitable for manufacturing natural fibre reinforced thermoset composites include the hand lay-up technique for unidirectional fibres/mats/fabric, and filament winding and pultrusion for continuous fibres. Resin transfer moulding (RTM) and prepegs can also be used. Semi-products, such as sheet moulding compounds (SMC) and bulk moulding compounds (BMC), can be obtained with short and chopped fibres.

19.5 COMPOSITE PROPERTIES

The major factors that govern the properties of short-fibre thermoplastic composites are fibre volume fraction, fibre dispersion, fibre aspect ratio and length distribution, fibre orientation and fibre–matrix adhesion. Each of these parameters is briefly discussed below.

19.5.1 Fibre volume fraction

Like other composite systems, the properties of short-fibre composites are strongly determined by the fibre concentration. The variation of the composite properties with fibre content can be predicted using the rule of mixtures, which involves the extrapolation of both matrix and fibre properties to a fibre volume fraction of 0 and 1. The following criteria must be taken into account:

(1) The composite fracture has to be fibre-controlled.
(2) The modulus of elasticity of the fibre should be greater than that of the matrix.
(3) The strain to failure of the matrix must be greater than that of the fibre.

In the case of unidirectional (or longitudinal) fibre reinforced composites, the stress is transferred from the matrix to the fibre by shear. When stressed in tension, both the fibre and the matrix elongate equally according to the principle of combined action [14]. Hence, the mechanical properties of the composite can be evaluated on the basis of the properties of the individual constituents. For a given elongation of the composite, both constituents, fibre and matrix, may be in elastic deformation; the fibre may be in elastic deformation whereas the matrix may be in plastic deformation, or both the fibre and the matrix may be in plastic deformation (Fig. 19.3).

At low fibre volume fraction, a decrease in the tensile strength is usually observed (Fig. 19.4). This is ascribed to the dilution of the matrix and the introduction of flaws at the fibre ends where a high stress concentration occurs, causing the bond between fibre and matrix to break. At high volume fraction, the stress is more evenly distributed and a reinforcement effect is observed. For all values of strain, the stress value in the composite is given by a simple mixing rule balanced by the volume fraction of each constituent, viz.:

$$\sigma_{\mathrm{c}}^{'} = \sigma_{\mathrm{f}}^{'} V_{\mathrm{f}} + \sigma_{\mathrm{m}}^{'} V_{\mathrm{m}} \tag{19.1}$$

where σ represents the stress value of each component at a particular strain value and V the volume fraction of each component of the composite. The subscripts c, f and m correspond to the composite, the fibre and the matrix, respectively.

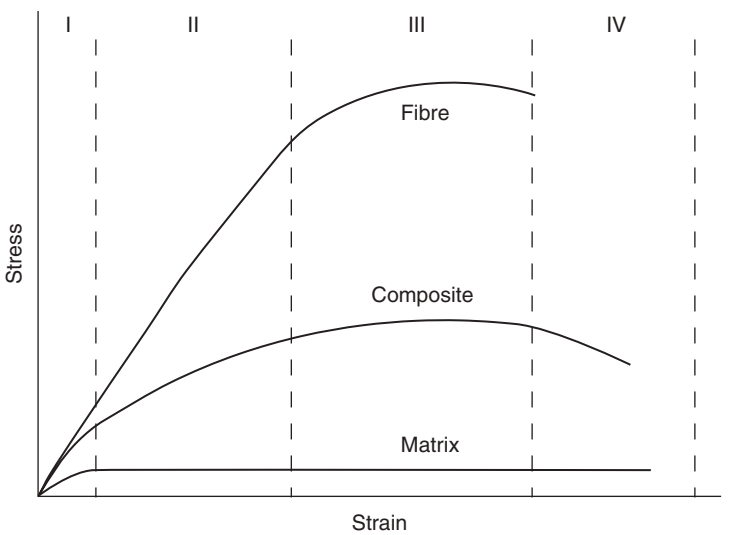

Figure 19.3 Illustration of four stages of deformation of fibres, matrix and composite. Stage I: elastic deformation of both fibres and matrix; stage II: elastic deformation of fibres and plastic deformation of matrix; stage III: plastic deformation of both fibres and matrix; stage IV: failure of both fibres and matrix. Reproduced with permission from Reference [14].

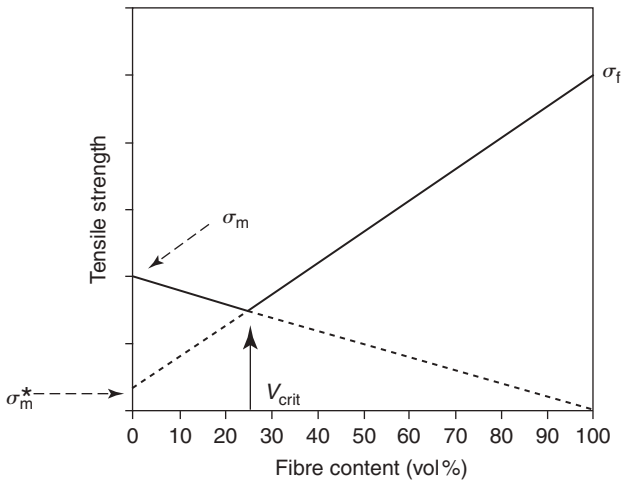

Figure 19.4 Model for the prediction of the ultimate tensile strength of unidirectional fibre-reinforced composites for which the fracture is fibre-controlled.

The fibre volume fraction for which the strength ceases to decrease and begins to increase is called the critical fibre volume fraction, V_{crit}. Below this value, the behaviour of the composite is only governed by the matrix:

$$\begin{aligned} &\text{For } V_f < V_{crit} \qquad \sigma_c = \sigma_m V_m \\ &\text{For } V_f > V_{crit} \qquad \sigma_c = \sigma_f V_f + \sigma_m^* V_m \end{aligned} \tag{19.2}$$

where σ_m is the ultimate tensile strength of the matrix, σ_f is that of the ultimate tensile strength of the fibre and σ_m^* is the stress on the matrix at a strain value where σ_f is reached. V_{crit} is an important parameter because it corresponds to the volume fraction of the fibres above which they begin to strengthen, rather than weaken the matrix. It can be calculated from the following equation:

$$V_{crit} = \frac{\sigma_m - \sigma_m^*}{\sigma_f - \sigma_m^*} \tag{19.3}$$

For a given matrix, the critical fibre volume fraction decreases with the increasing strength of the fibres. This means that for fibres which are much stiffer than the matrix, V_{crit} is very low.

The modulus of elasticity is also an important factor. Within strain limits for which both the fibre and the matrix are in elastic deformation, the modulus of the composite can be calculated using the rule of mixture:

$$E_c = E_f V_f + E_m V_m \tag{19.4}$$

where (Fig. 19.4) E_c, E_f and E_m are the modulus of elasticity of composite, fibre and matrix, respectively. When the fibre is in elastic and the matrix is in plastic deformation, the equation becomes:

$$E_c = E_f V_f + \left(\frac{\sigma_m^*}{\varepsilon}\right) V_m \tag{19.5}$$

The ratio σ_m^*/ε is the slope of the stress–strain curve of the matrix at a given strain beyond the proportional limit of the matrix.

The length of some individual natural fibres can reach up to 4 m, and when bundled with other fibres, this maximum length will be even higher. However, lignocellulosic materials are mainly used as discontinuous short fibres

and are ground into fine particles with relatively low aspect ratios. These fillers generally increase the stiffness of the composites, but the strength is generally lower than that of the pristine matrix [10]. For instance, residual softwood sawdust was used as a reinforcing material in PP [15] and it was found that the tensile strength decreased regularly from 35 MPa for the unfilled matrix down to 10 MPa for the 60 wt% filled system. On the contrary, the addition of henequen fibres to a low density polyethylene matrix increased the tensile strength by 50 per cent (from 9.2 to 14 MPa) at a fibre loading of 30 vol% [16]. At the same time, the modulus increased from 275 to 860 MPa and the strain at break decreased from 42 to 5 per cent. The increase in stiffness results from the fact that lignocellulosic fillers or fibres have a higher Young's modulus, as compared to commodity thermoplastics, thereby contributing to the higher stiffness of the composites. However, an anchoring effect of the lignocellulosic filler acting as nucleating agents for the polymeric chains has been reported [17] resulting in an increase in the degree of crystallinity of the matrix. This effect seems to be strongly influenced by the lignin content and the surface aspect of the fibre [18, 19]. This transcrystallization phenomenon at the fibre–matrix interphase participates in the reinforcing effect of the filler.

In order to use models to estimate composite properties, it is necessary to know the properties of the fibres, which vary widely depending on the source, age, separating techniques, moisture content, speed of testing, history of the fibre, etc. The properties of the individual fibres are therefore very difficult to measure. Moreover, in a natural fibre–polymer composite, the lignocellulosic phase is present in a wide range of diameters and lengths, some in the form of short filaments and others in forms that seem closer to the individual fibre.

Continuous regenerated cellulose fibres are extensively used as reinforcements in composites such as tyres. However, very few studies are available on their use as reinforcement for polymer composites. Because of the strong hydrogen bonds that occur between cellulose chains, cellulose does not melt or dissolve in common solvents. Thus, it is difficult to convert the short fibres from wood pulp into continuous filaments. Regenerated cellulose fibres are produced on a commercial scale under the generic name 'Lyocell' by a spinning process from a cellulose *N*-methylmorpholine-*N*-oxide/water solution. The mechanical properties of these fibres were found to depend on the draw ratio [20, 21]. The low mechanical properties reported for unidirectional composites composed of Lyocell fibres embedded in a poly(3-hydroxybutyrate-co-3-hydroxyvalerate) matrix were ascribed to weak interfacial adhesion due to both the smooth topography of the fibres and the hydrophobic properties of the matrix [22].

19.5.2 Fibre dispersion

The primary requirement for obtaining good performances from short-fibre composites is a good dispersion level in the host polymer matrix, which is obtained if the fibres are separated from each other and each fibre is surrounded by the matrix. Clumping and agglomeration must therefore be avoided. Insufficient fibre dispersion results in an inhomogeneous mixture composed of matrix-rich and fibre-rich domains. Mixing the polar and hydrophilic fibres with a non-polar and hydrophobic matrix, can result in dispersion difficulties.

There are two major factors affecting the extent of fibre dispersion: fibre–fibre interaction, such as hydrogen bonding between the fibres, and fibre length, because of the possibility of entanglements. As mentioned above, one of the specificity of cellulose fibres as reinforcement is their poor dispersion characteristics in many thermoplastic melts, due to their hydrophilic nature. Several methods have been suggested and described in the literature to overcome this problem and improve the dispersion. Among them are:

(1) Fibre surface modification. The surface energy is closely related to the hydrophilicity of the lignocellulosic fibres.
(2) Use of dispersing agents, such as stearic acid or a mineral oil. The dispersion of lignocellulosic fibres can be improved by pretreatment with lubricants or thermoplastic polymers. An addition of 1–3 per cent stearic acid is sufficient to achieve a maximum reduction in size and number of aggregates in PP and polyethylene [7]. The use of stearic acid in HDPE/wood fibres was reported to improve the fibre dispersion and the wetting between the fibre and the matrix [9].
(3) Fibre pre-treatments, such as acetylation, or use of a coupling agent.
(4) Increased shear force and mixing time. The best processing method involves twin-screw extruder.

Some physical methods have also been suggested to improve the dispersion of short fibres within the matrix. Treatments such as stretching, calandering, thermotreatment and the production of hybrid yarns do not change the chemical composition of the fibre, but modify their structural and surface properties and thus influence their mechanical bonding with polymers.

As already mentioned, the surface modification of lignocellulosic fibres is comprehensively dealt with in Chapter 18.

19.5.3 Fibre aspect ratio and length distribution

The efficiency of a composite also depends on the amount of stress transferred from the matrix to the fibres. This can be maximized by improving the interaction and adhesion between both phases and also by maximizing the length of the fibres retained in the final composite. However, long fibres sometimes increase the amount of clumping resulting in poor dispersion of the reinforcing phase within the host matrix. The ultimate fibre length present in the composite depends on the type of compounding and moulding equipment used and the processing conditions. Several factors contribute to the fibre attrition, such as the shearing forces generated in the compounding equipment, the residence time, the temperature and the viscosity of the compound. Using a polystyrene matrix, it was shown that the extent of breakage was most severe and rapid for glass fibres, less extensive for Kevlar fibres and the least for cellulose fibres [23]. The effect of twin-screw blending of wood fibres and polyethylene was also reported [12] and it was shown that the level of fibre attrition depended on the configuration and the processing temperature.

The fibre aspect ratio, which is its length to diameter ratio is a critical parameter in a composite. A relationship has been proposed by Cox to relate the critical fibre aspect ratio, l_c/d, to the interfacial shear stress, τ_y, viz.:

$$\frac{l_c}{d} = \frac{\sigma_{fu}}{2\tau_y} \tag{19.6}$$

where, σ_{fu} is the fibre ultimate strength in tension. At controlled fibre ultimate strength in tension, this equation shows an inverse relationship between the critical aspect ratio and the interfacial shear stress, where the former decreases as the latter increases, because of efficient transfer. This means that, for each short-fibre composite system, there is a critical fibre aspect ratio that corresponds to its minimum value for which the maximum allowable stress can be achieved for a given load. This parameter is determined by the fibre properties, the matrix properties and the quality of the fibre–matrix interface.

The condition for maximum reinforcement, that is the condition ensuring maximum stress transfer to the fibres, before the composite fails, is to have a length higher than the critical length l_c (Fig. 19.5). If the fibre aspect ratio is lower than its critical value, the fibres are not loaded to their maximum stress value. A specificity of cellulose fibres is their flexibility compared to glass fibres which allows a desirable fibre aspect ratio to be maintained after processing, which is around 100 or 200 for high performance short-fibre composites.

19.5.4 Fibre orientation

Fibre orientation is another important parameter that influences the mechanical behaviour of short-fibre composites. This is because the fibres in such composites are rarely oriented in a single direction, which is necessary to obtain the maximum reinforcement effects. During the processing of short-fibre composites, a continuous and

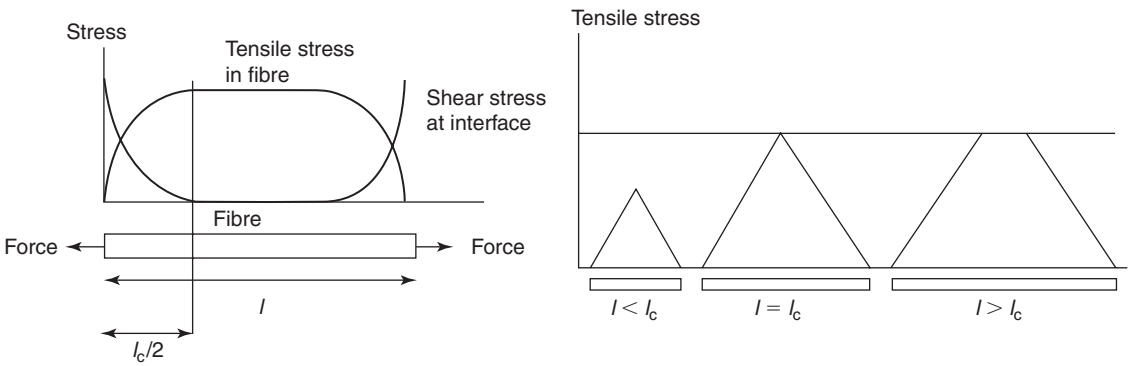

Figure 19.5 Variation of tensile stress in fibre and shear stress at interface occurring along the fibre length. If the fibre aspect ratio is lower than its critical value, l_c, the fibres are not loaded to their maximum stress value.

progressive orientation of individual fibres occurs (Fig. 19.6). This change is related to the geometrical properties of the fibres, the viscoelastic properties of the matrix and the change in shape produced by the processing. In these operations, the polymer melt undergoes both elongational and shear flow.

19.5.5 Fibre–matrix adhesion

Fibre to matrix adhesion plays a very important role in the reinforcement of composites with short fibres. During loading, loads are not applied directly to the fibres but to the matrix. It is necessary to have an effective load transfer from the matrix to the fibres for the ensuing composites to have good mechanical properties. This requires good interaction as well as adhesion between the fibres and the matrix, that is strong and efficient fibre–matrix interface.

As already pointed out, strongly hydrophilic cellulose fibres are inherently incompatible with hydrophobic polymers. When two materials are incompatible, it is often possible to introduce a third material having intermediate properties capable of reducing their interfacial energy. One way of applying this concept to the present context, is to impregnate the fibres with a polymer compatible with the matrix and, in general, this is achieved using low viscosity polymer solutions or dispersion. For a number of interesting polymers, however, the lack of solvents limits the use of this method. The compatibilization of the two components by specific chemical or physical treatments involving either is the most common approach to this problem as systematically reviewed in Chapter 18, with particular emphasis on the surface modification of the fibres. The following example illustrates the less frequent approach, based on the use of a surface modifier that bears a structure very close to that of the matrix, but which has been appropriately modified so that its macromolecules can react at the fibres' surface. Figure 19.7 shows SEM micrographs from the fractured surface of PP reinforced with cellulose fibres [15]. With the untreated matrix (Fig. 19.7(a)), a poor interfacial adhesion is clearly observed because of the absence of any physical contact between the fibre and the matrix. The micrograph in Fig. 19.7(b) corresponds to fibres in contact with a maleic

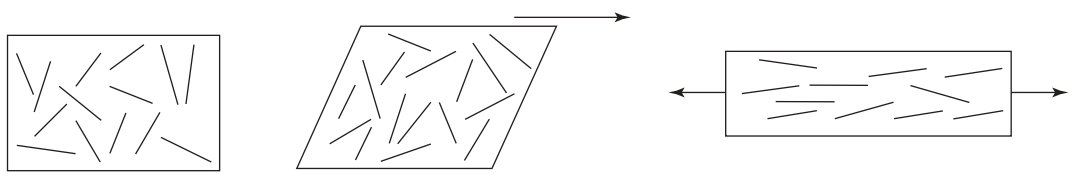

Figure 19.6 Orientation of individual fibres during processing: (a) initial random distribution, (b) rotation during shear flow and (c) alignment during elongational flow.

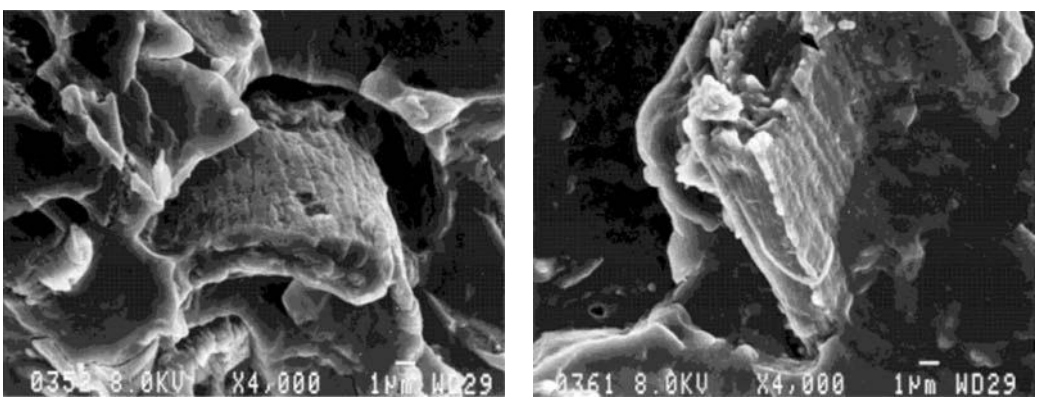

Figure 19.7 Scanning electron micrographs of a freshly fractured surface of a PP film filled with 20 wt% of raw untreated (a) and (b) MAPP coated softwood fibres. Reproduced with permission from Reference [24].

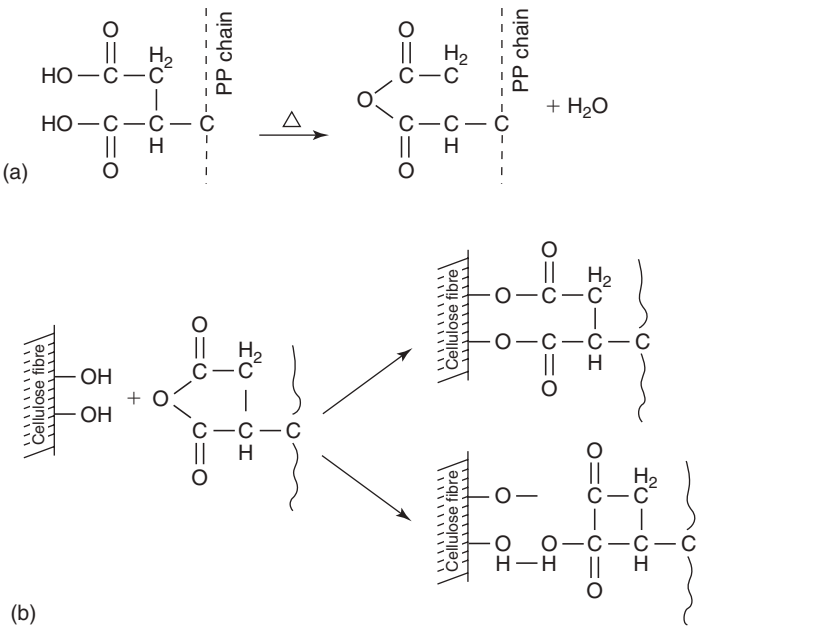

Figure 19.8 Reaction mechanism involved during the treatment of cellulose fibres with PP maleic anhydride copolymer (MAPP): (a) activation of MAPP ($T = 170°C$) before fibre treatment and (b) esterification of cellulose.

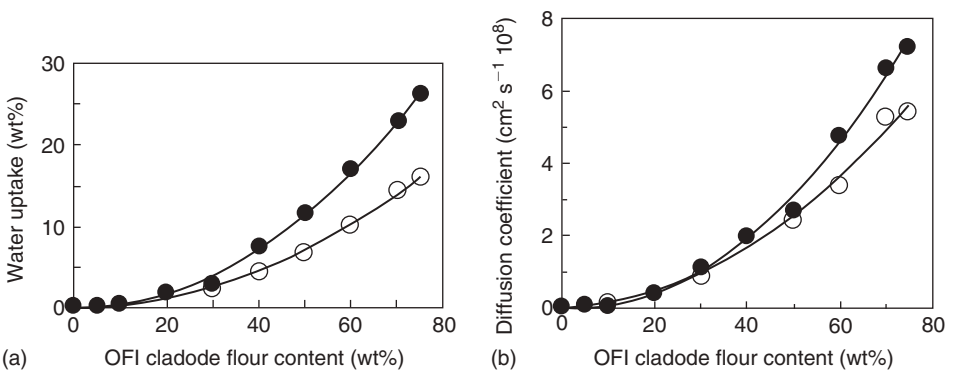

Figure 19.9 (a) Water uptake at equilibrium and (b) water diffusion coefficient of PP/*Opuntia ficus indica* cladode flour composites conditioned at 98 per cent RH versus filler loading: untreated filler (●) and MAPP coated filler (○) (the solid line serves to guide the eye). Reproduced with permission from Reference [25].

anhydride polypropylene (MAPP) graft copolymer (PP chains with pendant succinic acid moieties), which shows a good wetting, with absence of holes around the fibres. The mechanism of the reaction of MAPP with cellulose fibres can be divided into two steps (Fig. 19.8), the first being the activation of the copolymer by heat before the fibre treatment and the second, the esterification of cellulose. The fact of generating covalent bonds across the interface improved the adhesion between the matrix and the fibres, and both the Young modulus and the tensile strength were found to be higher than those obtained with the untreated fibres [15].

It has also been found that moisture absorbance of the natural fibre–polymer composite can be prevented if the fibre–matrix adhesion is optimized [15, 24]. Indeed, whereas composites based on standard PP and cellulosic fibres displayed high water content at the interphase, due to the presence of microcavities, the encapsulation of the fibres with MAPP decreased the water sensitivity of the composites in terms of both the water uptake and its diffusion coefficient [25], as shown in Fig. 19.9.

19.6 NANOCOMPOSITES

As previously mentioned, natural fibres present a multi-level organization and consist of several cells formed out of semi-crystalline oriented cellulose microfibrils. Each microfibril can be considered as a string of cellulose crystallites, linked along the chain axis by amorphous domains (Fig. 19.10) and having a modulus close to the theoretical limit for cellulose. They are biosynthesized by enzymes and deposited in a continuous fashion. A similar structure is reported for chitin, as discussed in Chapter 25. Nanoscale dimensions and impressive mechanical properties make polysaccharide nanocrystals, particularly when occurring as high aspect ratio rod-like nanoparticles, ideal candidates to improve the mechanical properties of the host material. These properties are profitably exploited by Mother Nature.

The promise behind cellulose-derived nanocomposites lies in the fact that the axial Young's modulus of the basic cellulose crystalline nanocrystal, derived from theoretical chemistry, is potentially higher than that of steel and similar to that of Kevlar. It was first experimentally studied in 1962 from the crystal deformation of cellulose I, using highly oriented fibres of bleached ramie [26]. A value of 137 GPa was reported, which differed from the theoretical estimate of 167.5 GPa calculated by Tashiro and Kobayashi [27]. The latter value is thought to be higher because the calculations had been carried out for low temperature. Force deflection data from the compression of cubes of potato tissues were fed into a model containing two structural levels, the cell structure and the cell wall structure [28], giving a maximum modulus value of 130 GPa. Eichhorn and Young [29] observed a decrease of cellulose crystallites when their crystallinity decreased. Recently, Raman spectroscopy was used to measure the elastic modulus of native cellulose crystals [30] and a value around 143 GPa was reported. However, it is worth noting that these measurements were made on epoxy/tunicin whiskers composites.

Stable aqueous suspensions of polysaccharide nanocrystals can be prepared by the acid hydrolysis of vegetable biomass. Different descriptors of the resulting colloidal suspended particles are used, including whiskers, monocrystals and nanocrystals. The designation 'whiskers' is used to describe elongated rod-like nanoparticles. These crystallites have also often been referred in the literature as microfibrils, microcrystals or microcrystallites, despite their nanoscale dimensions. Most of the studies reported in the literature refer to cellulose nanocrystals. A recent review described the properties and applications of cellulose whiskers in nanocomposites [31].

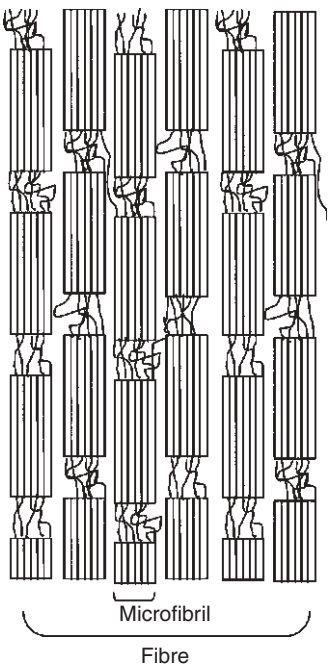

Figure 19.10 Schematic diagram showing the hierarchical structure of a semi-crystalline cellulose fibre.

The procedure for the preparation of such colloidal aqueous suspensions is described in detail in the literature for cellulose and chitin [32, 33]. The biomass is generally first submitted to a bleaching treatment with NaOH in order to purify cellulose or chitin by removing other constituents. The bleached material is then disintegrated in water, and the resulting suspension submitted to acid hydrolysis. The amorphous regions of cellulose or chitin act as structural defects and are responsible for the transverse cleavage of the microfibrils into short monocrystals by acid hydrolysis. Under controlled conditions, this transformation consists in the disruption of the amorphous regions surrounding and embedded within the cellulose or chitin microfibrils, while leaving the microcrystalline segments intact, because of the very large difference in the rate of hydrolysis between the amorphous and the crystalline domains, the latter obviously being much more resistant. The resulting suspension is subsequently diluted with water and washed by successive centrifugations. Dialysis against distilled water is then performed to remove the free acid in the dispersion. Complete dispersion of the whiskers is obtained by a sonication step. The dispersions are stored in a refrigerator after filtration to remove residual aggregates and addition of several drops of chloroform. This general procedure has to be adapted in terms of the acid hydrolysis conditions, such as time, temperature and purity of materials depending on the nature of the substrate and the geometrical characteristics of the nanocrystals.

The constitutive cellulose or chitin nanocrystals occur as elongated rod-like particles or whiskers. The length is generally of the order of a few hundreds nanometres and the width is of the order of a few nanometres. The aspect ratio of these whiskers is defined as the ratio of the length to the width. The high axial ratio of the rods is important for the determination of anisotropic phase formation and reinforcing properties. Figure 19.11 shows a transmission electron micrograph (TEM) obtained from a dilute suspension of tunicin whiskers, that is cellulose nanocrystals obtained from tunicate, a sea animal. Their average length and diameter are around 1 μm and 15 nm, respectively, and their aspect ratio was estimated to be around 67 [34].

Aqueous suspensions of starch nanocrystals can also be prepared by the acid hydrolysis of starch granules in aqueous medium using hydrochloric acid or sulphuric acid at 35°C (see also Chapter 15). Residues from the hydrolysis are called 'lintners' and 'nägeli' or amylodextrin. The degradation of native starch granules by acid hydrolysis depends on many parameters, which include the botanical origin of starch, namely crystalline type, granule morphology (shape, size, surface state) and the relative proportion of amylose and amylopectin. It also depends on the acid hydrolysis conditions, namely acid type, acid concentration, starch concentration, temperature, hydrolysis duration and stirring. A response surface methodology was used by Angellier *et al.* [35] to investigate the effect of five chosen factors on the selective sulphuric acid hydrolysis of waxy maize starch granules in order to optimize the preparation of aqueous suspensions of starch nanocrystals. These predictors were temperature, acid concentration, starch concentration, hydrolysis duration and stirring speed. The preparation of aqueous suspensions of starch nanocrystals with a yield of 15.7 wt%, was achieved after 5 days using 3.16 M H_2SO_4 at 40°C, 100 rpm and with a starch concentration of 14.7 wt%.

Compared to cellulose or chitin, the morphology of constitutive nanocrystals obtained from starch is completely different. Figure 19.12 shows a TEM obtained from a dilute suspension of waxy maize starch nanocrystals. They consist of 5–7 nm thick platelet-like particles with a length ranging 20–40 nm and a width in the range of 15–30 nm. The detailed investigation on the structure of these platelet-like nanoparticles was reported [36].

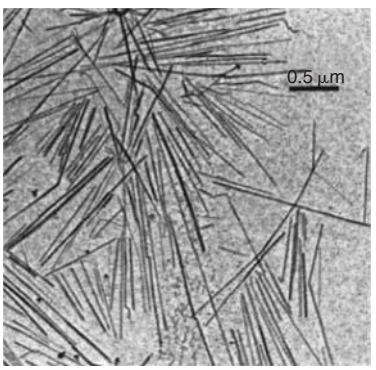

Figure 19.11 TEM of a dilute suspension of tunicin. Reproduced with permission from Reference [34].

Because of the high stability of aqueous polysaccharide nanocrystals dispersions, water is the preferred processing medium. High level of dispersion of the filler within the host matrix in the resulting composite is expected when processing nanocomposites in an aqueous medium. Therefore, this restricts the choice of the matrix to hydrosoluble polymers. The use of aqueous dispersed polymers, that is latexes, is a first alternative, which allows to employ hydrophobic polymers as matrices and ensure a good dispersion level of the filler, indispensable for homogenous composite processing. The possibility of dispersing polysaccharide nanocrystals in non-aqueous media is a second alternative which opens other possibilities for nanocomposite processing.

The first demonstration of the reinforcing effect of cellulose whiskers in a poly(St-co-BuA) matrix was reported by Favier *et al.* [37]. The authors measured, using DMA in the shear mode, a spectacular improvement in the storage modulus after adding tunicin whiskers, even at a low content, into the host polymer. This increase was especially significant above the glass–rubber transition temperature of the thermoplastic matrix, because of its poor mechanical properties in this temperature range. Figure 19.13 shows the isochronal evolution of the logarithm of the relative storage shear modulus (log G'_T/G'_{200}, where G'_{200} corresponds to the experimental value measured at 200 K) at 1 Hz as a function of temperature for such composites prepared by water evaporation. In the rubbery state of the thermoplastic matrix, the modulus of the composite with a loading level as low as 6 wt%, is more than two orders of magnitude higher than that of the unfilled matrix. Moreover, the introduction of 3 wt% or more

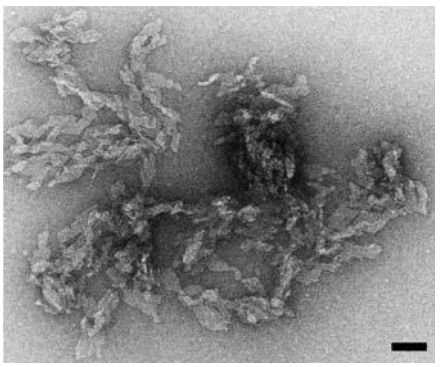

Figure 19.12 Transmission electron micrograph of a dilute suspension of hydrolyzed waxy maize starch (scale bar 50 nm). Reproduced with permission from Reference [35].

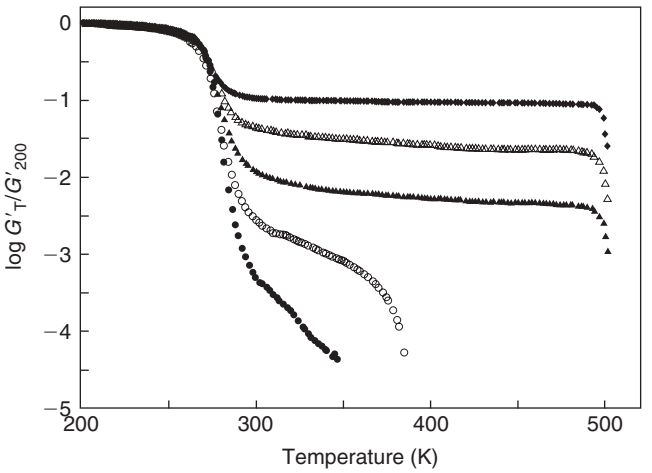

Figure 19.13 Logarithm of the normalized storage shear modulus (log G'_T/G'_{200}, where G'_{200} corresponds to the experimental value measured at 200 K) versus temperature at 1 Hz for tunicin whiskers reinforced poly(St-co-BuA) nanocomposite films, obtained by water evaporation and filled with 0 (●), 1 (○), 3 (▲), 6 (△) and 14 wt% (◆) of cellulose whiskers. Reproduced with permission from Reference [31].

cellulosic whiskers provides an outstanding thermal stability to the matrix modulus up to the temperature at which cellulose starts to degrade (500 K).

The macroscopic behaviour of polysaccharide nanocrystals-based nanocomposites depends, as for any heterogeneous materials, on the specific behaviour of each phase, the composition (volume fraction of each phase), the morphology (spatial arrangement of the phases) and the interfacial properties. The outstanding properties observed for these systems were ascribed to a mechanical percolation phenomenon [37]. A good agreement between experimental and predicted data was reported when using the series–parallel model of Takayanagi, modified to include a percolation approach. Therefore, the mechanical performance of these systems was not only the result of the high mechanical properties of the reinforcing nanoparticles. It was suspected that the stiffness of the material was due to infinite aggregates of cellulose whiskers. Above the percolation threshold, the cellulose nanoparticles can connect to form a three-dimensional continuous pathway through the nanocomposite film. For rod-like particles such as tunicin whiskers with an aspect ratio of 67, the percolation threshold is close to 1 vol%. The formation of this cellulose network was supposed to result from strong interactions, like hydrogen bonds, between whiskers. This phenomenon is similar to the high mechanical properties observed for a paper sheet, which result from the hydrogen-bonding forces that hold the percolating network of fibres. This mechanical percolation effect explains both the high reinforcing effect and the thermal stabilization of the composite modulus for evaporated composite films.

Any factor that affects the formation of the percolating whisker network, or interferes with it, changes the mechanical performances of the composite [38]. Three main parameters were reported to affect the mechanical properties of such materials, viz. the morphology and dimensions of the nanoparticles, the processing method, and the microstructure of the matrix and matrix–filler interactions.

Apart from the mechanical performances, some other properties are interesting and can be improved by adding polysaccharide nanocrystals, for instance swelling properties. It was shown that the water uptake of tunicin whiskers/thermoplastic starch nanocomposites decreased as a function of the filler content [34]. For starch nanocrystals/natural rubber nanocomposites, it was shown that both the toluene uptake at equilibrium and its diffusion coefficient decreased when adding starch nanocrystals [39]. The evolution of the diffusion coefficient of toluene displayed a discontinuity around 10 per cent, suggesting a possible percolation effect of the starch nanocrystals.

The barrier properties of starch nanocrystals/natural rubber nanocomposites were also investigated [39]. For these systems, the water vapour transmission rate, the diffusion coefficient of oxygen, the permeability coefficient of oxygen and its solubility, were measured. It was observed that the permeability to water vapour, as well as to oxygen, decreased when starch nanocrystals were added. These effects were ascribed to the platelet-like morphology of the nanocrystals.

19.7 CONCLUSIONS

There is a growing trend to use lignocellulosic fibres in applications for which synthetic fibres were traditionally employed, which is ascribed as their numerous well-known advantage. Present applications of natural fibre filled composites are in the field of energy and impact absorption, such as car fenders and bicycle helmets. They also include markets that target cheaper, renewable and non-recyclable, or biodegradable materials, such as packaging and structural elements. Other uses of natural fibre-based composites are deck surface boards, picnic tables, industrial flooring, etc. In cars, about 10–15 kg of these composites, typically made up of 50 per cent natural fibres and 50 per cent PP, along with other additives, are presently being used. Examples are door panels, roof headliners, seat backs, rear decks and trunkliners.

Another interesting property of natural fibres is their hierarchical structure and the possibility to choose the scale linked to the application. Polysaccharide nanocrystals are building blocks biosynthesized to provide structural properties to living organisms. They can be isolated from cellulose-containing materials under strictly controlled conditions. Polysaccharide nanocrystals are inherently low cost materials, available from a variety of natural sources in a wide range of aspect ratios. The corresponding polymer nanocomposites display outstanding mechanical properties and can be used to process high modulus thin films. Practical applications of such fillers and their transition into industrial technology require a favourable ratio between the expected performances of the composite material and its cost.

In conclusion, this area is moving fast towards novel outstanding composite materials based on renewable resources in the form of both traditional natural fibres and their nanomorphologies, but there are still significant scientific and technological challenges to be met.

REFERENCES

1. Rowell R.M., Property enhanced natural fiber composite materials based on chemical modification, in *Science and Technology of Polymers and Advanced Materials: Emerging Technologies and Business Opportunities*, (*Proceedings of the Fourth International Conference on Frontiers of Polymers and Advanced Materials*, Cairo, Egypt, 4–9 January 1997), Plenum Press, New York N.Y., 1998, pp. 717–732.
2. Anonym., *Information Bulletin of the FAO European Cooperative Research Network on Flax and other Bast Plants*, **2**(16), 2001; Institute of Natural Fibres Coordination Centre, Poznan, Poland, Dec. 2001.
3. Munder F., Fürll C., Hempel H., Processing of bast fiber plants for industrial application, in *Natural Fibers, Biopolymers and Biocomposites*, Eds.: Mohanty A.K., Misra M. and Drzal L.T., CRC Press Taylor & Francis Group, Boca Raton, 2005, pp. 109–140, Chapter 3.
4. Bismarck A., Aranberri-Askargorta I., Springer J., Lampke T., Wielage B., Stamboulis A., Shenderovich I., Limbach H.-H., Surface characterization of flax, hemp and cellulose fibers; surface properties and the water uptake behavior, *Polym. Compos.*, **23**(5), 2002, 872–894.
5. Rong M.Z., Zhang M.Q., Liu Y., Yang G.C., Zeng H.M., The effect of fiber treatment on the mechanical properties of unidirectional sisal-reinforced epoxy composites, *Compos. Sci. Technol.*, **61**(10), 2001, 1437–1447.
6. Katz H.S., Milewski J.V., in *Handbook of Fillers for Plastics*, Van Nostrand Reinhold, New York, 1987. p. 512
7. Bledzki A.K., Gassan J., Composites reinforced with cellulose based fibres, *Prog. Polym. Sci.*, **24**, 1999, 221–274.
8. Eichhorn S.J., Baillie C.A., Zafeiropoulos N., Mwaikambo L.Y., Ansell M.P., Dufresne A., Entwistle K.M., Herrera-Franco P.J., Escamilla G.C., Groom L., Hugues M., Hill C., Rials T.G., Wild P.M., Review: Current international research into cellulosic fibres and composites, *J. Mater. Sci.*, **36**, 2001, 2107–2131.
9. Woodhams R.T., Thomas G., Rodges D.K., Wood fibers as reinforcing fillers for polyolefins, *Polym. Eng. Sci.*, **24**(15), 1984, 1166–1171.
10. Kokta B.V., Raj R.G., Daneault C., Use of wood flour as filler in polypropylene: Studies on mechanical properties, *Polym. Plast. Technol. Eng.*, **28**(3), 1989, 247–259.
11. Bataille P., Ricard L., Sapieha S., Effect of cellulose in polypropylene composites, *Polym. Compos.*, **10**(2), 1989, 103–108.
12. Yam K.L., Gogoi B.K., Lai C.C., Selke S.E., Composites from compounding wood fibers with recycled high-density polyethylene, *Polym. Eng. Sci.*, **30**(11), 1990, 693–699.
13. Sanadi A.R., Young R.A., Clemons C., Rowell R.M., Recycled newspaper fibers as reinforcing fillers in thermoplastics: Part I. Analysis of tensile and impact properties in polypropylene, *J. Reinf. Plast. Comp.*, **13**(1), 1994, 54–67.
14. Weeton J.W., Peters D.M., Thomas K.L., in *Engineers' Guide to Composite Materials*, American Society for Metals, Metals Park, Ohio, 1987.
15. Anglès M.N., Salvadó J., Dufresne A., Mechanical behavior of steam exploded residual softwood filled polypropylene composites, *J. Appl. Polym. Sci.*, **74**, 1999, 1962–1977.
16. Herrera-Franco P.J., Aguilar-Vega M.J., Effect of fiber treatment on mechanical properties of LDPE-henequen cellulosic fiber composites, *J. Appl. Polym. Sci.*, **65**, 1997, 197–207.
17. Dufresne A., Dupeyre D., Paillet M., Lignocellulosic flour reinforced poly(hydroxybutyrate-co-valerate) composites, *J. Appl. Polym. Sci.*, **87**(8), 2003, 1302–1315.
18. Luo S., Netravali A.N., Mechanical and thermal properties of environment-friendly 'green' composites made from pineapple leaf fibers and poly(hydroxybutyrate-co-valerate) resin, *Polym. Compos.*, **20**(3), 1999, 367–378.
19. Reinsch V.E., Kelley S.S., Crystallization of poly(hydroxybutyrate-co-hydroxyvalerate) in wood fiber-reinforced composites, *J. Appl. Polym. Sci.*, **64**(9), 1997, 1785–1796.
20. Mortimer S.A., Peguy A.A., Ball R.C., Influence of the physical process parameters on the structure formation of Lyocell fibers, *Cell. Chem. Technol.*, **30**(3–4), 1996a, 251–266.
21. Mortimer S.A., Peguy A.A., The formation of structure in the spinning and coagulation of Lyocell fibers, *Cell. Chem. Technol.*, **30**(1–2), 1996b, 117–132.
22. Bourban C., Karamuk E., de Fondaumiere M.J., Rufieux K., Mayer J., Wintermantel E., Processing and characterization of a new biodegradable composite made of a PHB/V matrix and regenerated cellulosic fibers, *J. Environ. Polym. Degr.*, **5**(3), 1997, 159–166.
23. Czarnecki L., White J.L., Shear flow rheological properties, fiber damage and mastication characteristics of aramid-, glass-, and cellulose fiber-reinforced polystyrene melts, *J. Appl. Polym. Sci.*, **25**(6), 1980, 1217–1244.
24. Faria H., Cordeiro N., Belgacem M.N., Dufresne A., Dwarf cavendish as a source of natural fibers in polypropylene-based composites, *Macromol. Mater. Eng.*, **291**(1), 2006, 16–26.
25. Malainine M.E., Mahrouz M., Dufresne A., Lignocellulosic flour from cladodes of *Opuntia ficus-indica* reinforced polypropylene composites, *Macromol. Mater. Eng.*, **289**(10), 2004, 855–863.
26. Sakurada I., Nukushina Y., Ito T., Experimental determination of the elastic modulus of crystalline regions oriented polymers, *J. Polym. Sci.*, **57**(165), 1962, 651–660.

27. Tashiro K., Kobayashi M., Theoretical evaluation of three-dimensional elastic constants of native and regenerated celluloses: Role of hydrogen bonds, *Polymer*, **32**(8), 1991, 1516–1526.
28. Hepworth D.G., Bruce D.M., A method of calculating the mechanical properties of nanoscopic plant cell wall components from tissue properties, *J. Mater. Sci.*, **35**(23), 2000, 5861–5865.
29. Eichhorn S.J., Young R.J., The Young's modulus of a microcrystalline cellulose, *Cellulose*, **8**(3), 2001, 197–207.
30. Šturcová A., Davies G.R., Eichhorn S.J., Elastic modulus and stress-transfer properties of tunicate cellulose whiskers, *Biomacromolecules*, **6**(2), 2005, 1055–1061.
31. Azizi Samir M.A.S., Alloin F., Dufresne A., Review of recent research into cellulosic whiskers, their properties and their application in nanocomposite field, *Biomacromolecules*, **6**(2), 2005, 612–626.
32. Wise L.E., Murphy M., D'Addiecco A.A., Chlorite holocellulose, its fractionation and bearing on summative wood analysis and on studies on hemicelluloses, *Pap. Trade J.*, **122**, 1946, 35–43.
33. Marchessault R.H., Morehead F.F., Walter N.M., Liquid crystal systems from fibrillar polysaccharides, *Nature*, **184**, 1959, 632–633.
34. Anglès M.N., Dufresne A., Plasticized starch/tunicin whiskers nanocomposites: 1. Structural analysis, *Macromolecules*, **33**(22), 2000, 8344–8353.
35. Angellier H., Choisnard L., Molina-Boisseau S., Ozil P., Dufresne A., Optimization of the preparation of aqueous suspensions of waxy maize starch nanocrystals using a response surface methodology, *Biomacromolecules*, **5**(4), 2004, 1545–1551.
36. Putaux J.L., Molina-Boisseau S., Momaur T., Dufresne A., Platelet nanocrystals resulting from the disruption of waxy maize starch granules by acid hydrolysis, *Biomacromolecules*, **4**(5), 2003, 1198–1202.
37. Favier V., Canova G.R., Cavaillé J.Y., Chanzy H., Dufresne A., Gauthier C., Nanocomposites materials from latex and cellulose whiskers, *Polym. Adv. Technol.*, **6**, 1995, 351–355.
38. Dufresne A., Comparing the mechanical properties of high performances polymer nanocomposites from biological sources, *J. Nanosci. Nanotechnol.*, **6**(2), 2006, 322–330.
39. Angellier H., Molina-Boisseau S., Lebrun L., Dufresne A., Processing and structural properties of waxy maize starch nanocrystals reinforced natural rubber, *Macromolecules*, **38**(9), 2005, 3783–3792.

– 2 0 –

Chemical Modification of Wood

Mohamed Naceur Belgacem and Alessandro Gandini

ABSTRACT

The main emphasis of this chapter has to do with the shift from the traditional ways of treating woods in order to improve their resistance to atmospheric and biological degradation, to chemical modifications which eliminate the problem of leaching of toxic materials into the environment. Hence, recent contributions on the chemical modification of wood by different physico-chemical treatments, such as corona and plasma discharges, or its chemical grafting through esterification, etherification, as well as urethane and siloxane formation and the reaction of wood with furfuryl alcohol, are reviewed and discussed. The chapter also covers the topic of the preparation and characterization of composite materials made of wood fibres and polymeric matrices. These surface or bulk treatments point to the relevance of a novel green approach and show that very promising results can be obtained.

Keywords

Chemical modification of wood, Corona and plasma treatment, Wood esterification, Wood etherification, Reactions between wood and isocyanates, Reactions of wood with siloxanes, Reactions of wood with furfuryl alcohol, Wood-based composites

20.1 INTRODUCTION

Wood is one of the oldest renewable resources exploited by human activity in the form of timber, tools, source of energy and of shelter. Wood is a complex natural material whose structure represents the very paradigm of a composite assembly, as briefly outlined in Chapter 1, together with general references to the traditional uses of this multifarious vegetable manifestation. Its main components (see Chapter 1) are cellulose (**A**), hemicelluloses (**B**) and lignin (**C**), accompanied by minor contributions of low molecular weight compounds and mineral salts. This book includes several chapters devoted to the utilization of both the major and some of the minor components of wood considered individually as a source of polymers.

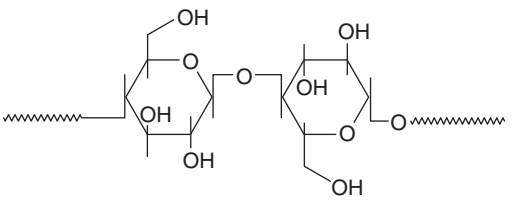

(**A**)

Wood, as such, finds numerous applications, often depending on the specific species, because it displays remarkable properties like good mechanical strength, easy processing and an attractive and warm appearance. None of these aspects bear a direct relationship with the purposes of this book, because they are essentially related to technological issues. The same considerations apply to the use of wood in papermaking, as already emphasized in Chapter 1.

The hydrophilic character of wood, intrinsically connected with the structure of its three main macromolecular components, has been a longstanding source of problems, mostly arising from its lack of dimensional stability in moist environments. An additional major drawback is its susceptibility to photolytic and biological degradation. The interest of both scientists and technologists in modifying wood in order to overcome these drawbacks has called upon specific treatments like chemical, thermal, enzymatic or purely physical modifications. This chapter examines recent contributions to these issues, based on approaches which only involve the chemical modification of wood, carried out in bulk or at its surface. The other treatments have been aptly covered in a recent book [1] and a thorough review [2].

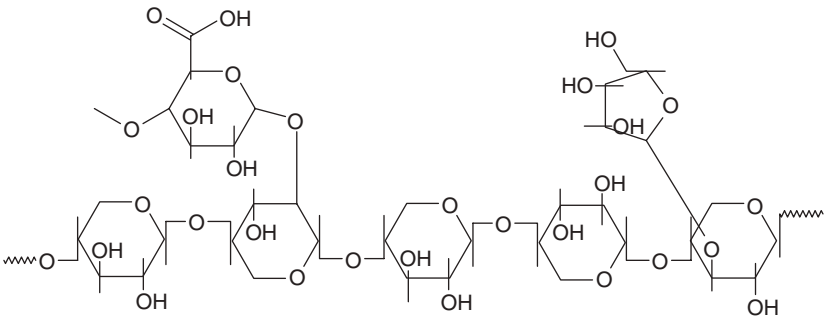

(**B**)

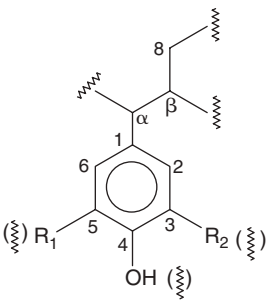

(**C**)

20.2 CHEMICAL MODIFICATION

The wood moieties exploited for chemical grafting are almost exclusively the hydroxyl functions present in the structure of the three polymers which constitute its essential composite morphology. Depending on the specific experimental conditions applied to achieve these modifications, they can be limited to the wood surface thereby preserving all its pristine bulk properties, or they can be extended inside the wood structure and, in this case, novel materials are therefore produced.

Both aspects are discussed here with a higher emphasis on surface modification.

20.2.1 Corona and plasma treatments

Corona and plasma treatments have been used to treat wood surfaces with the aim of increasing its wettability towards water and organic liquids, its adhesion with different coating lacquers and binders and its compatibility with polyolefins.

A corona treatment was applied to different wood tablets (Teak, Birch and Pine) and the wettability of the modified surfaces was measured by water contact angles which decreased from 90° to less than 40°, after a 24 kJ m^{-2} discharge [3]. The adhesion of a water-based lacquer was also improved.

Birch was treated with an oxygen plasma in the presence or absence of hexamethyldisiloxane (HMDS) [4] and the ensuing surface characterized by atomic force microscopy (AFM), contact angle measurements and adhesion strength with polypropylene. When the treatment was by oxygen alone, the water contact angle decreased from about 90° to 55°, at an optimal treatment time (*i.e.*, 60 s) and the polar component of the surface energy increased from 12 to 40 mJ m^{-2}. A 5 min plasma treatment with HMDS yielded a better adhesion between the modified surface and polypropylene. AFM showed that the deposited polymer followed the tortuosity of the birch surface without forming a continuous film.

Yellow pine was also submitted to a plasma oxygen treatment in order to reduce its degradation by weathering [5]. Different coatings were plasma-deposited, namely poly-(dimethylsiloxane) (PDMS), benzotriazole/PDMS, ZnO/PDMS, hydroxybenzophenone/PDMS, phthalocyanine/PDMS and graphite/PDMS. ATR-FTIR and XPS analyses showed the occurrence of the grafting and the latter coating was found to be the most efficient in terms of the stabilization of weight loss during weathering tests.

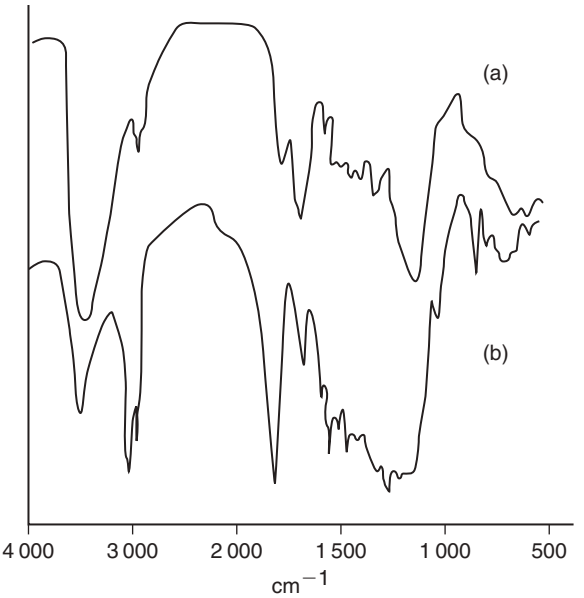

Figure 20.1 FTIR spectra of Oakwood sawdust before (a) and after (b) esterification with octanoyl chloride. (Reproduced by permission of Elsevier. Copyright 1995. Reprinted from Reference [10].)

Fir is another species whose surface was treated with oxygen plasma and corona in order to increase its adhesion with outdoor-coating systems and consequently the durability of the wood exposed to atmospheric conditions [6]. Different parameters were varied in this study and the wettability of the modified substrate tested which allowed the following optimal conditions to be established: a treatment time of 5 min, a plasma power of 600 W and a distance between the samples and the plasma source of 28 cm using oxygen or air as the plasma gas. The optimal corona voltage was around 15 kV, which yielded a drop in the water contact angle from 115° to less than 15°. Rehn and Viöl [7] showed that hydrophobic or hydrophilic wood surfaces can be generated by cold plasma treatment, depending on the gas used.

20.2.2 Esterification reactions

The esterification of wood has been investigated very extensively, as recently reviewed [1, 2]. Most of these investigations were carried out in a heterogeneous solid–liquid medium and only a few called upon the use of gaseous reagents. Only the very recent and scientifically relevant studies related to this topic will be reviewed here, since a much more detailed coverage of its historical development is available [8, 9].

Oakwood has been submitted to a solvent-free esterification procedure using fatty-acids of different chain lengths and their chlorides [10, 11]. These bulk reactions were carried out at high temperature in a nitrogen atmosphere and the modified wood samples characterized by weight gain, FTIR, SEM, moisture absorption, contact angle measurements and thermo-mechanical analyses. The weight gain reached 6 per cent for the highest grafting yields and the water contact angle was about 95°. Figure 20.1 shows the FTIR spectra of the wood sawdust before and after treatment with octanoyl chloride.

Pinus sylvestris was esterified using propionic anhydride and the FTIR spectroscopy of the ensuing sample proved that the grafting had indeed occurred [12]. *Pinus sylvestris* and mechanically pulped spruce fibres were also esterified with crotonic (**I**) and methacrylic anhydrides (**II**) and then copolymerized *in situ* with styrene (**ST**) [13].

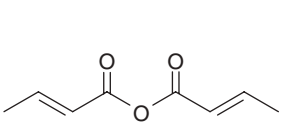

I

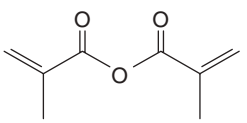

II

The fibres modified with **I** and copolymerized with **ST** using AIBN as the free-radical initiator, gave FTIR spectra with peaks which revealed the presence of C═O and C═C moieties after the first step, and the disappearance of the latter peak after the copolymerization with **ST**. The presence of grafted polystyrene was proven by the appearance of the characteristic double peak at 760 and 700 cm^{-1}, typical of monosubstituted benzene rings. The weight gain associated with these reactions was as high as 50 per cent. After the removal of wood, the FTIR and CP-MAS ^{13}C-NMR spectra of the residue were found to be similar to those of poly **ST** [13]. Figure 20.2 shows the ^{13}C-NMR spectra of the pine samples after different modifications.

Our group developed a novel strategy consisting in the use of planar stiff molecules bearing two identical reactive functions at the opposite end of their structure [14–17]. The working hypothesis was that *only one* of the functions can react with the wood OH group, whereas the other should be left to copolymerize with a subsequently

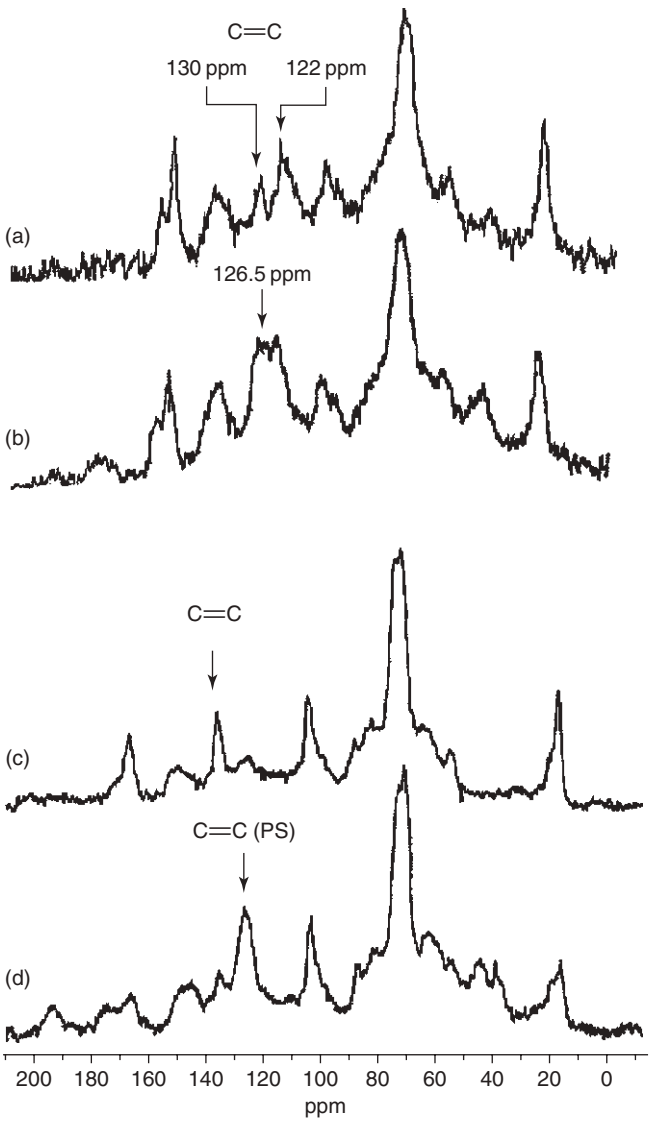

Figure 20.2 CP-MAS^{13}C-NMR spectra of pine samples treated with (a) crotonic anhydride, (b) crotonic anhydride followed by copolymerization with styrene, (c) methacrylic anhydride and (d) methacrylic anhydride followed by copolymerization with styrene. (Reproduced by permission of Elsevier. Copyright 2000. Reprinted from Reference [13].)

added monomer. Thus, wood was treated with pyromellitic anhydride (**III**) in a dry non-swelling medium. The recovered fibres showed clearly, after extraction of the excess reagent, the relevant infrared bands arising from anhydride carbonyl groups.

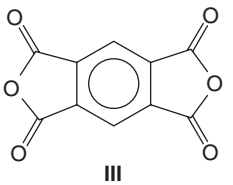

III

In another study, the treatment of pine wood with **III** (see Fig. 20.3) was followed by copolymerizations with **ST** and methyl methacrylate (**MMA**). After extraction of the ungrafted poly**ST**, the samples were characterized by FTIR, IGC, anti-swelling efficiency (ASE) and weight gain. The latter measurement showed a weight gain increase of 55 per cent. The water contact angle of the initial substrate surface was about 40° just after the drop deposition and decreased to zero within a few seconds, whereas that of a sample treated with **III**, followed by **MMA** polymerization and extraction, was about 100°. The ASE was improved after both copolymerizations. Finally, IGC showed that the surface energy of wood and its acid–base character had been lowered by this type of treatment [14–17].

III-treated wood tablets were further reacted with different biocide molecules, namely 2-phenylphenol (**IV**) and tebuconazole (**V**), chosen because they bore the hydroxy group necessary for their coupling with the unreacted anhydride function remaining after the single grafting of **III** [18]. All these reactions, carried out under nitrogen, were optimized after testing solvents of different polarity, various catalysts, temperatures and durations. After extracting all unbound species and drying, these modified wood samples were characterized by weight gain, FTIR spectroscopy (multiple reflections on the block surface at different depths and transmission on wood powders mixed into KBr pellets), elemental analysis and biological tests. The occurrence of grafting was proven with most systems, albeit to different extents depending on the actual conditions. More importantly, the presence of

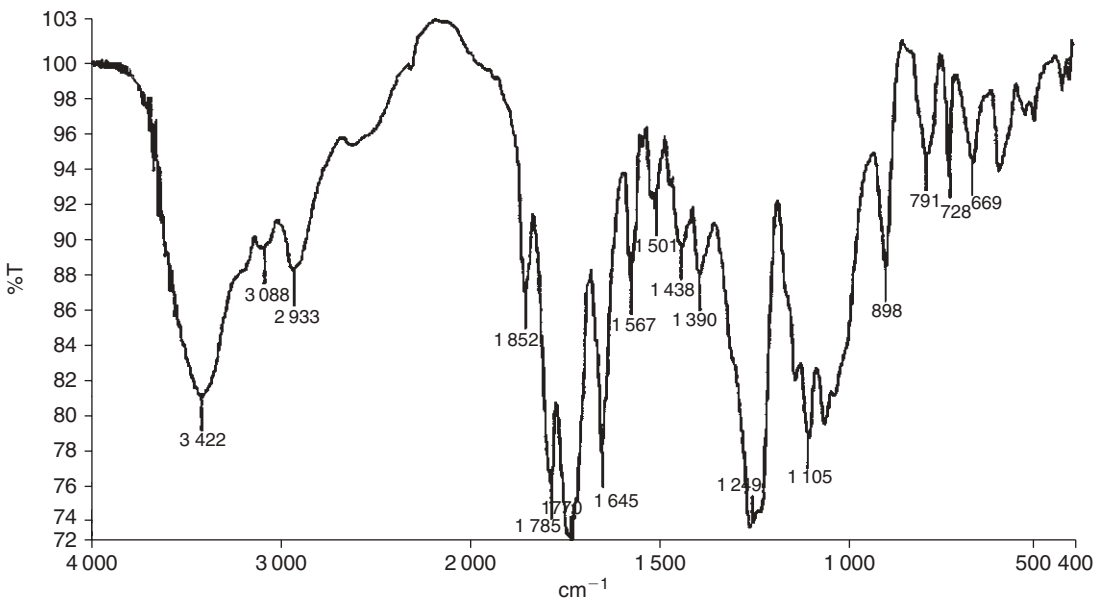

Figure 20.3 FTIR spectrum of **III**-modified pine wood [18].

the grafted biocide moieties arising from **IV** and **V** gave the correspondingly modified wood samples an excellent resistance to a wide selection of *fungi* [18].

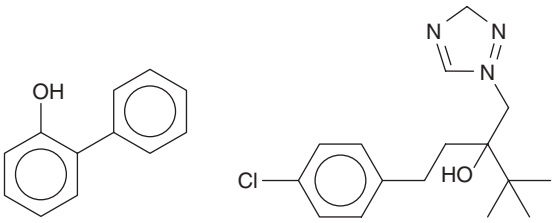

IV **V**

The esterification of sapwood using maleic anhydride (**MA**) in the vapour phase was recently reported [19, 20]. The weight gain varied as a function of the **MA/**wood weight ratio and reached about 70 per cent for the highest ratio studied, that is, 1.6. The dimensional and antifungal stability, as well as the ASE of the treated samples, improved considerably.

Poly-(*N*-acryloyl dopamine) (**PAD**) was developed as a new wood adhesive and used to bind maple specimens [21]. Scheme 20.1 shows the different steps involved in the **PAD** synthesis. Since **PAD** undergoes substantial oxidation and crosslinking reactions at 80°C, a **PAD**–polyethylenimine (**PAD–PEI**) mixture was used to bind wood. The glued samples were characterized in terms of adhesion strength and water resistance. The **PAD–PEI** system gave a much better shear strength and a higher water resistance, compared with the corresponding system in which

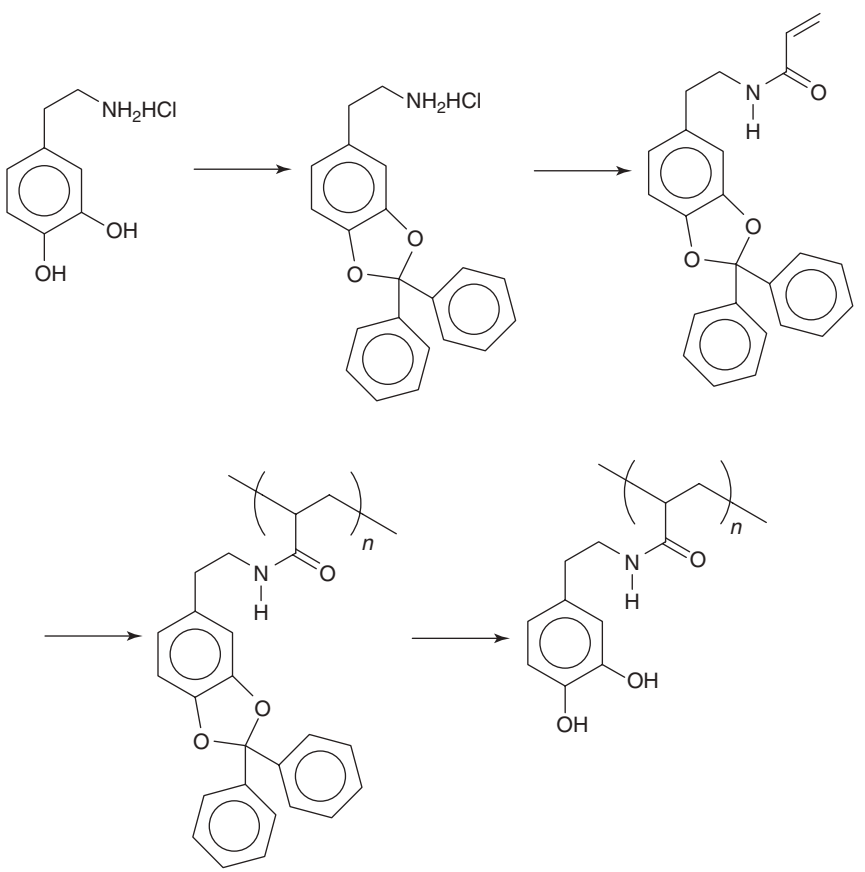

Scheme 20.1

the **PAD** homopolymer was used. However, this study did not provide any evidence about the occurrence of chemical bonding between wood and adhesive.

More recently [22], a poly-(aminoamide-epichlorohydrin)/stearic anhydride compatibilizer system was developed to optimize the interface between pine flour and polyethylene in the corresponding composites. FTIR spectra showed that the compatibilizer had indeed been grafted to the wood particles and the decrease in water uptake by the composite corroborated the interest in using this novel system.

Wood specimens from *P. Roxburgii* (Chir pine) were esterified with benzoyl chloride in order to enhance their photostability [23, 24]. The samples gained about 20 per cent in weight and, after their exposure for 500 h to a 100 W xenon arc light at 30°C and 65 per cent relative humidity, showed an improved resistance to photoyellowing, thanks to a reduced extent of lignin degradation. A review dealing with the photodegradation and photostabilization of wood was recently reported [25].

20.2.3 Etherification reactions

Allyl glycidyl ether (**VI**) and glycidyl methacrylate (**VII**) were used to etherify wood blocks of *Pinus sylvestris* and mechanically pulped spruce fibres. The mechanism of the reaction consisted in the chain extension of the wood OH functions by the epoxy groups of **VI** and **VII**. The modified samples were characterized by FTIR and ^{13}C-NMR spectroscopy and by weight gain, which amounted to 7 and 20 per cent for **VI** and **VII**, respectively [12].

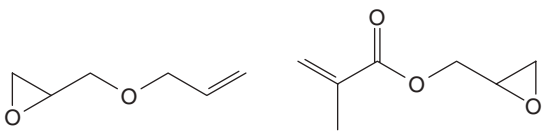

VI **VII**

Much more recently, **VII** was used to graft pine wood using different solvents, temperatures, catalysts and reaction times [14]. After the removal of the excess of **VII** by extraction, a weight gain of ~20 per cent was measured. These modified wood samples were then copolymerized with **MMA** or **ST**. The ensuing solvent-extracted materials (wood + **VII** + **MMA** or wood + **VII** + **ST**) had gained a further 35 per cent in weight. FTIR spectra showed unequivocally the occurrence of grafting at each step. The water contact angles on these modified wood surfaces were higher than 110° after the second grafting reactions, as shown in Fig. 20.4.

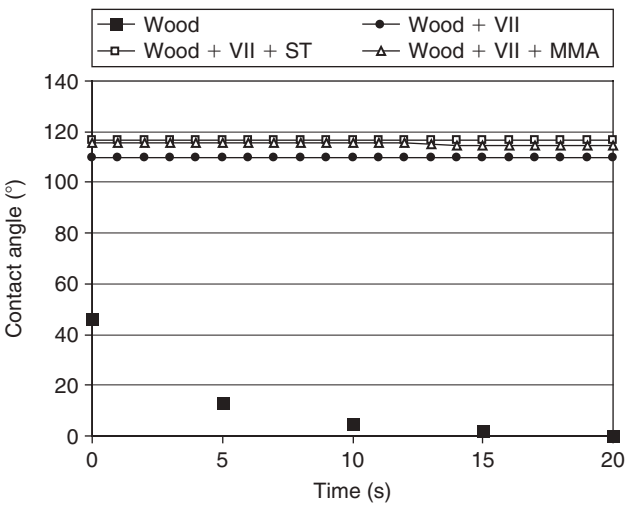

Figure 20.4 Water contact angles measured on the surface of wood before and after different modifications [18].

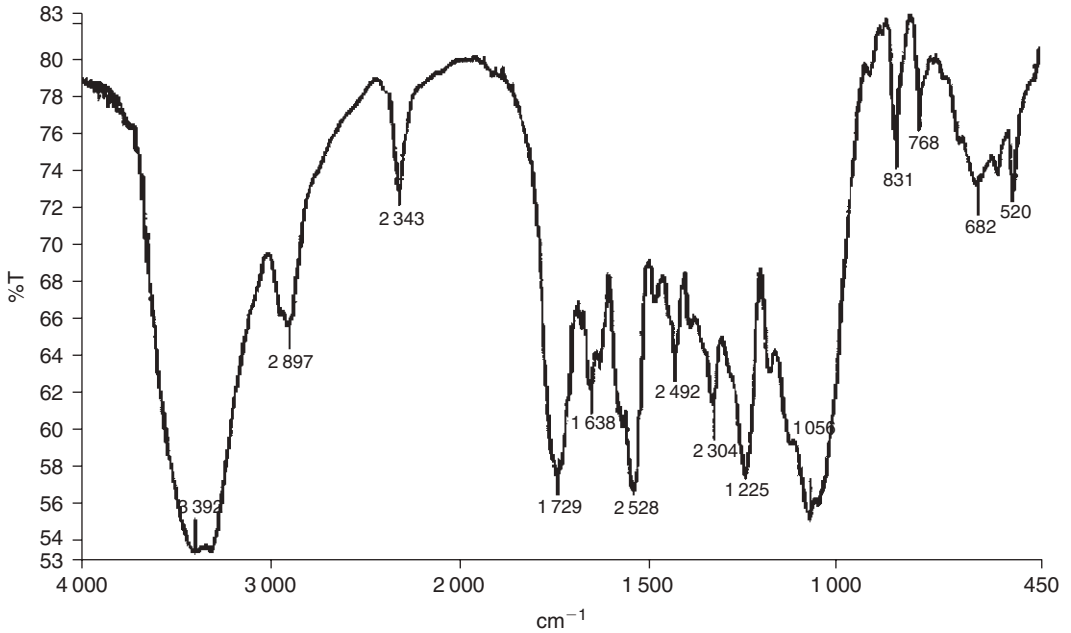

Figure 20.5 FTIR spectrum of **VIII**-modified wood [18].

Pine tablets were treated successively with **VII** and **ST** [26]. The ensuing materials were characterized by FTIR, weight gain, ASE, thermogravimetry and mechanical testing. Surprisingly, the authors claimed that wood can be grafted directly with **ST**, just by heating **ST**-impregnated wood samples in the presence of AIBN. They succeeded to graft up to 25 per cent w/w with respect to wood. Even more surprising was the reported lower weight gain associated with the double grafting strategy (wood + **VII** + **ST**), which however yielded much better results in terms of mechanical, ASE and thermal properties.

20.2.4 Reactions with isocyanates

The reaction of wood with isocyanate coupling agents was first reported in 1957 and concerned the use of phenyl isocyanate at 100–120°C [27]. Since then, numerous other reagents and wood substrates have been used, as recently reviewed [8, 9]. Hence only very recent investigations will be reported here.

1,4-Phenyl diisocyanate (**VIII**) was used as a grafting molecule following the same strategy discussed above in the case of the double anhydride **III** [14–17]. As expected, the FTIR spectrum of the modified wood surface, after extraction of the unreacted **VIII**, displayed a strong peak at 2 250 cm^{-1}, characteristic of the presence of isocyanate functions (see Fig. 20.5). These modified wood samples were treated with the biocides **IV** and **V**, which provided an excellent resistance to fungi [18].

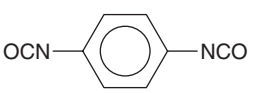

VIII

20.2.5 Reactions with siloxanes

A recent series of articles [28–30] describes the treatment of maritime pine sapwood with three different siloxanes, namely 3-isocyanatopropyl trimethoxysilane (**IX**), 3-glycidoxypropyltriethoxysilane (**X**) and *n*-propyltriethoxysilane (**XI**).

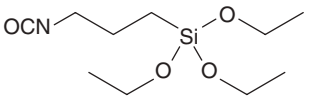

IX

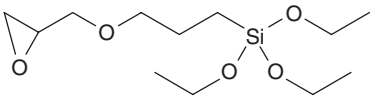

X

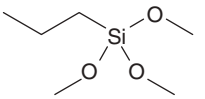

XI

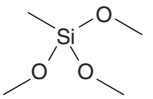

XII

These wood samples were solvent extracted and dried before grafting by impregnating them with a reagent solution under nitrogen using dibutyltin dilaurate as a catalyst and pyridine or dimethyl formamide as solvents. After these reactions, the treated samples were extracted with methylene chloride, before being characterized by weight gain, FTIR and CP-MAS NMR spectroscopy, SEM–EDX and ASE. Considerable weight gains were obtained after the optimization of the treatment. The atomic cartography showed that **IX** was mostly located in the primary wall and middle lamella regions, that is, in the lignin-rich zones. ^{29}Si-CP-MAS-NMR spectroscopy showed that the triethoxysilane moieties were not hydrolyzed during the different modification and characterization steps. The **IX**-modified wood was hydrolyzed and cocondensed with methyltrimethoxysilane (**XII**), as sketched in Scheme 20.2.

20.2.6 Reactions with furfuryl alcohol

Pinus sylvestris L. was treated with an aqueous solution of furfuryl alcohol (**XIII**) and catalyst at 80–100°C, using a process developed by Wood Polymer Technologies (Oslo, Norway) [31, 32]. The acid-catalyzed polycondensation of **XIII** has been thoroughly described in the literature [33–35].

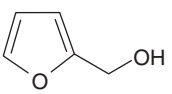

XIII

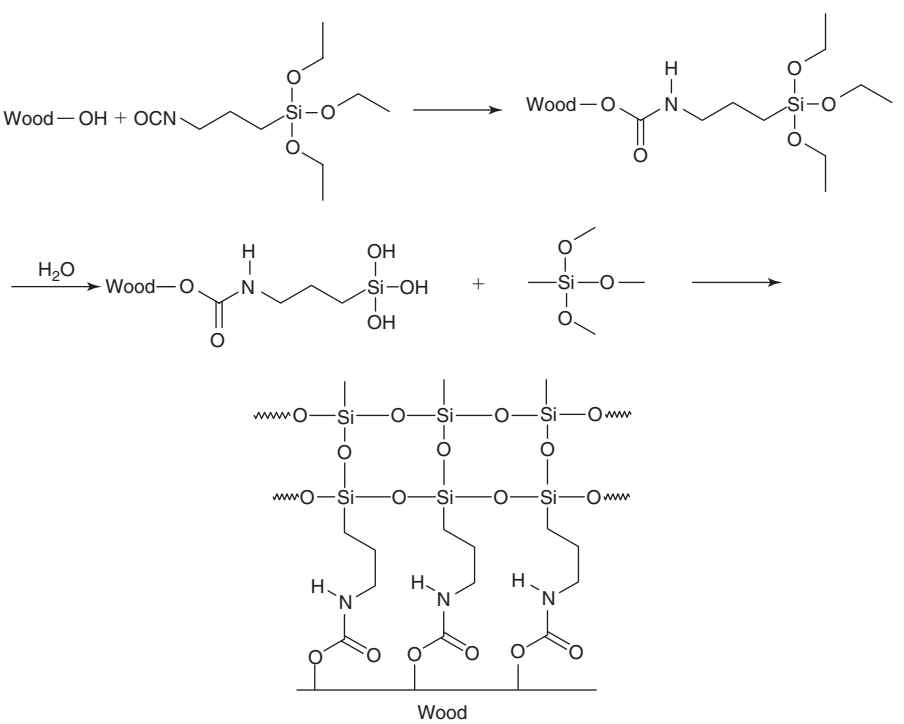

Scheme 20.2

The application of this Norwegian process has been shown to produce modified wood samples with exceptional resistance to both microbial decay and insect attacks, improved mechanical properties and remarkable dimensional stability.

Another study dealing with the treatment of wood with **XIII** involved the use of boric acid and ammonium borate as catalysts [36] and produced modified woods with improved ASE and water repellence efficiency and reduced water absorption. It is important to mention, however, that leaching tests showed that boron was slowly released into the washing water.

20.2.7 Reactions with other molecules

Ketene has been used to esterify wood (Scheme 20.3) because this reaction does not produce any condensation product, as in the case of anhydrides. However, the use of this reagent is associated with serious handling problems, since it is both toxic and explosive. Recently, Morozovs *et al*. [37] reported that, in the context of the reaction between wood and ketene gas, hardwoods are more reactive than softwoods and that the optimal reaction temperature is about 50°. The reaction with diketene (Scheme 20.3) gave a weight gain of 35 per cent, when carried out at 52°C for 3 h.

Reactions on wood with more exotic compounds have been reviewed systematically in Hill's book [1] and since then no other relevant study has appeared to the best of our knowledge.

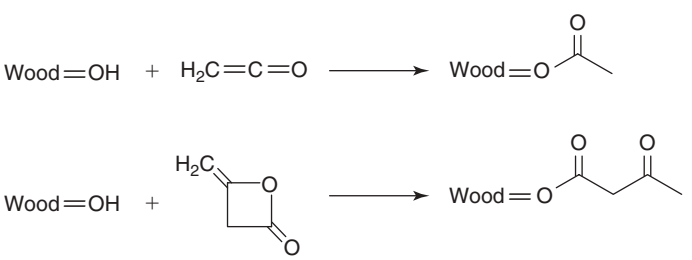

Scheme 20.3

20.2.8 Wood-based composites

The use of wood fibres as reinforcing elements in macromolecular composite materials has recently gained considerable attention, as witnessed by the numerous reviews on the topic [38–42]. The main driving force related to this new strategy in composite materials is the fact that glass fibre based composites cannot be recycled at the end of their life cycle, because their burning to recover energy is accompanied by the formation of a glass residue which is particularly difficult to handle. This problem is obviously not encountered with wood fibre based counterparts, which are fully organic and therefore totally combustible. The additional advantages related to the use of wood fibres are the same as those already emphasized in Chapters 18 and 19 in the context of cellulose fibres, namely their low density, renewable character and ubiquitous availability at low cost and in a variety of forms.

Very recently, siloxane-crosslinked wood plastic composites based on the use of spruce and pine wood fibres and high density polyethylene in the presence of varying amounts of vinyltrimethoxysilane (**XIV**) have been reported [43].

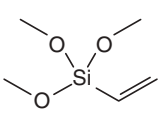

XIV

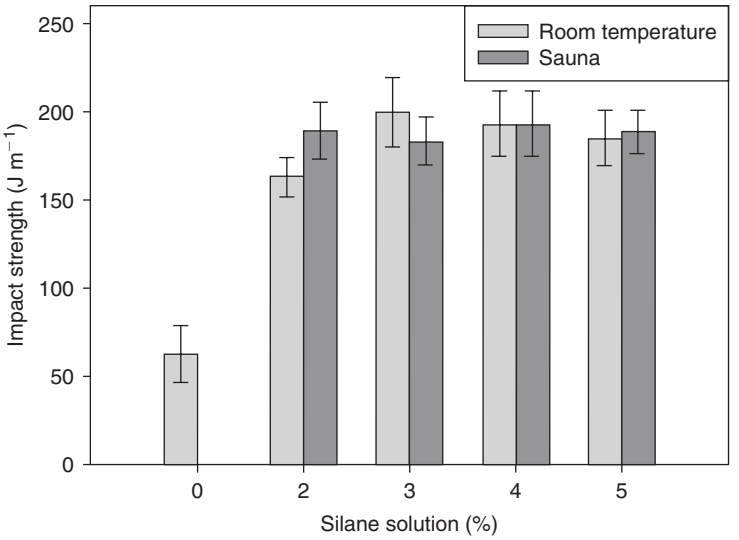

Figure 20.6 Average values of impact strength as a function of added **XIV**. (Reproduced by permission of Elsevier. Copyright 2006. Reprinted from Reference [43].)

These novel materials showed improved toughness, impact strength and creep properties compared with those of the siloxane-free counterpart, as shown in Fig. 20.6 for impact strength measurements.

The treatment of wood fibres with isocyanate-bearing molecules and their incorporation into polyethylene were also recently studied [44]. In particular, the use of poly-(diphenylmethane diisocyanate) (**XV**) increased both the modulus of rupture (MOR) and the modulus of elasticity (MOE) of the ensuing composites. The use of stearic anhydride (**XVI**) as a novel compatibilizer further improved both MOR and MOE and enhanced the water resistance of the composites.

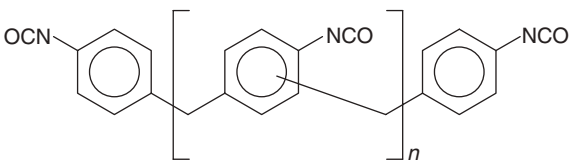

$n = 0, 1, 2,...$

XV

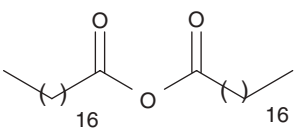

XVI

The incorporation of sisal fibres into composites containing wood particles has also attracted some attention [45]. This system involved an unsaturated polyester/styrene matrix and pine wood flour. A composite with 12 per cent (v/v) of wood particles displayed a 10-fold increase in the work of fracture upon the addition of 7 per cent (v/v) of sisal fibres.

Wood-based composites with a phenolic resin matrix have been transformed into silicon-infiltrated silicon carbide ceramics by carbonization at about 1 650°C [46]. The bending strength and the elastic modulus of these original ceramics were better than those of conventionally manufactured counterparts, whereas the fracture toughness was lower.

The performance of wood–polyethylene composites was found to improve by an appropriate compatibilization with different **MA**s and the additional incorporation of organo-clay particles [47] consisting of natural montmorillonite modified with quaternary ammonium salt. The thermal expansion coefficient and the heat of deflection values indicated that these materials displayed an improved interfacial adhesion.

The processing and processes of microcellular-foamed wood plastic composites have been the subject of a recent review [48].

20.3 CONCLUSIONS

The main emphasis of this chapter has to do with the shift from the traditional ways of treating woods involving the physical incorporation of stabilizers in order to enhance some of their physical properties but, more importantly, to improve their resistance to atmospheric and biological degradation through chemical modifications which eliminate the problem of leaching of toxic materials into the environment. The variety of these surface or bulk treatments published in the recent literature points to the relevance of this novel green approach and shows that very promising results can be obtained.

REFERENCES

1. Hill C.A.S., *Wood Modification: Chemical, Thermal and Other Processes*, John Wiley & Sons, Ltd, Chichester, 2006.
2. Lu J.Z., Wu Q., McNabb, Jr. H.S., *Wood Fibre Sci.*, **32**, 2000, 88.
3. Back E.L., Danielsson S., *Nord. Pulp Pap. Res. J.*, **2**, 1987, 53.
4. Mahlberg R., Niemi H.E.M., Denes F., Rowell R.M., *Int. J. Adhes. Adhes.*, **18**, 1998, 283.
5. Denes A.R., Young R.A., *Holzforschung*, **53**, 1999, 632.
6. Podgorski L., Chevet B., Onic L., Marlin A., *Int. J. Adhes. Adhes.*, **20**, 2000, 103.
7. Rehn P., Vlöl W., *Holz. Roh. Werkst.*, **61**, 2003, 145.
8. Ref. 1, Chapters 3 and 4.
9. Belgacem M.N., Gandini A., *Compos. Interface*, **12**, 2005, 41.
10. Thiebaud S., Borredon M.E., Baziard G., Senocq F., *Bioresource Technol.*, **59**, 1997, 103.
11. Thiebaud D., Borredon M.E., *Bioresource Technol.*, **52**, 1995, 169.
12. Cetin N.S., Hill C.A.S., *J. Wood Chem. Technol.*, **19**, 1999, 247.
13. Hill C.A.S., Cetin N.S., *Int. J. Adhes. Adhes.*, **20**, 2000, 71.
14. Bach S., Belgacem M.N., Gandini A., *Holzforschung*, **59**, 2005, 389.
15. Gandini A., Belgacem M.N., *Macromol. Symp.*, **221**, 2005, 257.
16. Gandini A., Botaro V.R., Zeno E., Bach S., *Polym. Intern.*, **50**, 2000, 7.
17. Gandini A., Belgacem M.N., *ACS Symp. Ser.*, **954**, 2007, 93.
18. Bach S., Le Sage L., Belgacem M.N., Gandini A., unpublished results. Bach, S., Doctorate Thesis, Grenoble National Polytechnic Institute, 2000.
19. Iwamoto Y., Ito T., *J. Wood Sci.*, **51**, 2005, 595.
20. Iwamoto Y., Ito T., Minato K., *J. Wood Sci.*, **51**, 2005, 601.
21. Zhang C., Li K., Simonsen J., *J. Appl. Polym. Sci.*, **89**, 2003, 1078.
22. Geng Y., Li K., Simonsen J., *J. Appl. Polym. Sci.*, **99**, 2006, 712.
23. Pandey K.K., *Polym. Degrad. Stabil.*, **90**, 2005, 9.
24. Pandey K.K., Chandrashekar N., *J. Appl. Polym. Sci.*, **99**, 2006, 2367.
25. George B., Suttie E., Merlin A., Deglise X., *Polym. Degrad. Stabil.*, **88**, 2005, 268.
26. Devi R.R., Maji T.K., *Polym. Composite*, **28**, 2007, 1.
27. Clermont L.P., Bender F., *Forest Prod. J.*, **7**, 1957, 167.
28. Sèbe G., Tingaut P., Safou-Tchiama R., Pétraut M., Grelier S., De Jéso B., *Holzforschung*, **58**, 2004, 511.
29. Tingaut P., Weigenand O., Militz H., De Jéso B., Sèbe G., *Holzforschung*, **59**, 2005, 397.
30. Tingaut P., Weigenand O., Mai C., Militz H., Sèbe G., *Holzforschung*, **60**, 2006, 271.
31. Lande S., Eikenes M., Westin M., *Scand. J. Forest Res.*, **19**, 2004, 14.
32. Lande S., Westin M., Schneider M., *Scand. J. Forest Res.*, **19**, 2004, 22.
33. Choura M., Belgacem M.N., Gandini A., *Macromolecules*, **29**, 1996, 3839.
34. Choura M., Belgacem M.N., Gandini A., *Macromol. Symp.*, **122**, 1997, 263.
35. Gandini A., Belgacem M.N., *Prog. Polym. Sci.*, **22**, 1997, 1203.
36. Baysal E., Ozaki S.K., Yalinkilic M.K., *Wood Sci. Technol.*, **38**, 2004, 405.
37. Morozovs A., Aboltins A., Zoldners J., Akerfelds I., in *Proceedings of the first European Conference on Wood Modification*, Eds.: Van Acker J. and Hill C.A.S., Ghent, Belgium, 2003, pp. 351–362.
38. Eichhorn S.J., Baillie C.A., Zafeiropoulos N., Mwaikambo L.Y., Ansell M.P., Dufresne A., Entwistle K.M., Herraro-Franco P.J., Escamilla G.C., Groom L., Hughes M., Hill C., Rials T.G., Wild P.M., *J. Mater. Sci.*, **36**, 2001, 2107.
39. Eco-Composites: A special issue of *Composite Sci. Technol.* **63**, 2004, 112, collection of 14 publications all dedicated to cellulose and wood fibres-based composite materials.
40. Mohanty A.K., Misra M., Hinrichsen G., *Macromol. Mater. Eng.*, **276/277**, 2000, 1.

41. Gassan J., Bledzki A.K., *Prog. Polym. Sci.*, **24**, 1999, 221.
42. Lu J.Z., Wu Q., McNabb, Jr. H.S., *Wood Fibre Sci.*, **32**, 2000, 88.
43. Bentsson M., Oksman K., *Comp. Sci. Technol.*, **66**, 2006, 2177.
44. Geng Y., Li K., Simonsen J., *J. Adhes. Sci. Technol.*, **19**, 2005, 987.
45. Nuñez A.J., Aranguren M.I., Berglund L.A., *J. Appl. Polym. Sci.*, **101**, 2006, 1982.
46. Hofenauer A., Treusch O., Tröger F., Wegener G., Fromm J., *Holz. Roh. Werkst.*, **64**, 2006, 165.
47. Zhong Y., Poloso T., Hetzer M., De Kee D., *Polym. Eng. Sci.*, **47**, 2007, 797.
48. Faruk O., Bledzki A.K., Matuana L.M., *Macromol. Mater. Eng.*, **292**, 2007, 113.

This page is intentionally left blank.